COLLOID BEHAVIOR IN FRACTURED AQUIFER SYSTEMS

PHYSICS-BASED AND DATA-DRIVEN STRATEGIES FOR SIMULATING COLLOID BEHAVIOR IN FRACTURED AQUIFER SYSTEMS

By

Ahmed Mohamed Yosri Ahmed

BSc., MSc.

A Thesis Submitted to the School of Graduate Studies in Partial Fulfillment of the Requirements for the Degree

Doctor of Philosophy

Doctor of Philosophy (2019) (Civil Engineering)	McMaster University Hamilton, Ontario
TITLE:	Physics-based and data-driven strategies for simulating colloid behavior in fractured aquifer systems
AUTHOR:	Ahmed Mohamed Yosri Ahmed BSc., MSc. (Cairo University)
SUPERVISORS:	Dr. Sarah Dickson-Anderson Dr. Wael El-Dakhakhni
NUMBER OF PAGES:	xix, 180

Dedications

To Mohamed Yosri & Nadia,

Shimaa & Mennatallah,

Laila

Lay Abstract

Microorganisms, microplastics, clay, and fine silt are classified as *colloids* within the spectrum of contaminants that might exist in groundwater. Although some colloids are benign (e.g., clay and fine silt), they can still affect the groundwater quality and aquifer porosity. Colloids can also enhance or inhibit the migration of other contaminants in groundwater because of their high adsorption capacity. Several remediation strategies are being envisioned to remove pathogenic colloids and eliminate other contaminants adsorbed onto benign colloids, where effective design of such strategies requires reliable models of colloid behavior. The present study aims at enhancing the reliability of simulating colloid behavior in fractured aquifers through: *i*) developing models that capture the effects of the aquifer's physical and chemical properties on colloid behavior; and, *ii*) designing a framework that improves the reliability of aquifer conceptualization. Effective remediation strategies can then be designed for contaminated fractured aquifers based on the developed tools.

Abstract

The design of effective quality management strategies in groundwater systems is crucial, as clean water is essential for livelihood, health, and development. Colloids represent a class of contaminants that might be pathogenic or benign. Colloids can also enhance or inhibit the transport of dissolved contaminants in groundwater, which has inspired the use of benign colloids in the remediation of contaminated aquifers. Reliable modelling of colloid behavior is therefore essential for the design of effective remediation strategies, both those employing benign colloids and those aiming at the removal of pathogenic colloids. While colloid transport is controlled by groundwater velocity, colloid retention is governed by the physical and chemical properties of the aquifer together with those of the colloid. The present study aims at enhancing the reliability of modelling colloid behavior in fractured aquifers through: *i*) developing a synchronization-based framework that can effectively identify hydraulic connections within the aquifer; *ii*) developing a mathematical model for the relationship between the fraction of colloids retained along a fracture (F_r) and the parameters describing the aquifer's physical and chemical properties; *iii*) developing an analytical model for the relationship between F_r and the coefficient describing irreversible colloid deposition in single fractures; and, *iv*) developing a numerical technique that can efficiently simulate colloid behavior in single fractures and fracture networks under different physical, chemical, and matrix conditions. The performance of the synchronization-based framework, mathematical and analytical models, and the numerical technique was assessed separately for different verification cases, and the corresponding efficacy was confirmed. Coupling the tools developed in the present study enables the reliable prediction of colloid behavior in response to changes in the groundwater-colloid-fracture system's physical and chemical properties, which can aid in understanding how to manipulate the system's

properties for the effective design of groundwater quality management and remediation strategies.

Acknowledgement

I would like to express my sincere appreciation to my supervisors Dr. Sarah Dickson-Anderson and Dr. Wael El-Dakhakhni for their continuous help and guidance all the way during my study. It was a great opportunity to work with such amazing supervisors. I really did not feel that I am away from my home as they really gave me all the support and provided me with a family-like environment. Special thanks are due to my supervisory committee members Dr. Dieter Stolle and Dr. Shinya Nagasaki for their constructive feedback that helped me expanding my work. I also want to thank the external examiner, Dr. Constantinos Chrysikopoulos, for supporting my work and giving me valuable advices for extending this study.

I am also very grateful to Dr. Ahmed Hassan and Dr. Mohamed Attia for their long-distance support. Special thanks are due to my brothers before being friends: Maysara Ghaith, Mohamed El-Sefy, Mohamed El-Ganzory, Ahmed El-Sayed, Ahmed Yassin, and my sister before being a friend Mouna Reda. I also want to thank my peers and colleagues: Mohamed Salama, Ahmed Gondia, Yassin Salaheldin, Ahmed Ghith, Heba Gamal, Mohamed Khafagy, Brinda Narayanan, Zoha Anjum, Katie White, and Kayla Lucier. I owe special thanks to my friends and supporters: Dr. Shady Salem, Dr. Tarek El-Hashimy, Dr. Mohamed Ezzeldin, Dr. Moataz Mohamed, and Dr. Ahmad Siam.

At last but not the least, I want to express my sincere gratitude to my mother (Nadia) who supported me all the way during my study, even before starting my journey in Canada. Actually, my mother Nadia supported and encouraged me in everything in my life. Also, this work could not be completed without the support from my sister (Mennatallah) and her children (Miral and Marwan), my brother-in-law (Abd El-Hamid), my father-in-law (Salah), my mother-in-law (Nagat), and my cousins (Amr, Hind, and Ali). Most importantly, I would like to express my deep

appreciation to my wife (Shimaa) for supporting me, for sustaining a lot of stresses, and for accepting to join me in this tough journey. Shimaa really helped me in everything, and I really could not achieve anything without her support. I also would like to thank my little princess (Laila) for giving me the power to love everything, for her wonderful smile, and for being the source of my happiness. Finally, I would like to say that no words can express my sincere gratitude to my father (Mohamed Yosri) who is my role model, my backbone, and my source of wisdom. I really missed him in this journey, but cannot forget him smiling and pushing me towards a better life.

Table of contents

List of Figures

List of Tables

Declaration of Academic Achievement

This dissertation was prepared in accordance with the guidelines set by the school of graduate studies at McMaster University for sandwich theses that contain a compilation of research papers published or prepared for publishing as journal articles. Chapters 2, 4, and 5 were prepared for publication as journal articles whereas the research paper presented in Chapter 3 is already published. This dissertation presents the work carried out solely by Ahmed Yosri, where technical advice and guidance were provided for the whole thesis by the academic supervisors Dr. Sarah Dickson-Anderson and Dr. Wael El-Dakhakhni. Some editorial comments for the papers presented in Chapters 2, 3, and 4 were provided by Dr. Ahmad Siam. Information from outside sources, which has been used towards analysis or discussion, has been cited where appropriate. The original contributions of the author to each paper (Chapter) and the reasons for including them in this dissertation are outlined below:

Chapter 2: Yosri, Ahmed, Sarah Dickson-Anderson, Ahmad Siam, and Wael El-Dakhakhni. "**Hydraulic Connection Identification in Fractured Aquifers: A Stochastic Event Synchrony-Based Framework.**" *Journal of Hydrology*. Submitted for publication in April 2019.

The idea for this paper came from Ahmed Yosri who also prepared the framework and tested it in different cases. Ahmed Yosri prepared the manuscript, and Ahmad Siam provided editorial comments to an earlier version of it. The

manuscript was then reviewed and edited by Sarah Dickson-Anderson and Wael El-Dakhakhni. This work should be included in this dissertation as it introduces a cost-effective alternative for fractured aquifer characterization which is essential for preparing reliable conceptual flow and transport models.

Chapter 3: Yosri, Ahmed, Ahmad Siam, Sarah Dickson-Anderson, and Wael El-Dakhakhni. 2019. "**A Genetic Programming–Based Model for Colloid Retention in Fractures.**" *Groundwater* 1–11. https://doi.org/10.1111/gwat.12860

The idea for this paper came from Ahmed Yosri. The dataset employed in this paper was provided by Sarah Dickson-Anderson. Ahmed Yosri conducted the analysis and prepared the manuscript that was reviewed and edited by Ahmad Siam, Sarah Dickson-Anderson, and Wael El-Dakhakhni. This work should be included in this dissertation as it provides an accurate mathematical model to predict colloid retention in single fractures under a range of physical and chemical conditions; and therefore, aid in the design of water quality management and remediation plans in contaminated fractured systems.

Chapter 4: Yosri, Ahmed, Sarah Dickson-Anderson, Ahmad Siam, and Wael El-Dakhakhni. "**Analytical description of colloid behavior in single fractures under irreversible deposition.**" *Groundwater*. Submitted for publication in July 2019.

The idea for this paper came from Ahmed Yosri who also developed the analytical solution and tested it in different cases. Ahmed Yosri prepared the

manuscript, and Ahmad Siam provided editorial comments to an earlier version of it. The manuscript was then reviewed and edited by Sarah Dickson-Anderson and Wael El-Dakhakhni. This work should be included in this dissertation as it enables the prediction of colloid retention in single fractures analytically, and can be coupled with the mathematical model developed in Chapter 3 to enhance the prediction of colloid behavior in single fractures under different physical and chemical conditions.

Chapter 4: Yosri, Ahmed, Sarah Dickson-Anderson, and Wael El-Dakhakhni. "**A Modified Time Domain Random Walk Approach for Simulating Colloid Behavior in Fractures: Method Development and Verification.**" Prepared for submission to the Journal of Water Resources Research.

The idea for this paper came from Ahmed Yosri who also developed the numerical technique and verified its efficiency in different cases. Ahmed Yosri prepared the manuscript that was reviewed and edited by Sarah Dickson-Anderson and Wael El-Dakhakhni. This work should be included in this dissertation as it provides an effective simulation tool for colloid behavior in fractured systems. This numerical technique can be coupled with the tools presented in other chapters for effective simulation of colloid behavior in fractures under different physical and chemical conditions. This can aid in the design of effective water quality management and remediation strategies through understanding how to modify the system's physical and chemical properties to enhance or inhibit colloid migration.

Chapter 1

INTRODUCTION

1.1. BACKGROUND AND MOTIVATION

Water is the essence of life, and clean water is crucial for livelihood, health, and development. Terrestrial water is found in different forms including saline-water in oceans and seas, as well as freshwater in ice caps and glaciers, surface-water, and groundwater. More than 90% of the terrestrial water is saline, and two-thirds of the freshwater resources are groundwater (Freeze and Cherry 1979; Fetter 2001). Furthermore, approximately 50% of the global population depends on groundwater for drinking (WWAP 2015), which highlights the need of effective management of groundwater quantity and quality.

Groundwater aquifers are generally classified into: *i*) unconsolidated (porous media) aquifers, in which connected pores represent the preferential pathways for water and contaminants (e.g., Collins 1961); *ii*) fractured aquifers, in which interconnected fractures are the main conduits (e.g., Snow 1970); and, *iii*) karst aquifers, in which water conduits range in size from a centimeter to multiple meters (e.g., White 2019), with the consensus being that a combination of different types of aquifers might exist in the same groundwater system. Increasing reliance on groundwater, due to population growth and industrialization, has led to an extensive overuse of this resource and subsequent acceleration of aquifer depletion (e.g., Castellazzi et al. 2018; Rahmati et al. 2018). This necessitates extracting water from

increasing depths where fractured aquifers are most likely to be found. Therefore, effective modelling of groundwater flow and contaminant transport in fractured aquifers is needed.

Contaminants in groundwater may be dissolved, particulate, or non-aqueous in phase. Colloids represent a subset of particulates that range in size from a nanometer to ten micrometers (e.g., Buddemeier and Hunt 1988), and are negatively charged under normal groundwater conditions (e.g., Zvikelsky and Weisbrod 2006). Colloids may be pathogenic (e.g., microorganisms, anthropogenic materials) or benign (e.g., clay, fine silt), and are introduced to groundwater systems through different mechanisms, including: the infiltration of contaminated water or wastewater (Gschwend et al. 1990); the micro-erosion of rock matrix minerals due to chemical perturbations (McCarthy et al. 2002); tectonic movements in fragile rock materials (Degueldre et al. 1989); the scouring of fracture fillings (Zhang et al. 2012); and, the precipitation of colloidal mineral phases (Ryan and Elimelech 1996).

Colloids have been proven to behave differently than dissolved contaminants and other larger particulates due to the significant effects of their surface characteristics (e.g., electrical charge density, and chemical groups) (Reimus 1995), particularly in fractured systems. Colloids typically have a large specific surface area and high adsorption capacity, which enable them to facilitate or inhibit the transport of dissolved contaminants (e.g., McDowell-Boyer et al. 1986). As such, some colloidal particles have been employed for the water quality management and

remediation of contaminated aquifers (NRC 2015; Hamamoto et al. 2017; Koju et al. 2019; Sousa Neto et al. 2019; T. Wang et al. 2019).

Colloids in fractures are subject to several transport (i.e., advection and dispersion) and retention (e.g., attachment, matrix diffusion, physical straining, and sedimentation) mechanisms (Zhang et al. 2012). While colloid transport is controlled by groundwater velocity and its variation across the fracture, colloid retention is governed by the physical (e.g., specific discharge, aperture variability, colloid size and density) and chemical (e.g., water ionic strength and pH) properties of the groundwater-colloid-fracture system (Zhang et al. 2012). However, to the best of the author's knowledge, an accurate mathematical quantification of the combined effect of these parameters (or even the effect of each parameter individually) on colloid behavior does not exist. Therefore, the preparation of action plans to remove or inactivate pathogenic colloids and the design of colloid-based remediation strategies in fractured aquifers necessitate: *i*) effective characterization of the aquifer (e.g., identification of hydraulic connections), which is essential for the development of reliable flow and transport models; and, *ii*) effective modelling of colloid behavior in single fractures and fracture networks under different physical and chemical conditions, which enables the simulation of the system's response during remediation.

1.1.1. CHARACTERIZATION OF FRACTURED AQUIFERS

Around 20% of the earth's groundwater aquifers are fractured (Chandra et al. 2019), and fractured aquifers represent the primary water resource in the regions where they exist (e.g., Shapiro 2002). Simulating groundwater flow and contaminant transport in fractured systems is generally carried out through: *i*) equivalent porous media models, where fractures must be dense and highly interconnected within the aquifer (e.g., Berkowitz 2002); *ii*) dual continuum models, where the aquifer is divided into two interacting mediums with different hydraulic properties (e.g., Dershowitz and Miller 1995); and, *iii*) discrete fracture network models, where an explicit representation of fractures and the surrounding matrix is used (e.g., Cacas et al. 1990). Each of these modelling approaches requires a number of parameters that are difficult to obtain without adequate characterization of the aquifer at the single-fracture (e.g., location, length, aperture, orientation) and fracture network (e.g., fracture density and interconnectivity, statistical distribution of fracture properties) scales (Dorn et al. 2013).

Several effective field techniques have been developed over the past few decades for the hydraulic and geometric characterization of fractures (e.g., Klepikova et al. 2014; Guiltinan and Becker 2015; Quinn et al. 2015; Kang et al. 2016; Klammler et al. 2016; Alexis Shakas et al. 2016; Klepikova et al. 2018; Persaud et al. 2018; Hsu et al. 2019; Maldaner et al. 2019; Vitale et al. 2019; W. Wang et al. 2019). These techniques include hydraulic and tracer tests, and

geophysical investigations. Extensive, and therefore costly and time-consuming, *in-situ* investigations are typically required for the full characterization of an aquifer (e.g., Liu and Kitanidis 2011). Therefore, groundwater flow and contaminant transport in fractured aquifers are most often simulated in fracture networks that are generated stochastically based on statistical distributions of fracture characteristics (e.g., Dorn et al. 2013). These distributions are typically obtained through a combination of limited, rather than extensive, field- and laboratory investigations. While stochastically generated fractured networks may not necessarily preserve the actual hydraulic connections within the aquifer, these networks are modified through inverse modelling to preserve head/concentration observations to enhance their reliability (e.g., Somogyvári et al. 2017).

Inverse modelling has been, however, shown to be computationally intensive (e.g., X. Wang et al. 2017; Dong et al. 2019). As such, the reliability of flow and transport models in fractured aquifers can be enhanced through the effective identification of hydraulic connections within the aquifer. These connections can be identified using observations from field experiments (i.e., hydraulic and tracer tests), in which the aquifer ambient conditions (e.g., head in hydraulic tests, and concentration in tracer tests) are perturbated at a specified (test) location. The propagation of this perturbation to a downstream (monitoring) location indicates that a test and monitoring locations are hydraulically connected. Nonetheless, hydrogeologic properties within the connection are still obtained through inverse modelling.

Cost-effective tools can be developed to identify the hydraulic connection between two locations based on mass replication at these locations, instead of just monitoring perturbation arrival. The hydrogeologic properties within the connection can then be obtained through assessing the lagged interdependence between time series representing mass arrival at the two locations. Several interdependence measures have been developed to date (e.g., nonlinear interdependences, phase synchronization, mutual information, cross-correlation, and coherence function) (e.g., JuNG Hsu 1992; Quiroga et al. 2002; Schreiber et al. 2003), each of which has its own strengths and limitations.

Stochastic event synchrony (SES) is an alternative way to assess the interdependence between multiple point processes (Dauwels et al. 2009). SES can be applied to observations from field tracer experiments conducted in a fractured aquifer using a group of wells, and subsequently, hydraulic connections between well pairs can be identified. In addition, the hydrogeological properties within each connection can be obtained based on the SES metrics. The SES-based hydraulic connections can be utilized as an additional constraint during the stochastic generation of fracture networks, which enhances the reliability of flow and transport models in fractured aquifers. It should be mentioned that multiple test and monitoring locations might be used during a field tracer experiment; however, the concept of mass replication is still applicable.

1.1.2. COLLOID BEHAVIOR IN FRACTURED AQUIFERS

Colloid behavior has been studied extensively in unconsolidated aquifers (e.g., Lehoux et al. 2017; Kamrani et al. 2018; Yang et al. 2019), fractured aquifers (e.g., Neukum 2018; C. Wang et al. 2019; Stoll et al. 2019), and karst aquifers (e.g., Schiperski et al. 2016; Bandy et al. 2019; Vesper 2019). Colloid suspensions most often contain multiple sized (i.e., polydisperse) rather than single sized (i.e., monodisperse) particulates, with diameters following a normal or a lognormal distribution (Ledin et al. 1994; Reimus 1995). Colloid size, or diameter, falls within a relatively wide range (i.e., one nanometer up to ten micrometers). Therefore, colloids in fractures are affected by forces associated with both molecules (e.g., Van der Waals forces, Brownian motion) and larger particles (e.g., drag force, gravity force) (Reimus 1995). All these forces are affected by the physical and chemical characteristics of the groundwater-colloid-fracture system, and their net effect determines whether a colloid migrates or is retained within the fracture.

While the transport of colloids in fractures is due to advection and longitudinal dispersion, *attachment* was identified as their primary retention mechanism (e.g., Rodrigues and Dickson 2014; Stoll et al. 2017; Cohen and Weisbrod 2018). The terms “attachment” and “deposition” have been used interchangeably in the literature to describe colloid interaction with fracture surfaces, and they are also used interchangeably in the present study. Colloid attachment occurs when the Van der Waals attractive forces overcome the repulsive

double layer forces (O'Melia and Stumm 1967), and it requires a prior collision between the colloid and the fracture surface. Colloid-substrata interfacial interactions have been described in porous media using colloid filtration theory (CFT) (Yao et al. 1971), and this description was further enhanced via the Derjaguin-Landau-Verwey-Overbeek (DLVO) theory (Derjaguin and Landau 1941; Verwey and Overbeek 1984). DLVO theory describes the combined effect of the Van der Waals attractive forces and the electric double layer repulsive forces (e.g., Elimelech and O'Melia 1990), and was developed under the assumptions of (e.g., Degueldre et al. 1996): *i*) the short range chemical effects are negligible; *ii*) the colloid and collector are idealized as spheres with a homogenous surface charge; and, *iii*) the DLVO theory cannot be applied at the atomic scale. An extended DLVO theory was developed to include other non-DLVO forces (e.g., steric, bridging, and hydration forces) (e.g., Hoek and Agarwal 2006; Syngouna and Chrysikopoulos 2013; Molnar et al. 2019); however, neither DLVO nor extended DLVO theory can be applied to colloids in fractures as they violate the assumptions used to develop these theories (e.g., Christenson 1988; Degueldre et al. 1996). Nevertheless, DLVO theory and its extended version can provide a conceptual description, rather than predictive tools, for colloid-fracture surface interactions (e.g., An et al. 2000).

The deficiencies of CFT, DLVO, and extended DLVO in the context of fractures have restricted the modelling of the forces causing colloid deposition. Instead, colloid deposition has been described macroscopically using a deposition

coefficient (κ) that combines the effects of the different mechanisms leading to deposition (Abdel-Salam and Chrysikopoulos 1994). This coefficient depends on the parameters describing the physical and chemical properties of the groundwater-colloid-fracture system (Abdel-Salam and Chrysikopoulos 1994); however, to the best of the author's knowledge, the mathematical relationship between κ and these parameters has not yet been developed. Therefore, simulating colloid behavior in fractures has been limited to groundwater-colloid-fracture systems with homogenous physical and chemical properties.

Colloid behavior has been described analytically (i.e., Abdel-Salam and Chrysikopoulos, 1994; James and Chrysikopoulos, 2003) in single fractures under different matrix and boundary conditions, with the consensus being that κ is constant and estimated from laboratory or field experiments (Abdel-Salam and Chrysikopoulos 1994). The application of these analytical solutions at the fracture network scale has not yet been verified, and thus, numerical techniques verified at the single-fracture scale are typically adopted. These numerical techniques can be designed based on different perspectives, including: *i*) the spatiotemporal evolution of contaminant concentration (e.g., random walk particle tracking, finite difference, finite element approaches); or, *ii*) the temporal evolution of contaminant concentration (i.e., time domain approaches). Although the first perspective has been extensively employed to simulate colloid behavior in fractures (e.g., Abdel-Salam and Chrysikopoulos 1995; Chrysikopoulos and Abdel-Salam 1997; James and Chrysikopoulos 1999; Bagalkot and Suresh Kumar 2017; James et al. 2018),

accuracy is typically achieved at the expenses of a high computational cost. On the other hand, the second perspective represents an efficient alternative without loss of accuracy. However, the application of this perspective to colloid transport in fractures has not been established yet.

1.2. RESEARCH OBJECTIVES

The main goal of the work in this dissertation is to enhance the reliability of modelling colloid behavior in fractures such that physical and chemical properties of the groundwater-colloid-fracture system can be explicitly considered, which can subsequently aid in the design of effective water quality management and remediation strategies in fractured aquifers. As such, the following specific objectives were envisioned:

- Develop a cost-effective characterization framework that can efficiently identify hydraulic connections within fractured aquifers.
- Develop a mathematical relationship between F_r and the parameters describing the physical (i.e., fracture geometry, colloid size, specific discharge, diffusion coefficient) and chemical (i.e., ionic strength, surface charges of colloid and matrix) properties of the groundwater-colloid-fracture system.
- Develop an analytical relationship between F_r and κ in a saturated fracture; subsequently, κ can be quantified mathematically based on the parameters

describing the physical and chemical properties of the groundwater-colloid-fracture system.

- Develop a numerical approach that can efficiently simulate colloid behavior at the single-fracture and fracture network scales under different boundary and matrix conditions, and is also able to simulate the physical and chemical heterogeneity over the fracture network.

The present study was conducted under the following general assumptions (additional assumptions are highlighted in specific sections where applicable):

- Fracture surfaces are idealized as two parallel plates, and a constant aperture is assigned to the fracture.
- The Cubic Law is valid and can be employed to describe flow in a single fracture.
- Colloid deposition is an irreversible process, and irreversible deposition is dominant over other colloid retention mechanisms in fractures.
- Colloid's deposition and dispersion coefficients are constant within a fracture; however, they might vary over a network.

1.3. THESIS ORGANIZATION

This section summarizes the content of each of the six chapters in this dissertation:

- Chapter 1 provides the background required for this research, an overview of the objectives, and a description of the thesis organization.
- Chapter 2 discusses the development of a SES-based framework to identify hydraulic connections between different locations within a fractured aquifer. The framework was developed based on the coherence between solute transport in a fracture and time series synchronization. In addition to identifying a hydraulic connection between two locations, the hydrogeologic properties (groundwater velocity or the ratio between groundwater velocity and dispersion coefficient) within the connection can be estimated based on the SES metrics. The capability of the framework was verified for: a single fracture with- and without matrix diffusion under an instantaneous colloid release at the inlet; a single fracture under a range of Peclet numbers and a decaying colloid release at the inlet; and a simple impermeable fracture network under a decaying colloid release at the inlet boundary.
- Chapter 3 discusses the use of multigene genetic programming (MGGP) to develop a mathematical relationship between F_r and the parameters describing the physical and chemical properties of the groundwater-colloid-fracture system. The MGGP-based model was developed using the dataset collected by Rodrigues and Dickson (2014) from a series of laboratory-scale colloid tracer experiments, and was validated using a subset of the same dataset. A global sensitivity analysis (GSA) was

conducted to identify the most dominant parameters contributing to the variability of F_r.

- Chapter 4 presents the development of an analytical relationship between F_r and κ in a semi-infinite, saturated fracture with an impermeable matrix and under an instantaneous colloid release at the inlet. This relationship was developed through conceptualizing irreversible colloid deposition as first-order decay, and was verified using the dataset collected by Rodrigues and Dickson (2014). A GSA was applied to the F_r–κ relationship to determine the parameters dominating the variability of F_r.
- Chapter 5 discusses the development of a modified time domain random walk (MTDRW) approach that is capable of simulating colloid behavior at the single-fracture and fracture network scales under different matrix conditions. The MTDRW approach was developed based on the similarity between colloid breakthrough curves and the probability density function of colloid travel time in a fracture. The efficacy of the MTDRW approach was confirmed after comparing its results to the corresponding estimates of analytical and semi-analytical solutions in single fractures and a fracture network, respectively.
- Chapter 6 provides a summary of this research, the overall conclusions, and suggestions for future work.

It should be noted that Chapters 2 through 5 represent standalone manuscripts that are already published, submitted, or prepared for publishing as journal articles;

nonetheless, these chapters collectively describe cohesive research body as outlined in this introductory chapter of the dissertation. However, some overlap might exist for the completeness of each standalone chapters/manuscripts.

1.4. NOTATIONS

F_r: Fraction of colloids retained along a fracture

Greek Letters:

κ: Deposition coefficient

1.5. ACRONYMS

CFT: Colloid filtration theory

DLVO: Derjaguin-Landau-Verwey-Overbeek theory

GSA: Global sensitivity analysis

MGGP: Multigene genetic programming

MTDRW: Modified time domain random walk approach

SES: Stochastic event synchrony

1.6. REFERENCES

Abdel-Salam, Assem, and Constantinos V. Chrysikopoulos. 1994. "Analytical Solutions for One-Dimensional Colloid Transport in Saturated Fractures." *Advances in Water Resources* 17(5): 283–96.

Abdel-Salam, Assem, and Constantinos V. Chrysikopoulos. 1995. "Modeling of Colloid and Colloid-Facilitated Contaminant Transport in a Two-Dimensional Fracture with Spatially Variable Aperture." *Transport in Porous Media* 20(3): 197–221.

An, Yuehuei H., Richard B. Dickinson, and Ronald J. Doyle. 2000. "Mechanisms of Bacterial Adhesion and Pathogenesis of Implant and Tissue Infections." *In Handbook of Bacterial Adhesion,* eds. Y.H. An and R.J. Friedman. Totowa, NJ: Humana Press, 1–27.

Bagalkot, Nikhil, and Govindarajan Suresh Kumar. 2017. "Effect of Random Fracture Aperture on the Transport of Colloids in a Coupled Fracture-Matrix System." *Geosciences Journal* 21(1): 55–69.

Bandy, Ashley M., Kimberly Cook, Alan E. Fryar, and Junfeng Zhu. 2019. "Differential Transport of Escherichia Coli Isolates Compared to Abiotic Tracers in a Karst Aquifer." *Groundwater*.

Berkowitz, Brian. 2002. "Characterizing Flow and Transport in Fractured Geological Media: A Review." *Advances in Water Resources* 25(8–12): 861–84.

Buddemeier, Robert W., and James R. Hunt. 1988. "Transport of Colloidal Contaminants in Groundwater: Radionuclide Migration at the Nevada Test Site." *Applied Geochemistry* 3(5): 535–48.

Cacas, M. C., E. Ledoux, G. de Marsily, B. Tillie, A. Barbreau, E. Durand, B. Feuga, and P. Peaudecerf. 1990. "Modeling Fracture Flow with a Stochastic Discrete Fracture Network: Calibration and Validation: 1. The Flow Model." *Water Resources Research banner* 26(3): 479–89.

Castellazzi, Pascal, Laurent Longuevergne, Richard Martel, Alfonso Rivera, Charles Brouard, and Estelle Chaussard. 2018. "Quantitative Mapping of Groundwater Depletion at the Water Management Scale Using a Combined GRACE/InSAR Approach." *Remote Sensing of Environment* 205(1): 408–18.

Chandra, Subash, Esben Auken, Pradip K. Maurya, Shakeel Ahmed, and Saurabh K. Verma. 2019. "Large Scale Mapping of Fractures and Groundwater Pathways in Crystalline Hardrock By AEM." *Scientific Reports* 9(1): 1–11.

Christenson, H. K. 1988. "Non-DLVO Forces between Surfaces - Solvation, Hydration and Capillary Effects" *Journal of Dispersion Science and Technology* 9(2): 171–206.

Chrysikopoulos, Constantinos V., and Assem Abdel-Salam. 1997. "Modeling Colloid Transport and Deposition in Saturated Fractures." *Colloids and Surfaces A: Physicochemical and Engineering Aspects* 121(2–3): 189–202.

Cohen, Meirav, and Noam Weisbrod. 2018. "Transport of Iron Nanoparticles through Natural Discrete Fractures." *Water Research* 129(1): 375–83.

Collins, RE. 1961. *Flow of Fluid Trough Porous Materials*. New York: Reinhold Publishing Co.

Dauwels, J, F Vialatte, T Weber, T Musha, and A Cichocki. 2009. "Quantifying Statistical Interdependence by Message Passing on Graphs-Part I: One-Dimensional Point

Processes.” *Neural computation* 21: 2152–2202.

Degueldre, C., B. Baeyens, W. Goerlich, J. Riga, J. Verbist, and P. Stadelmann. 1989. “Colloids in Water from a Subsurface Fracture in Granitic Rock, Grimsel Test Site, Switzerland.” *Geochimica et Cosmochimica Acta* 53(3): 603–10.

Degueldre, C, R Grauer, A Laube, A Oess, and H Silby. 1996. “Colloid Properties in Granitic Groundwater Systems. II: Stability and Transport Study.” *Applied Geochemistry* 11(5): 697–710.

Derjaguin, B., and L. D. Landau. 1941. “Theory of the Stability of Strongly Charged Lyophobic Sols and of the Adhesion of Strongly Charged Particles in Solutions of Electrolytes.” *Acta Physicochimica U.R.S.S.* 14: 633–62.

Dershowitz, W., and Ian Miller. 1995. “Dual Porosity Fracture Flow and Transport.” *Geophysical Research Letters* 22(11): 1441–44.

Dong, Yanhui, Yunmei Fu, Tian Chyi Jim Yeh, Yu Li Wang, Yuanyuan Zha, Liheng Wang, and Yonghong Hao. 2019. “Equivalence of Discrete Fracture Network and Porous Media Models by Hydraulic Tomography.” *Water Resources Research* 55(4): 3234–47.

Dorn, Caroline, Niklas Linde, Tanguy Le Borgne, Olivier Bour, and Jean-Raynald de Dreuzy. 2013. “Conditioning of Stochastic 3-D Fracture Networks to Hydrological and Geophysical Data.” *Advances in Water Resources* 62: 79–89.

Elimelech, Menachem, and Charles R. O’Melia. 1990. “Kinetics of Deposition of Colloidal Particles in Porous Media.” *Environmental Science and Technology* 24(10): 1528–36.

Fetter, C.W. 2001. *Applied Hydrogeology*. 4th ed. Upper Saddle River, N.J.: Prentice Hall.

Freeze, R. Allan, and John A. Cherry. 1979. *Groundwater*. Englewood Cliffs, New Jersey: Prentice-Hall, Inc.

Gschwend, Philip M., Debera A. Backhus, John K. MacFarlane, and A.L. Page. 1990. "Mobilization of Colloids in Groundwater Due to Infiltration of Water at a Coal Ash Disposal Site." *Journal of Contaminant Hydrology* 6(4): 307–20.

Guiltinan, Eric, and Matthew W. Becker. 2015. "Measuring Well Hydraulic Connectivity in Fractured Bedrock Using Periodic Slug Tests." *Journal of Hydrology* 521: 100–107.

Hamamoto, Shoichiro, Takato Takemura, Kenichiro Suzuki, and Taku Nishimura. 2017. "Effects of PH on Nano-Bubble Stability and Transport in Saturated Porous Media." *Journal of Contaminant Hydrology* 208: 61–67.

Hoek, Eric M V, and Gaurav K Agarwal. 2006. "Extended DLVO Interactions between Spherical Particles and Rough Surfaces." *Journal of colloid and interface science* 298(1): 50–58.

Hsu, Shih Meng, C. C. Ke, Y. T. Lin, C. C. Huang, and Y. S. Wang. 2019. "Unravelling Preferential Flow Paths and Estimating Groundwater Potential in a Fractured Metamorphic Aquifer in Taiwan by Using Borehole Logs and Hybrid DFN/EPM Model." *Environmental Earth Sciences* 78(5): 1–22.

James, Scott C., and Constantinos V. Chrysikopoulos. 2003. "Analytical Solutions for Monodisperse and Polydisperse Colloid Transport in Uniform Fractures." *Colloids and Surfaces A: Physicochemical and Engineering Aspects* 226: 101–18.

James, Scott C., Lichun Wang, and Constantinos V. Chrysikopoulos. 2018. "Modeling Colloid Transport in Fractures with Spatially Variable Aperture and Surface Attachment." *Journal of Hydrology* 566: 735–42.

James, Scott C, and V Chrysikopoulos. 1999. "Transport of Polydisperse Colloid Suspensions in a Single Fracture." *Water Resources Research* 35(3): 707–18.

JuNG Hsu, KUANG. 1992. "Time Series Analysis of the Interdependence Among Air Pollutants." *Atmospheric Environment* 26(4): 491–503.

Kamrani, Salahaddin, Mohsen Rezaei, Mehdi Kord, and Mohammed Baalousha. 2018. "Transport and Retention of Carbon Dots (CDs) in Saturated and Unsaturated Porous Media: Role of Ionic Strength, PH, and Collector Grain Size." *Water Research* 133(1): 338–47.

Kang, Peter K., Yingcai Zheng, Xinding Fang, Rafal Wojcik, Dennis McLaughlin, Stephen Brown, Michael C. Fehler, Daniel R. Burns, and Ruben Juanes. 2016. "Sequential Approach to Joint Flow-Seismic Inversion for Improved Characterization of Fractured Media." *Water Resources Research* 52(2): 903–19.

Klammler, Harald, Kirk Hatfield, Mark A. Newma, Jaehyun Cho, Michael D. Annable, Beth L. Parker, John A. Cherry, and Irina Perminova. 2016. "A New Device for Characterizing Fracture Networks and Measuring Groundwater and Contaminant Fluxes in Fractured Rock Aquifers." *Water Resources Research* 52: 5400–5420.

Klepikova, Maria V., Tanguy Le Borgne, Olivier Bour, Kerry Gallagher, Rebecca Hochreutener, and Nicolas Lavenant. 2014. "Passive Temperature Tomography Experiments to Characterize Transmissivity and Connectivity of Preferential Flow

Paths in Fractured Media." *Journal of Hydrology* 512(1): 549–62.

Klepikova, Maria V., Clement Roques, Simon Loew, and John Selker. 2018. "Improved Characterization of Groundwater Flow in Heterogeneous Aquifers Using Granular Polyacrylamide (PAM) Gel as Temporary Grout." *Water Resources Research* 54(2): 1410–19.

Koju, Neel Kamal, Xin Song, Na Lin, Keke Xu, and Heng Fu. 2019. "Enhanced Distribution of Humic Acid-Modified Nanoscale Magnesia for in Situ Reactive Zone Removal of Cd from Simulated Groundwater." *Environmental Pollution* 245: 9–19.

Ledin, Anna, Stefan Karlsson, Anders Düker, and Bert Allard. 1994. "Measurements in Situ of Concentration and Size Distribution of Colloidal Matter in Deep Groundwaters by Photon Correlation Spectroscopy." *Water Research* 28(7): 1539–45.

Lehoux, Alizée P., Pamela Faure, François Lafolie, Stéphane Rodts, Denis Courtier-Murias, Philippe Coussot, and Eric Michel. 2017. "Combined Time-Lapse Magnetic Resonance Imaging and Modeling to Investigate Colloid Deposition and Transport in Porous Media." *Water Research* 123(1): 12–20.

Liu, X., and P. K. Kitanidis. 2011. "Large-Scale Inverse Modeling with an Application in Hydraulic Tomography." *Water Resources Research* 47(2): 1–9.

Maldaner, Carlos H., Jonathan D. Munn, Thomas I. Coleman, John W. Molson, and Beth L. Parker. 2019. "Groundwater Flow Quantification in Fractured Rock Boreholes Using Active Distributed Temperature Sensing Under Natural Gradient Conditions." *Water Resources Research* 55(4): 3285–3306.

McCarthy, John F., Larry D. McKay, and Deirdre Diana Bruner. 2002. “Influence of Ionic Strength and Cation Charge on Transport of Colloidal Particles in Fractured Shale Saprolite.” *Environmental Science and Technology* 36(17): 3735–43.

McDowell-Boyer, Laura M., James R. Hunt, and Nicholas Sitar. 1986. “Particle Transport through Porous Media.” *Water Resources Research* 22(13): 1901–21.

Molnar, Ian L., Erica Pensini, Md Abdullah Asad, Chven A. Mitchell, Ludwig C. Nitsche, Laura J. Pyrak-Nolte, Gastón L. Miño, and Magdalena M. Krol. 2019. “Colloid Transport in Porous Media: A Review of Classical Mechanisms and Emerging Topics.” *Transport in Porous Media* 1-28.

Neukum, Christoph. 2018. “Transport of Silver Nanoparticles in Single Fractured Sandstone.” *Journal of Contaminant Hydrology* 209(1): 61–67.

National Academies of Sciences, Engineering, and Medicine. 2015. “Characterization, Modeling, Monitoring, and Remediation of Fractured Rock”. Washington, D.C: The National Academies Press.

O’Melia, Charles R., and Werner Stumm. 1967. “Theory of Water Filtration.” *Journal (American Water Works Association)* 59(11): 1393–1412.

Persaud, Elisha, Jana Levison, Peeter Pehme, Kentner Novakowski, and Beth Parker. 2018. “Cross-Hole Fracture Connectivity Assessed Using Hydraulic Responses during Liner Installations in Crystalline Bedrock Boreholes.” *Journal of Hydrology* 556: 233–46.

Quinn, Patryk, John A. Cherry, and Beth L. Parker. 2015. “Combined Use of Straddle Packer Testing and FLUTe Profiling for Hydraulic Testing in Fractured Rock

Boreholes." *Journal of Hydrology* 524: 439–54.

Quiroga, R. Quian, A. Kraskov, T. Kreuz, and P. Grassberger. 2002. "Performance of Different Synchronization Measures in Real Data: A Case Study on Electroencephalographic Signals." *Physical Review E* 65(4): 041903.

Rahmati, Omid, Seyed Amir Naghibi, Himan Shahabi, Dieu Tien Bui, Biswajeet Pradhan, Ali Azareh, Elham Rafiei-Sardooi, Aliakbar Nazari Samani, and Assefa M. Melesse. 2018. "Groundwater Spring Potential Modelling: Comprising the Capability and Robustness of Three Different Modeling Approaches." *Journal of Hydrology* 565: 248–61.

Reimus, Paul W. 1995. "Transport of Synthetic Colloids through Single Saturated Fractures: A Literature Review". New Mexico. (https://digital.library.unt.edu/ark:/67531/metadc793343/: accessed July 11, 2019)

Rodrigues, Sandrina, and Sarah Dickson. 2014. "A Phenomenological Model for Particle Retention in Single, Saturated Fractures." *Groundwater* 52(2): 277–83.

Ryan, Joseph N., and Menachem Elimelech. 1996. "Colloid Mobilization and Transport in Groundwater." *Colloids and Surfaces A* 107(95): 1–56.

Schiperski, Ferry, Johannes Zirlewagen, and Traugott Scheytt. 2016. "Transport and Attenuation of Particles of Different Density and Surface Charge: A Karst Aquifer Field Study." *Environmental Science and Technology* 50(15): 8028–35.

Schreiber, S., J.M. Fellous, D. Whitmer, P. Tiesinga, and T.J. Sejnowski. 2003. "A New Correlation-Based Measure of Spike Timing Reliability." *Neurocomputing* 52–54: 925–31.

Shakas, Alexis, Niklas Linde, Ludovic Baron, Olivier Bochet, Olivier Bour, and Tanguy Le Borgne. 2016. "Hydrogeophysical Characterization of Transport Processes in Fractured Rock by Combining Push-Pull and Single-Hole Ground Penetrating Radar Experiments." *Water Resources Research* 52: 938–53.

Shapiro, A M. 2002. "Fractured-Rock Aquifers; Understanding an Increasingly Important Source of Water. " *USGS Fact Sheet 112-02*.

Snow, D. T. 1970. "The Frequency and Apertures of Fractures in Rock." *International Journal of Rock Mechanics and Mining Sciences & Geomechanics Abstracts* 7(1): 23–40.

Somogyvári, Márk, Mohammadreza Jalali, Santos Jimenez Parras, and Peter Bayer. 2017. "Synthetic Fracture Network Characterization with Transdimensional Inversion." *Water Resources Research* 53(6): 5104–23.

Sousa Neto, Vicente de Oliveira, Paulo de Tarso Cavalcante Freire, and Ronaldo Ferreira do Nascimento. 2019. "Groundwater Remediation Using Nanomaterials." *In Nanomaterials Applications for Environmental Matrices*, eds. Ronaldo Fereira do Nascimento, Odair Pastor Ferreira, Amauri Jardim De Paula, and Vicente de Oliveira Sousa Neto. Elsevier, 381–402.

Stoll, M., F. M. Huber, E. Schill, and T. Schäfer. 2017. "Parallel-Plate Fracture Transport Experiments of Nanoparticulate Illite in the Ultra-Trace Concentration Range Investigated by Laser-Induced Breakdown Detection (LIBD)." *Colloids and Surfaces A: Physicochemical and Engineering Aspects* 529(1): 222–30.

Stoll, M., F. M. Huber, M. Trumm, F. Enzmann, D. Meinel, A. Wenka, E. Schill, and T.

Schäfer. 2019. “Experimental and Numerical Investigations on the Effect of Fracture Geometry and Fracture Aperture Distribution on Flow and Solute Transport in Natural Fractures.” *Journal of Contaminant Hydrology* 221: 82–97.

Syngouna, Vasiliki I, and Constantinos V Chrysikopoulos. 2013. “Cotransport of Clay Colloids and Viruses in Water Saturated Porous Media.” *Colloids and Surfaces A: Physicochemical and Engineering Aspects* 416: 56–65.

Verwey, E. J. W., and J. TH. G. Overbeek. 1984. Theory of Stability of Lyophobic Colloids. Elsevier, Amsterdam.

Vesper, Dorothy J. 2019. “Contamination of Cave Waters by Heavy Metals.” *In Encyclopedia of Caves*, eds. William B. White, David C. Culver, and Tanja Pipan. Academic Press, 320–25.

Vitale, Sarah A., Gary A. Robbins, and Edwin Romanowicz. 2019. “Identifying Cross-Well Fracture Connections Using the Dissolved Oxygen Alteration Method.” *Journal of Hydrology* 572: 781–89.

Wang, Chaozi et al. 2019. “Particle Tracer Transport in a Sloping Soil Lysimeter under Periodic, Steady State Conditions.” *Journal of Hydrology* 569(June 2018): 61–76.

Wang, Tao, Yuanyuan Liu, Jiajia Wang, Xizhi Wang, Bin Liu, and Yingxu Wang. 2019. “In-Situ Remediation of Hexavalent Chromium Contaminated Groundwater and Saturated Soil Using Stabilized Iron Sulfide Nanoparticles.” *Journal of Environmental Management* 231: 679–86.

Wang, Wendong, Kaijie Zhang, Yuliang Su, Meirong Tang, Qi Zhang, and Guanglong Sheng. 2019. “Fracture Network Mapping Using Integrated Micro-Seismic Events

Inverse with Rate-Transient Analysis." *In International Petroleum Technology Conference,* Beijing, China.

Wang, Xiaoguang, Abderrahim Jardani, and Hervé Jourde. 2017. "A Hybrid Inverse Method for Hydraulic Tomography in Fractured and Karstic Media." *Journal of Hydrology* 551: 29–46.

White, William B. 2019. "Hydrogeology of Karst Aquifers." *In Encyclopedia of Caves,* eds. William White, David Culver, and Tanja Pipan. Elsevier Inc., 537–45.

WWAP (United Nations World Water Assessment Programme), 2015. "The United Nations World Water Development Report 2015: Water for a Sustainable World." *Paris, UNESCO*.

Yang, Junwei, Mengtuan Ge, Qiang Jin, Zongyuan Chen, and Zhijun Guo. 2019. "Co-Transport of U(VI), Humic Acid and Colloidal Gibbsite in Water-Saturated Porous Media." *Chemosphere* 231: 405–14.

Yao, Kuan Mu, Mohammad T. Habibian, and Charles R. O'Melia. 1971. "Water and Waste Water Filtration: Concepts and Applications." *Environmental Science and Technology* 5(11): 1105–12.

Zhang, Wei, Xiangyu Tang, Noam Weisbrod, and Zhuo Guan. 2012. "A Review of Colloid Transport in Fractured Rocks." *Journal of Mountain Science* 9(6): 770–87.

Zvikelsky, Ori, and Noam Weisbrod. 2006. "Impact of Particle Size on Colloid Transport in Discrete Fractures." *Water Resources Research* 42(12): 1–12.

Chapter 2

HYDRAULIC CONNECTION IDENTIFICATION IN FRACTURED AQUIFERS: A STOCHASTIC EVENT SYNCHRONY-BASED FRAMEWORK

ABSTRACT

Several approaches are commonly applied to modeling fractured aquifers, including discrete fracture networks and stochastic continuums. However, vast and accurate input data are required for these models to facilitate understanding and enable prediction in the complex physical systems they represent, which are necessary in the development of sound planning, management, and remediation strategies. The extensive resources required to collect such data are often prohibitive. The present study addresses this issue by utilizing the coherence between solute transport in a fracture and the lagged interdependence between two time series through a stochastic event synchrony (SES) technique. A SES-based framework was developed and applied to solute breakthrough curves obtained *i*) analytically at different locations along a single, synthetic fracture both with and without matrix diffusion; and, *ii*) numerically at the outlets of a synthetic, impervious fracture network. In all cases, the framework was capable of accurately mapping the hydraulic connections represented by a direct path between the locations considered. The framework was also capable of identifying the hydrogeologic characteristics within each connection (i.e., flow velocity or its relationship to the dispersion coefficient). This framework is expected to

significantly reduce the extensive resources required to identify the hydraulic connections within complex fractured aquifers. Additionally, the SES-based hydraulic connections identified may represent an additional constraint within other fracture network generation approaches to enhance their reliability. This study is the first in the field of hydrogeology to adopt synchronization analysis and is expected to open the gate for using SES to address related problems.

Keywords: Synchronization Analysis, Fractured Aquifers, Hydraulic Connection

2.1. INTRODUCTION

Understanding groundwater flow and contaminant transport in fractured aquifers is of critical importance to resource extraction (e.g., potable water, fracking) and waste management (e.g., industrial wastewater, nuclear waste, carbon sequestration) (Singhal and Gupta 2010), as they provide source water to support these activities and storage for the wastes they produce (Shapiro 2002). Although open, connected fractures in these aquifers represent only a small fraction of the porosity, they are the primary conduits for groundwater and contaminants (NRC, 1996; Tsang et al. 1998). Simulating groundwater flow and contaminant transport in fractured aquifers is challenging due to the heterogeneous nature of fracture characteristics, which often vary significantly within short distances (Dorn et al. 2013). The development of effective flow and transport models in fractured aquifers requires adequate characterization at the scale of a single fracture (e.g., location, length, size, orientation) and at the network scale (e.g., statistical distributions of fracture properties, connectivity, fracture density) (Dorn et al. 2013). However, it is prohibitive to obtain these characteristics for each individual fracture in a network; and therefore, stochastically generated fracture networks based on data collected from field and laboratory investigations are typically adopted for model development (Somogyvári et al. 2017).

Extensive research has been conducted over the past several decades to develop effective field-based techniques for the hydraulic and geometric

characterization of individual fractures, the surrounding rock matrix, and the network (e.g., Burbey 2010; Alexis Shakas et al. 2016; Kang et al. 2016; Klammler et al. 2016; A. Shakas et al. 2018; Klepikova et al. 2018; Persaud et al. 2018; Ren et al. 2018; Vitale et al. 2019; Chandra et al. 2019; Hsu et al. 2019). These techniques can be classified into (Berkowitz 2002): *i*) hydraulic tests (e.g., packer and slug tests); *ii*) tracer tests (e.g., solute, heat); and *iii*) geophysical techniques (e.g., seismic methods, ground penetrating radar), all of which can be applied within or between boreholes in conjunction with visual inspection of cores and outcrops, and areal photographs. Numerous field-based characterization techniques for fractured aquifers have been presented (NRC 1996, 2015) with the consensus being that these methods aim at measuring the response to the presence of fractures (i.e., hydraulic connections) rather than mapping the physical fractures (Berkowitz 2002). Since field-based approaches only provide information about fractures that intersect boreholes, the heterogenous nature of fractured aquifers requires extensive resources to conduct comprehensive and detailed field investigations. Therefore, field data are often limited, and are subsequently extrapolated to the whole aquifer through generating stochastically conditioned fracture networks (e.g., Dorn et al. 2013; Klepikova et al. 2014; Somogyvári et al. 2017). However, this is an iterative, and therefore computationally expensive, approach. Additionally, it is not always appropriate to extrapolate characteristics from one part of an aquifer to another due to the heterogeneous nature of fractured aquifers.

It is postulated herein that a small subset of the aforementioned field-based approaches can be utilized to map fracture networks directly by evaluating the interdependence between temporally varying data (i.e., time series) acquired from several locations within the aquifer. However, classic correlation measures (e.g., Kendall's tau coefficient, Spearman's rank correlation coefficient) cannot be used to evaluate the interdependence in fracture networks as they cannot adequately address the lag between temporally varying variables. A more appropriate method for evaluating interdependence is by measuring the degree of synchronization, based on the fact that the perturbation of an ambient condition (e.g., pressure, solute concentration, temperature) at a specific location will cause an effect at a downstream location(s), after some time lag, if the two locations are hydraulically connected either directly (i.e., through a fracture) or indirectly (i.e., both locations are part of the same fracture network). The resulting fracture map then represents possible hydraulic connections, rather than the physical fractures, between the locations from which the data were collected. Different synchronization measures have been discussed in detail in earlier studies (e.g., JuNG Hsu, 1992; Quiroga et al. 2002; Schreiber et al. 2003), and include nonlinear interdependences, phase synchronization, mutual information, cross-correlation, and coherence function. Some of these measures are only suitable for linearly related time series, while others do not use the series values or do not distinguish between the different values within each series. Dauwels et al. (2009) presented stochastic event synchrony (SES) as an alternative approach for assessing the synchronization between two

time series. In the SES, specific values/events are chosen from each series and their occurrence times are aligned iteratively. The reliability of the SES-based synchrony is determined by the fraction of events aligned at a specific time lag, and its precision is measured by the accuracy of alignment of these events at that time lag. Despite the usefulness of synchronization analysis in assessing the interdependence between two or more time series, its application in the field of water resources has been vey limited to date (i.e., Malik et al. 2010, 2012).

The objective of the present study is to develop a SES-based framework for identifying hydraulic connections within fractured aquifers based on solute concentration data, obtained over time and space, through: *i*) confirming the ability of SES to identify hydraulic connections in a single fracture based on solute transport; *ii*) exploring the relationship between SES measures (i.e., reliability and precision) and the transport parameters within a single fracture; and, *iii*) demonstrating the application of the SES-based framework to multiple locations within a fracture network to determine the hydraulic connections between these locations, and thereby develop a fracture network map. This technique is expected to significantly reduce the extensive field-based resources typically required to identify hydraulic connections within fractured aquifers. SES can also be combined with discrete fracture network models by adding a constraint to represent the SES-based connections when generating stochastically-based fracture networks.

2.2. METHODS

2.2.1. SOLUTE TRANSPORT IN FRACTURES

In fractured aquifers, groundwater flow and solute transport occur in both fractures and the surrounding rock matrix (Bear et al. 1993; Rausch et al. 2005). While advection and dispersion are primarily responsible for solute transport within the fractures, molecular diffusion is the dominant transport mechanism in the matrix (Bear et al. 1993; Rausch et al. 2005). Other mechanisms influencing solute transport in fractured systems include sorption and decay (Bear et al. 1993). Modeling solute transport in these systems requires coupling the solute behavior in fractures with that in the rock matrix; the resulting coupled governing equations can be solved analytically (Tang et al. 1981; Sudicky and Frind 1982; Maloszewski and Zuber 1990; Liu et al. 2017; Meng et al. 2018) or numerically (Abdel-salam and Chrysikopoulos 1995; James and Chrysikopoulos 1999; Natarajan 2014; Brutz and Rajaram 2017; He et al. 2017; Suzuki et al. 2018) in different configurations of a single fracture under specified boundary condition at the inlet (i.e., constant concentration, constant flux, instantaneous or time-dependent function). When the solute is released into the fracture following a time-dependent function, the breakthrough curve (BTC) at any location along the fracture is the convolution of that function and the analytical solution of an instantaneous injection (Bodin et al. 2007). Analytical solutions developed to date have not been confirmed at the network scale, and thus numerical techniques are typically adopted (Bodin et al.

2007; Makedonska et al. 2015; Ngo et al. 2017). Only the instantaneous or time-dependent injection schemes are of interest in the present study, as these conditions represent the typical procedures of field-based tracer tests.

When a conservative solute is introduced to a fracture with an impervious matrix (i.e., no matrix diffusion), the injected mass is preserved along the fracture. However, hydrodynamic dispersion causes the residence time of each solute particle between any two locations in the fracture to be a random variable with a lognormal probability density function (Bodin and Delay 2001). The theoretical mean residence time ($\bar{t}$) is the average time lag between the appearance of the injected mass at the two locations, and depends on the distance between these locations (d) and the flow velocity (u) as follows:

$$\bar{t} = \frac{d}{u} \qquad (2-1)$$

However, matrix diffusion cannot be neglected when the matrix is permeable; solute may diffuse into or out of the matrix depending on the direction of the concentration gradient across the fracture wall. When matrix diffusion is considered, the BTC at any location along the fracture can be expressed as the convolution of two functions: *i*) the BTC resulting from an instantaneous injection of a conservative solute when matrix diffusion is negligible; and, *ii*) a retention function representing the fracture-matrix system response to the solute input function when hydrodynamic dispersion along the fracture is neglected (Cvetkovic et al. 1999; Hassan et al. 2001; Liu et al. 2017). The migration of solute particles

between two points in a fracture is typically governed by advection and dispersion only, even when matrix diffusion is not negligible. However, calculating $\bar{t}$ according to Equation (2-1) is not valid in this case as it does not account for fracture-matrix interactions. The retention function, representing the matrix response to the input source, acts as a decay function and results in a heavy-tailed BTC. Therefore, matrix diffusion can be represented by a retardation factor (*R*) that delays solute migration in the fracture (Bodin and Delay 2001), and depends on *u*, *d*, the hydrodynamic dispersion coefficient (*D*), the matrix porosity (θ), and the effective diffusion coefficient (D_e). Subsequently, $\bar{t}$ is estimated as follows (Bodin and Delay 2001):

$$\bar{t} = \frac{d}{u} + R \times \frac{d}{u} \times erfc\left[\Omega\left(\frac{4d^3}{uD}\right)^{\frac{1}{4}}\right] \qquad (2-2)$$

where $\Omega = \sqrt{\theta D_e}/b$, and *b* is the fracture aperture.

The same concept is utilized when the solute interacts with impervious fracture wall, however, the mass retained is adsorbed onto the surface of the fracture rather than within the matrix. Another retardation factor is introduced in this case, based on the relationship between the sorbed and non-sorbed fractions of the solute. A more complex transport scenario includes a reactive solute moving along a fracture with permeable surfaces which combines advection, hydrodynamic dispersion, sorption, and matrix diffusion.

In all cases, $\bar{t}$ is the theoretical time lag between the centers of mass (CM) of two BTCs at two distinct locations along the fracture, as shown in Figure 2-1, considering all possible transport mechanisms. Such BTCs can be obtained from a field-based tracer test, and the interdependence between them can be used to reveal the hydraulic connection between the two locations. However, such a hydraulic connection will always be represented by a straight path connecting the two locations.

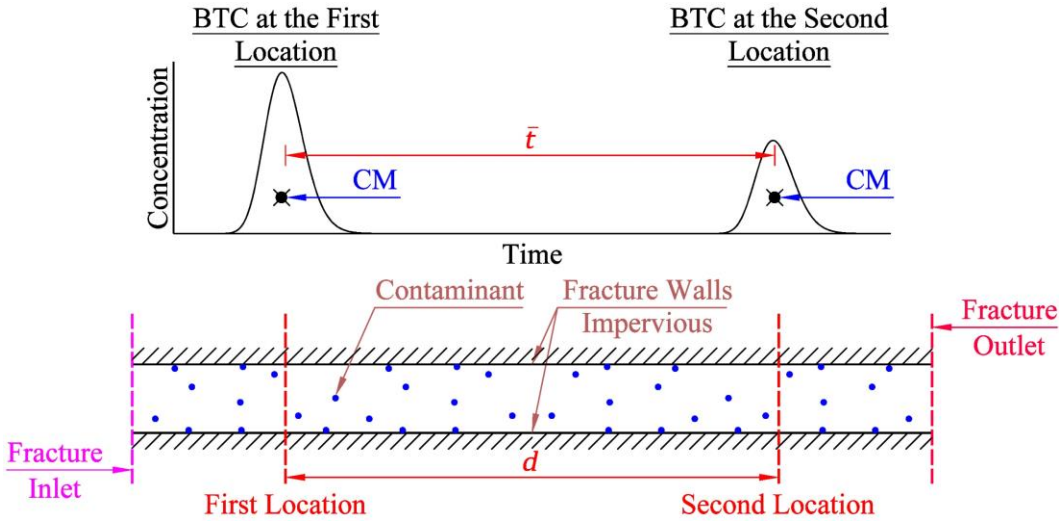

Figure 2-1: Typical BTCs at two different locations along a fracture when the solute is introduced to the fracture either instantaneously or over a specified time

2.2.2. STOCHASTIC EVENT SYNCHRONY

Synchronization is defined as the agreement or correlation in time between different processes (Boccaletti et al. 2002), and it indicates the interdependence between systems coupled through such processes (Boccaletti et al. 2018). Different synchronization measures have been developed over the past two centuries, each of which has its own strengths and limitations. Stochastic event synchrony (SES) was

first introduced by Dauwels et al. (2009) to overcome the limitations of other measures, and it can be used to uncover the interdependence between two or more linearly or nonlinearly coupled time series. The first step in the application of SES is to identify specific events from each time series (e.g., maximum values, minimum values, or values larger than a specific threshold), and subsequently align (or pair) these events at a pre-defined time lag. The fraction of paired events, known as the coincidence ratio (ρ), indicates the reliability of pairing/synchronization between the two series. Higher values of ρ indicate that more events from the first series are replicated in the second one at the chosen lag. However, the paired events may not be aligned exactly at that lag, leading to a time jitter (τ) as shown in Figure 2-2. Therefore, two synchronized time series can be characterized by higher ρ and lower τ. The events shown in Figure 2-2 can represent any processes such as signals transmitted through the human neural system or concentrations of a solute observed at two locations within a fractured network. The latter example is the focus of the present study. It must be noted here that concentration-based events may find pairs where hydraulic connections do not exist. Thus, more confidence can be placed in the legitimacy of mass-based event pairs as mass represents the cumulation of concentration over time.

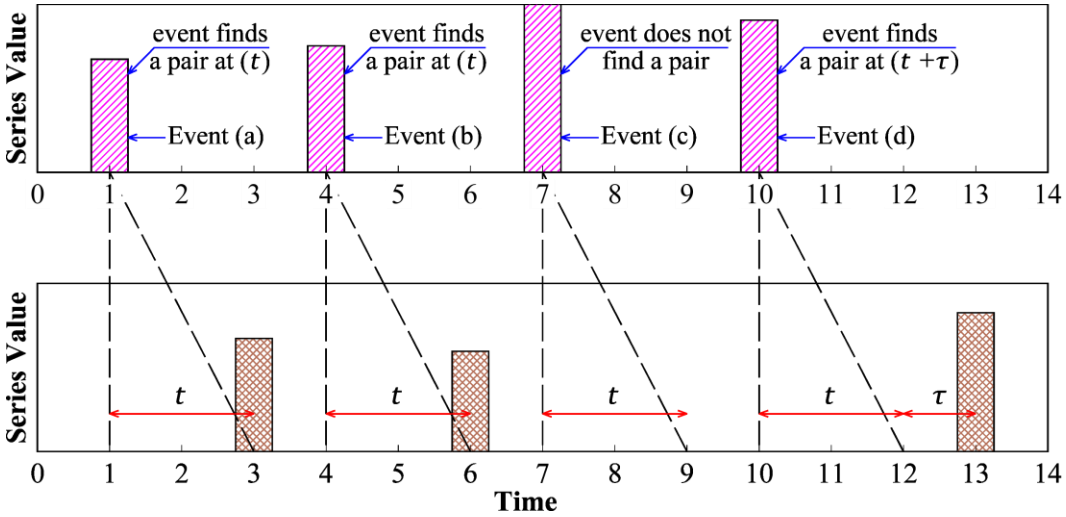

Figure 2-2: Illustration of time lag and jitter where the top panel represents events selected from the first series, and the bottom panel represents events selected the second one

2.2.3. THE SES-BASED FRAMEWORK

A single and unique hydraulic connection (i.e., a fracture) between two locations in a fractured aquifer represents a transmission path for a solute; however, the distance (x) travelled by each solute particle in that fracture within a time (dt) is not deterministic due the range of mechanisms influencing transport (e.g., hydrodynamic dispersion, matrix diffusion). Therefore, dt between two specific locations (i.e., x is constant) is a random variable described as (Bodin et al. 2007):

$$dt = dt_{con} + \left[\frac{\Omega x}{u \times erfc^{-1}(U_{01})}\right]^2 \qquad (2-3)$$

where dt_{con} is a lognormal random number with a mean of x/Ru and a variance of $2Dx/u^3$, and U_{01} is a uniform random number between 0 and 1. The first term on the right-hand-side of Equation (2-3) represents the travel time imposed by advection, dispersion, and matrix diffusion, and the second term represents the solute particle

residence time within the rock matrix. The mean value of *dt* is $\bar{t}$ calculated using Equation (2-1) when matrix diffusion is neglected, or Equation (2-2) when matrix diffusion is considered. The BTC at any location along the fracture is the relationship between the concentration of solute particles arriving at that location and time. The CM of a BTC represents the mean residence time (i.e., $\bar{t}$) of all solute particles migrating from the point at which they were released to that location, and the BTC spreading can be described by higher moments of *dt*.

Synchronization between two BTCs (i.e., BTC 1 and BTC 2) acquired from two locations (i.e., location 1 and location 2) along a fracture can be assessed through discretizing them into N_t and L_t segments, respectively. Subsequently, the arrival of a mass $M_2(t_k; \bar{t}_k)$ at location 2 following its release at location 1 as $M_1(t_j; \bar{t}_j)$ is assessed, where t_j is the arrival time of the j^{th} segment of BTC 1 (j = 1, 2, …., N_t), t_k is the arrival time of the k^{th} segment of BTC 2 (k = 1, 2, …., L_t), $\bar{t}_j$ is the mean travel time of all solute particles arriving at location 1 up to time t_j (i.e., CM_j), $\bar{t}_k$ is the mean travel time of all solute particles arriving at location 2 up to time t_k (i.e., CM_k), and M_m is the mass arriving at the m^{th} location (m = 1, 2 in this example), as shown in Figure 2-3. After its release at location 1, the mass $M_1(t_j; \bar{t}_j)$ migrates along the fracture and is expected to reach location 2 after $\bar{t}$ as $\overline{M_2}(t_j + \bar{t}; \bar{t}_j + \bar{t})$. When matrix diffusion is negligible, masses $\overline{M_2}(t_j + \bar{t}; \bar{t}_j + \bar{t})$ and $M_1(t_j; \bar{t}_j)$ must be the same; whereas, when matrix diffusion is considered, the two masses will be mathematically related through available analytical solutions (e.g., Tang et al. 1981;

Maloszewski and Zuber 1990). The j^{th} segment of BTC 1 is paired with the k^{th} segment of BTC 2 if $M_2(t_k; \bar{t}_k) = \overline{M_2}(t_j + \bar{t}; \bar{t}_j + \bar{t})$. Subsequently, the k^{th} segment of BTC 2 is referred to as the n^{th} segment. While the time lag between the two BTCs is theoretically $\bar{t}$, the actual lag between two paired segments (t_{jn}) is $\bar{t}_j - \bar{t}_n$ which may be different from $\bar{t}$, leading to a time jitter (τ_{jn}) equal to $t_{jn} - \bar{t}$. During a field-based tracer experiment, t_j and t_k represent the sampling times at locations 1 and 2, respectively. In addition, prior knowledge of the volumetric flow rate (Q) is required to calculate the mass $M_m(t_i, \bar{t}_i)$ at time (t_i) based on the observed BTC. Since Q is often unknown prior to proper characterization of a fractured aquifer, time integral of the BTC can be used as an indicator of $M_m(t_i, \bar{t}_i)$, where the CM of that portion of the BTC is at $\bar{t}_i$.

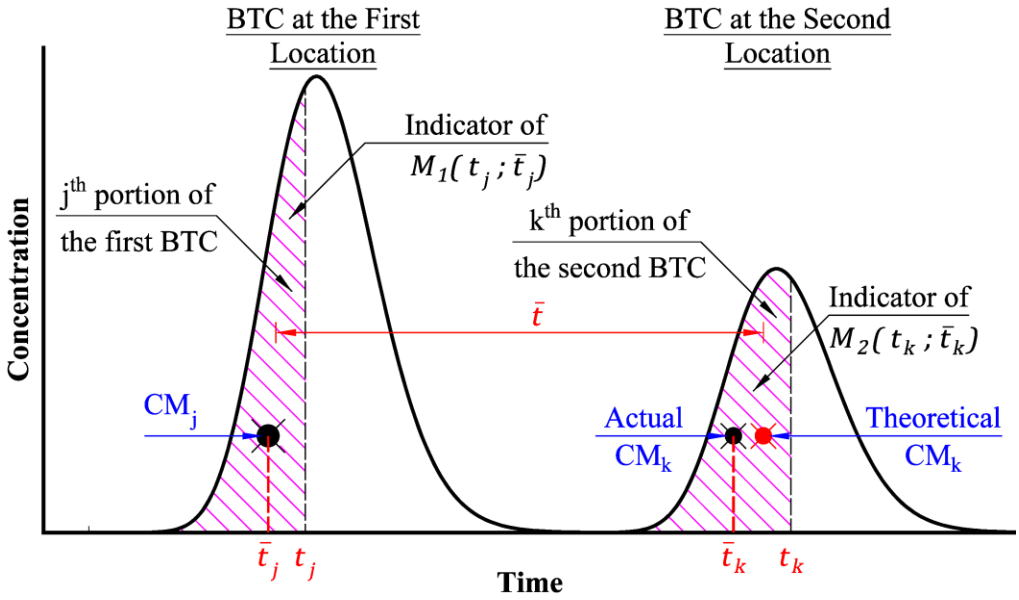

Figure 2-3: Application of SES to BTCs obtained at two locations along a fracture

The application of SES utilizing two BTCs results in a set of paired segments (N), each of which is lagged by time t_{jn} that differs from $\bar{t}$ by a jitter τ_{jn}. The actual mean lag ($\bar{t}_{act}$) and average jitter ($\bar{\tau}$) between the two BTCs are thus, respectively:

$$\bar{t}_{act} = \frac{1}{N}\sum_{j=1}^{N}\left(\bar{t}_j - \bar{t}_n\right) \qquad (2-4a)$$

$$\bar{\tau} = \frac{1}{N}\sum_{j=1}^{N}\left(t_{jn} - \bar{t}\right) \qquad (2-4b)$$

The degree of synchronization between the two BTCs at $\bar{\tau}$ and $\bar{t}_{act}$, expressed by ρ, is the ratio between N and N_t. For a hydraulic connection to exist between the locations where the BTCs are acquired, ρ must be equal to or exceed a threshold value, ρ_{acc}, calculated by:

$$\rho_{acc} = \boldsymbol{P}\left[\bar{t}_{act} - \min\left(\tau_{jn}\right) \le dt \le \bar{t}_{act} + \max\left(\tau_{jn}\right)\right] \qquad (2-5)$$

where $\boldsymbol{P}$ represents the probability that the travel time between locations 1 and 2 is within the time interval $\left[\bar{t}_{act} - \min\left(\tau_{jn}\right)\right.$ and $\left.\bar{t}_{act} + \max\left(\tau_{jn}\right)\right]$. In other words, $\boldsymbol{P}$ represents the fraction of solute particles (expressed through the number of segments of BTC 1 (i.e., N)) expected to migrate from location 1 to location 2 within that time interval under the transport mechanisms considered. For a conservative solute not subject to matrix diffusion, dt is lognormally distributed with a mean of x/u and a variance of $2Dx/u^3$ (Bodin and Delay 2001), and subsequently, ρ_{acc} can be evaluated analytically. However, the statistical distribution of dt is not well known when matrix diffusion is considered. In this

case, for simplicity, the residence time in the rock matrix (t_m) is assumed to be the same for all solute particles and is given by:

$$t_m = R \times \frac{x}{u} \times erfc\left[\Omega\left(\frac{4x^3}{uD}\right)^{1/4}\right] \qquad (2-6)$$

Subtracting t_m from each term on the right-hand side of Equation (2-5) yields a modified expression to estimate dt, $dt_{con,}$ which is lognormally distributed with a mean of x/Ru and a variance of $2Dx/u^3$, and therefore, ρ_{acc} can be evaluated analytically. When a hydraulic connection is detected (i.e., $\rho \geq \rho_{acc}$), the coupling of Equations (2-4a) and (2-4b) enables estimating the flow velocity (u) when the matrix diffusion is negligible, or provides a relationship between u and D when the matrix properties (i.e., D_e and θ) and fracture aperture (i.e., b) are known. Based on the discussion above, a SES-based framework is proposed to assess the presence of a hydraulic connection between two locations along a single fracture, and the application procedures of this framework are shown in Figure 2-4.

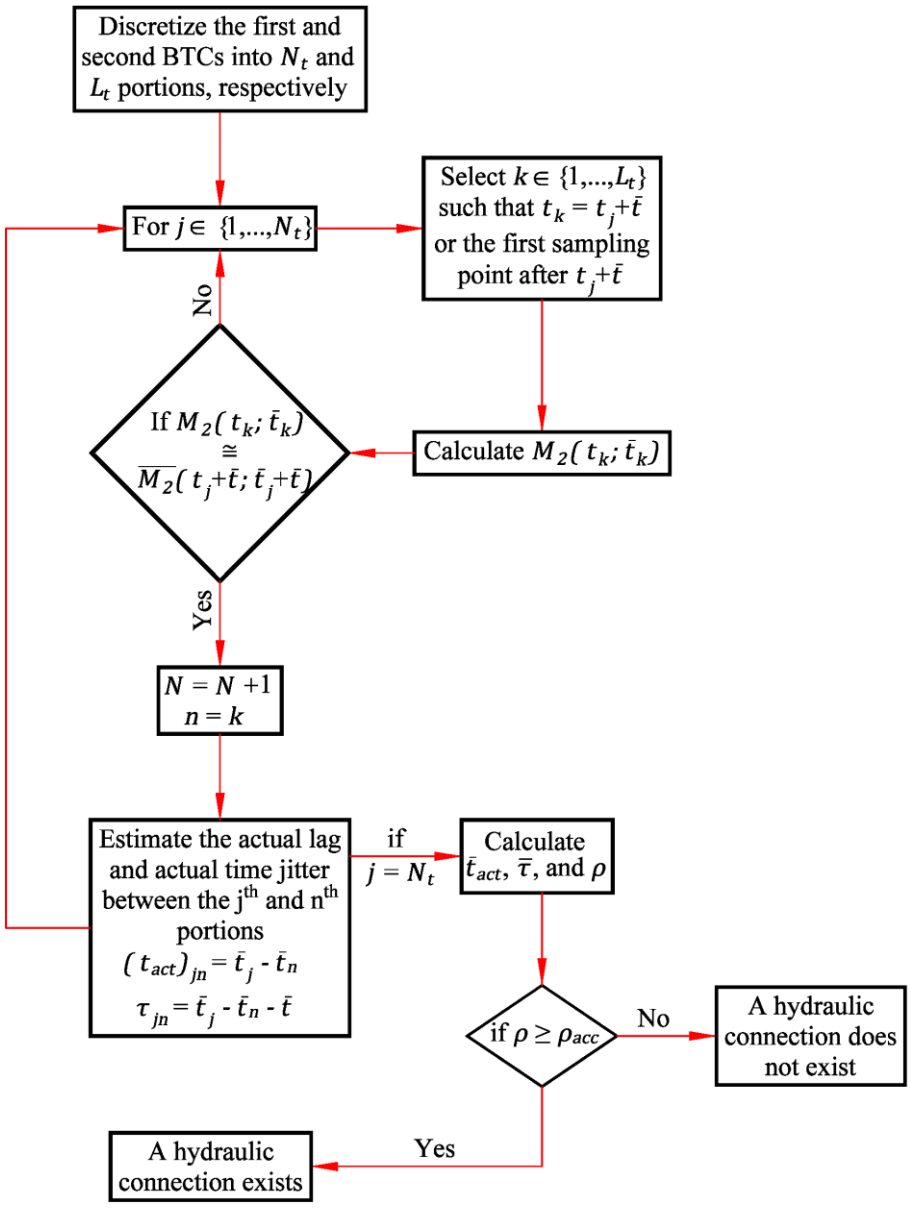

Figure 2-4: The application procedures of the SES-based framework proposed to asses the presence of a hydraulic connection between two locations along a single fracture using BTCs acquired at these locations

2.3. RESULTS AND DISCUSSION

Three different cases were chosen to demonstrate the efficacy of the SES-based framework in identifying hydraulic connections: 1) a single, synthetic

fracture with an instantaneous solute injection at the inlet under both pervious and impervious matrix conditions; 2) a single, synthetic fracture with an impervious matrix and an exponentially decaying solute release at the inlet; and, 3) a synthetic fracture network with an impermeable matrix and exponentially decaying solute releases at two distinct points along the inlet boundary.

The SES-based framework was first applied to a single, synthetic fracture with specified hydrogeologic characteristics to assess its efficacy in identifying interdependence between BTCs acquired from two locations along that fracture, thus demonstrating the existence of a hydraulic connection between these locations. The hydrogeologic characteristics of the synthetic fracture is (Bodin and Delay 2001): length (L) = 2 m, b = 200 μm, u = 5x10^{-6} m/s, D = 5x10^{-7} m^2/s. For the case with a permeable matrix, θ = 0.35 and D_e = 10^{-13} m^2/s (Tang et al. 1981) were used. A mass of 100 g of a conservative solute was released at the fracture inlet through an instantaneous injection and BTCs were calculated at 0.2L, 0.4L, 0.6L, 0.8L, and L using the analytical solutions reported in (Kreft and Zuber 1978) and (Maloszewski and Zuber 1990) for impermeable and permeable matrix conditions, respectively as shown in Figure 2-5.

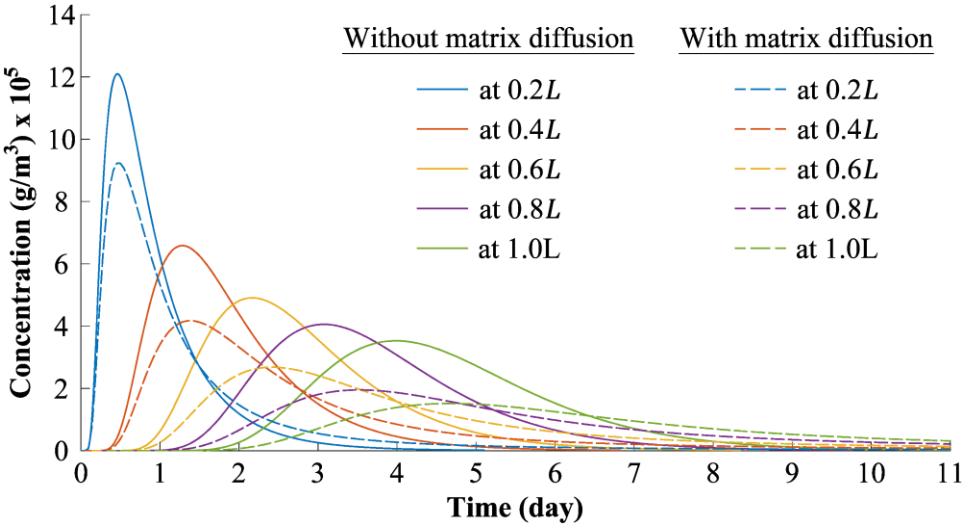

Figure 2-5: BTCs calculated analytically at various locations along a synthetic fracture with and without matrix diffusion

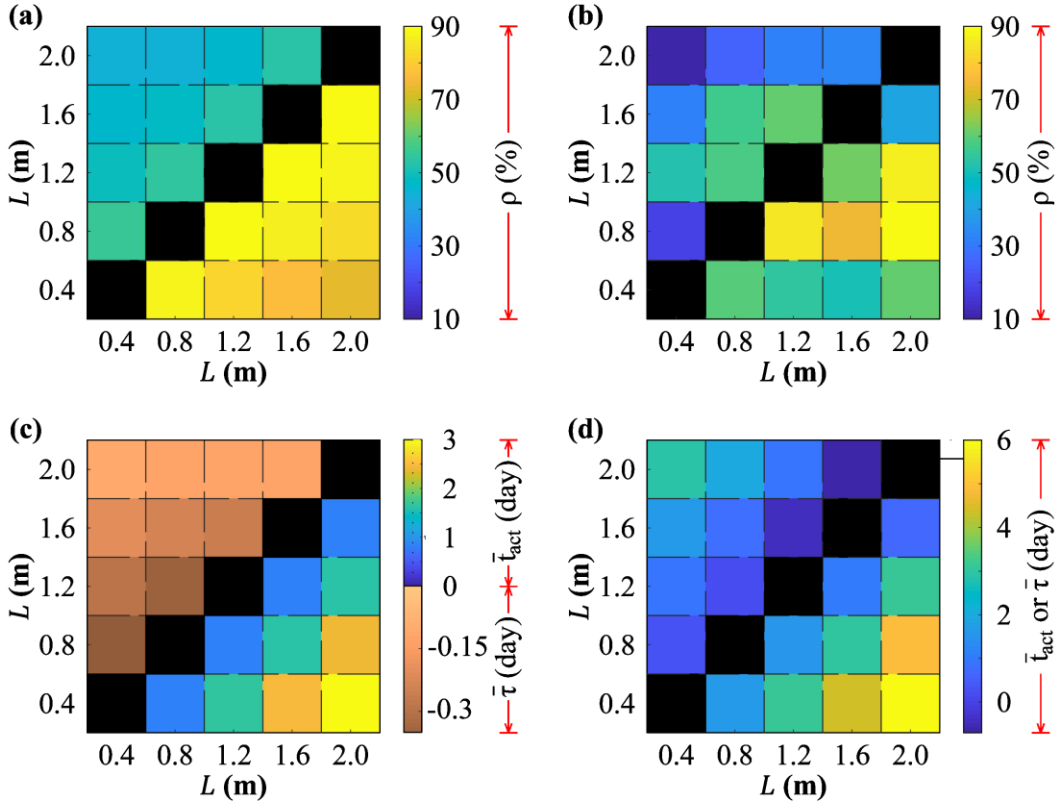

Figure 2-6: Synchronization reliability (i.e., ρ compared to ρ_{acc}) for (a) no matrix diffusion, and (b) matrix diffusion is considered, and precision (i.e., $\bar{t}_{act}$ and $\bar{\tau}$) values for (c) no matrix diffusion, and (d) with matrix diffusion

A second case is employed to assess the efficacy of the SES-based framework under different boundary conditions. In this case, 100 g of a conservative solute was introduced at the inlet of a single fracture (with impervious walls) through an exponentially decaying release, exp $(-\gamma t)$ where γ = 1x10^{-5} s^{-1} is the decay rate (Bodin et al. 2003). Peclet numbers (P_e) ranging from 0.2 to 100 were adopted, and the corresponding effluent BTC was estimated using the Time Domain Random Walk (TDRW) approach (Bodin and Delay 2001). BTCs at the inlet and outlet (represented by BTC 1 and 2, respectively) were discretized into 500 segments (i.e., N_t = L_t = 500) for each P_e. The SES-based framework was subsequently applied, and the corresponding ratios ρ/ρ_{acc} and $(\bar{t}_{act} - \bar{\tau})/\bar{t}$ are shown in Figure 2-7. The SES-based framework effectively detected the hydraulic connection between the fracture inlet and outlet for the range of P_e investigated as indicated by the fact that ρ/ρ_{acc} is consistently greater than 1. Furthermore, $(\bar{t}_{act} - \bar{\tau})/\bar{t}$ is always equal to 1.0, supporting the use of SES metrics ($\bar{t}_{act}$ and $\bar{\tau}$) to determine the transport parameters (u in this case).

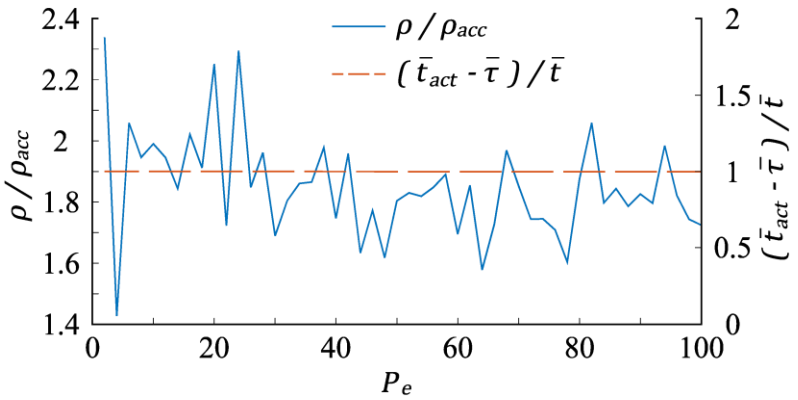

Figure 2-7: Reliability and precision metrics for the case of an exponentially decaying solute release at the inlet of a fracture under a range of P_e

The results from both cases support the efficacy of the SES-based framework in determining hydraulic connections along a single fracture, with and without a permeable matrix, and under different inlet boundary conditions. Of even a greater interest is the ability of the SES-based framework to detect multiple connections within a fracture network. Therefore, a third case using a simple, impermeable, synthetic fracture network within a 2500 m^2 square domain is developed as shown in Figure 2-8a. The fractures are assumed to have equal apertures of 200 μm, and constant heads of 100 m and 99 m are assigned to the inlet (West) and outlet (East) boundaries, respectively. A conservative solute was injected through the inlet boundary following the release scheme described in the previous case (case 2); however, the particles were injected at point 1 prior to point 2 to reduce their coupled interaction in the BTCs at the outlets. The TDRW approach was adopted to simulate solute transport through the synthetic network, and the BTCs at points 3 and 4 on the outlet boundary were obtained as shown in Figure 2-8c. The BTCs at points 1, 2, 3, and 4 were divided into 500 segments, and the SES-based framework was employed. The framework was applied to each point pair twice; the first one (case *i*) included the BTC at a source (i.e., point 1 or 2) and the BTC at an outlet (i.e., point 3 or 4), and the second case (case *ii*) included the BTC at a source (i.e., point 1 or 2) and the combined BTC at the outlet (i.e., mass at points 3 and 4 summed at each time). The resulting synchronization metrics, $\rho = (\rho^{i}, \rho^{ii})$ and the corresponding $\rho_{acc} = (\rho_{acc}^{i}, \rho_{acc}^{ii})$, where the superscripts (*i*) and (*ii*) refer to the case, are shown in Figure 2-8b. For each pair of points, the theoretical time lag (i.e., the

theoretical mean residence time $\bar{t}$) was assumed to be the difference between the CMs of their BTCs. A direct hydraulic connection is assumed to exist between an inlet and an outlet when $\rho^{i} \geq \rho_{acc}^{i}$ and $\rho^{ii} \leq \rho_{acc}^{ii}$, whereas the inlet point is assumed to be directly hydraulically connected to both outlets when $\rho^{ii} \geq \rho_{acc}^{ii}$ and $\rho^{i} \leq \rho_{acc}^{i}$. A zero value of ρ_{acc}^{i}, or ρ_{acc}^{ii}, indicates that there is no probability for the solute particles released at an inlet to exit the domain through either, or both, outlet within the time interval $[\bar{t}_{act} - \min(\tau_{jn})$ and $\bar{t}_{act} + \max(\tau_{jn})]$; therefore, corresponding hydraulic connection(s) is rejected.

The SES-based framework effectively detected the direct hydraulic connections in the synthetic fracture network (see Figure 2-8a). A hydraulic connection was also detected between points 1 and 4, where one does not currently exist (see Figure 2-8b), due to the similarities between the BTCs at points 1 and 4. This connection was subsequently rejected as $\rho_{acc} = 0$ for both cases (*i*) and (*ii*). These results demonstrate the efficacy of the SES-based framework in reconstructing the hydraulic connections within a fracture network. For a larger number of outlets, an optimization technique can be coupled with the SES-based framework to detect the most reliable hydraulic connections.

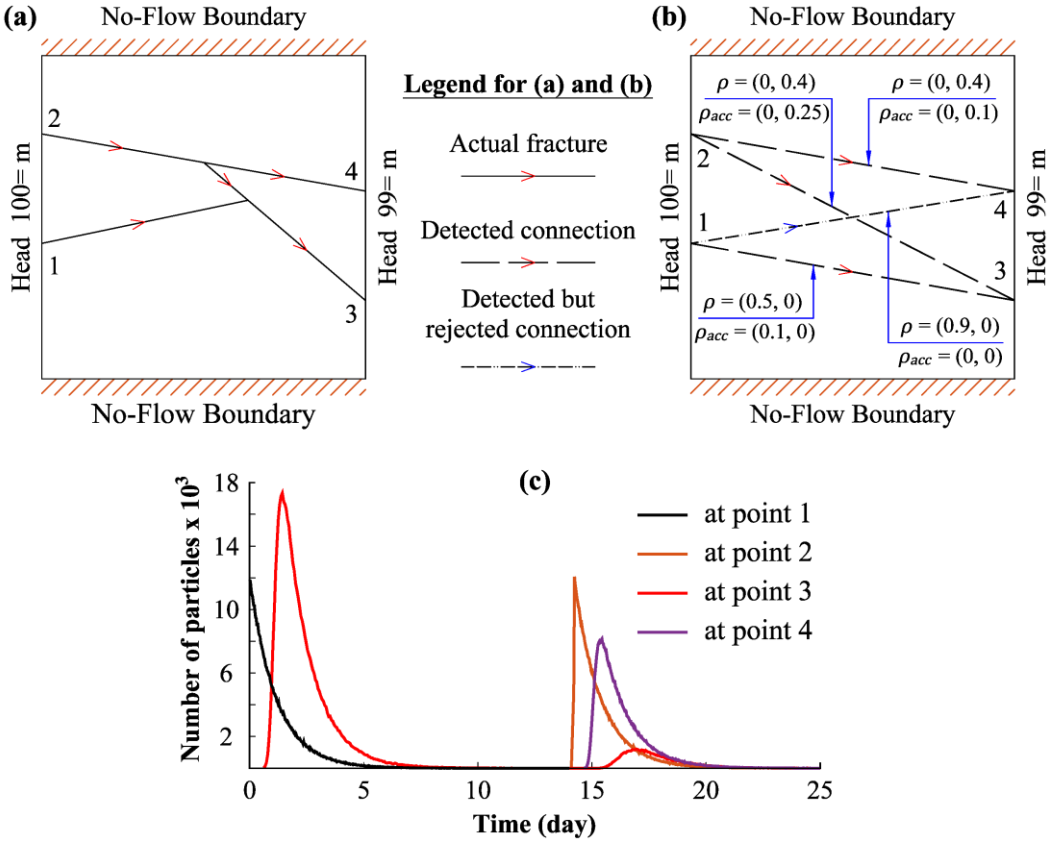

Figure 2-8: Application of the SES-based framework to (a) a synthetic fracture network. The results show (b) hydraulic connections detected based on (c) the BTCs at points 1, 2, 3, and 4

2.4. CONCLUSIONS

The coherence between solute transport in a fracture and time series synchronization enabled the development of a SES-based framework that is able to detect hydraulic connections between two points in a fractured aquifer. The efficacy of the SES-based framework was demonstrated through its ability to map the hydraulic connection(s) based on the solute BTCs at two distinct locations within: *i*) a single, synthetic fracture with an impermeable matrix under instantaneous and exponentially decaying solute releases at the inlet; *ii*) a single synthetic fracture

with permeable matrix under an instantaneous solute injection at the inlet; and *iii*) a fracture network, with an impermeable matrix, under exponentially decaying solute releases at two points along the inlet boundary. Additionally, the SES-based framework is able to determine u or the relationship between u and D for impermeable and permeable matrix conditions, respectively. This SES-based framework was able to map hydraulic connections using sparsely located concentration profiles rather than hydraulic, geometrical, and connectivity data, all of which require far more intensive resources to collect in the field. The hydraulic connections mapped using the SES-based framework can be utilized to condition stochastically generated fracture networks that are typically employed to model these systems, which is necessary to develop effective planning, management, or remediation strategies. This study is the first to introduce the synchronization analysis in the field of hydrogeology and is expected to be the basis for applying the same analysis to solve complex relevant problems in similar systems.

2.5. ACKNOWLEDGEMENT

This research was supported by NSERC through the Canadian Nuclear Energy Infrastructure Resilience under Systemic Risk (CaNRisk) – Collaborative Research and Training Experience (CREATE) and Discovery Grant programs.

2.6. NOTATIONS

b:	Fracture aperture	R:	Retardation factor
d:	Distance between two locations along a fracture	t:	Time lag between two BTCs
D:	Hydrodynamic dispersion coefficient	$\bar{t}$:	Theoretical time lag between two BTCs
D_e:	Effective diffusion coefficient	$\bar{t}_{act}$:	Actual mean lag between two BTCs
dt:	Total particle travel time for a distance x (including residence time within the matrix)		
dt_{con}:	Particle travel time imposed by advection, dispersion, and matrix diffusion		
L:	Fracture length	t_j:	The arrival time of the j^{th} segment of BTC 1
L_t:	Number of segments in the BTC at location 2	$\bar{t}_j$:	Mean travel time of solute particles arriving at location 1 up to time t_j
M_1:	Mass arrival at location 1	t_{jn}:	The actual lag between two paired segments (j and n, respectively)
M_2:	Mass arrival at location 2	t_k:	The arrival time of the k^{th} segment of BTC 2
M_m:	Mass arriving at location m	$\bar{t}_k$:	Mean travel time of solute particles arriving at location 2 up to time t_k
N:	Number of paired events	t_m:	Particle residence time in the rock matrix

N_t:	Number of segments in the BTC at location 1	u:	Flow velocity
$\boldsymbol{P}$:	Probability that particle travel time between locations 1 and 2 is within the time interval $\left[\bar{t}_{act} - \min(\tau_{jn})\right.$ and $\left.\bar{t}_{act} + \max(\tau_{jn})\right]$		
P_e:	Peclet number	U_{01}:	Uniform random number
Q:	Volumetric flow rate	x:	Distance travelled by a particle within a time dt

Greek Letters:

θ:	Matrix porosity
γ:	Decay rate
ρ:	The coincidence ratio
ρ_{acc}:	The threshold of the coincidence ratio
$\bar{\tau}$:	Average time jitter between two BTCs
τ:	Time jitter between two events
τ_{jn}:	Actual time jitter between two paired segments (j and n, respectively)

2.7. ACRONYMS

BTC: Solute breakthrough curve

CM: Center of mass of a BTC

SES: Stochastic event synchrony

TDRW: Time domain random walk

2.8. REFERENCES

Abdel-salam, Assem, and Constantinos V Chrysikopoulos. 1995. "Analysis of a Model for Contaminant Transport in Fractured Media in the Presence of Colloids." *Journal of Hydrology* 165(1–4): 261–81.

Bear, Jacob, Chin-Fu Tsang, and Ghislain de Marsily. 1993. *Flow and Contaminant Transport in Fractured Rock*. San Diego: Academic Press, Inc.

Berkowitz, Brian. 2002. "Characterizing Flow and Transport in Fractured Geological Media: A Review." *Advances in Water Resources* 25(8–12): 861–84.

Boccaletti, S., J. Kurths, G. Osipov, D.L. Valladares, and C.S. Zhou. 2002. "Synchronization of Chaotic Systems." *Physics Reports* 366(1–2): 1–101.

Boccaletti, Stefano, Alexander N. Pisarchik, Charo I. del Genio, and Andreas Amann. 2018. *Synchronization: From Coupled Systems to Complex Networks*. 1st ed. Cambridge University Press.

Bodin, Jacques, and Frederick Delay. 2001. "Time Domain Random Walk Method to Simulate Transport by Advection-Dispersion and Matrix Diffusion in Fracture Networks." *Geophysical research Letters* 28(21): 4051–54.

Bodin, Jacques, Gilles Porel, and Fred Delay. 2003. "Simulation of Solute Transport in Discrete Fracture Networks Using the Time Domain Random Walk Method." *Earth and Planetary Science Letters* 208(3–4): 297–304.

Bodin, Jacques, Gilles Porel, Fred Delay, Fabrice Ubertosi, Stéphane Bernard, and Jean Raynald de Dreuzy. 2007. "Simulation and Analysis of Solute Transport in 2D

Fracture/Pipe Networks: The SOLFRAC Program." *Journal of Contaminant Hydrology* 89(1–2): 1–28.

Brutz, Michael, and Harihar Rajaram. 2017. "Coarse-Scale Particle Tracking Approaches for Contaminant Transport in Fractured Rock." *Applied Mathematical Modelling* 41(1): 549–61.

Burbey, Thomas J. 2010. "Fracture Characterization Using Earth Tide Analysis*." Journal of Hydrology* 380(3–4): 237–46.

Chandra, Subash, Esben Auken, Pradip K. Maurya, Shakeel Ahmed, and Saurabh K. Verma. 2019. "Large Scale Mapping of Fractures and Groundwater Pathways in Crystalline Hardrock by AEM." *Scientific Reports* 9(1): 1–11.

Cvetkovic, V., J. O. Selroos, and H. Cheng. 1999. "Transport of Reactive Tracers in Rock Fractures." *Journal of Fluid Mechanics* 378: 335–56.

Dauwels, J, F Vialatte, T Weber, T Musha, and A Cichocki. 2009. "Quantifying Statistical Interdependence by Message Passing on Graphs-Part I: One-Dimensional Point Processes." *Neural computation* 21: 2152–2202.

Dorn, Caroline, Niklas Linde, Tanguy Le Borgne, Olivier Bour, and Jean-Raynald de Dreuzy. 2013. "Conditioning of Stochastic 3-D Fracture Networks to Hydrological and Geophysical Data." *Advances in Water Resources journal* 62: 79–89.

Hassan, A., K. Pohlmann, and J. Chapman. 2001. "Uncertainty Analysis of Radionuclide Transport in a Fractured Coastal Aquifer with Geothermal Effects." *Transport in Porous Media* 43(1): 107–36.

He, Cairong, Tongke Wang, Zhixue Zhao, Yonghong Hao, Tian Chyi J. Yeh, and Hongbin Zhan. 2017. "One-Dimensional Analytical Solution for Hydraulic Head and Numerical Solution for Solute Transport through a Horizontal Fracture for Submarine Groundwater Discharge." *Journal of Contaminant Hydrology* 206(1): 1–9.

Hsu, Shih Meng, C. C. Ke, Y. T. Lin, C. C. Huang, and Y. S. Wang. 2019. "Unravelling Preferential Flow Paths and Estimating Groundwater Potential in a Fractured Metamorphic Aquifer in Taiwan by Using Borehole Logs and Hybrid DFN/EPM Model." *Environmental Earth Sciences* 78(5): 1–22.

James, Scott C, and V Chrysikopoulos. 1999. "Transport of Polydisperse Colloid Suspensions in a Single Fracture." *Water Resources Research* 35(3): 707–18.

JuNG Hsu, KUANG. 1992. "Time Series Analysis of the Interdependence Among Air Pollutants." *Atmospheric Environment* 26(4): 491–503.

Kang, Peter K., Yingcai Zheng, Xinding Fang, Rafal Wojcik, Dennis McLaughlin, Stephen Brown, Michael C. Fehler, Daniel R. Burns, and Ruben Juanes. 2016. "Sequential Approach to Joint Flow-Seismic Inversion for Improved Characterization of Fractured Media." *Water Resources Research* 52: 903–19.

Klammler, Harald, Kirk Hatfield, Mark A. Newma, Jaehyun Cho, Michael D. Annable, Beth L. Parker, John A. Cherry, and Irina Perminova. 2016. "A New Device for Characterizing Fracture Networks and Measuring Groundwater and Contaminant Fluxes in Fractured Rock Aquifers." *Water Resources Research* 52: 5400–5420.

Klepikova, Maria V., Tanguy Le Borgne, Olivier Bour, Kerry Gallagher, Rebecca Hochreutener, and Nicolas Lavenant. 2014. "Passive Temperature Tomography Experiments to Characterize Transmissivity and Connectivity of Preferential Flow Paths in Fractured Media." *Journal of Hydrology* 512(1): 549–62.

Klepikova, Maria V., Clement Roques, Simon Loew, and John Selker. 2018. "Improved Characterization of Groundwater Flow in Heterogeneous Aquifers Using Granular Polyacrylamide (PAM) Gel as Temporary Grout." *Water Resources Research* 54(2): 1410–19.

Kreft, A, and A Zuber. 1978. "On the Physical Meaning of the Dispersion Equation and Its Solutions for Different Initial and Boundary Conditions." *Chemical Engineering Science* 33(11): 1471–80.

Liu, Longcheng, Ivars Neretnieks, Pirouz Shahkarami, Shuo Meng, and Luis Moreno. 2017. "Solute Transport along a Single Fracture in a Porous Rock: A Simple Analytical Solution and Its Extension for Modeling Velocity Dispersion." *Hydrogeology Journal* 26(1): 297–320.

Makedonska, Nataliia, Scott L. Painter, Quan M. Bui, Carl W. Gable, and Satish Karra. 2015. "Particle Tracking Approach for Transport in Three-Dimensional Discrete Fracture Networks." *Computational Geosciences* 19(5): 1123–37.

Malik, N., N. Marwan, and J. Kurths. 2010. "Spatial Structures and Directionalities in Monsoonal Precipitation over South Asia." *Nonlinear Processes in Geophysics* 17(5): 371–81.

Malik, Nishant, Bodo Bookhagen, Norbert Marwan, and Jürgen Kurths. 2012. "Analysis of Spatial and Temporal Extreme Monsoonal Rainfall over South Asia Using Complex Networks." *Climate Dynamics* 39(3): 971–87.

Maloszewski, Piotr, and Andrzej Zuber. 1990. "Mathematical Modeling of Tracer Behavior in Short-term Experiments in Fissured Rocks." *Water Resources Research* 26(7): 1517–28.

Meng, S., L. Liu, B. Mahmoudzadeh, I. Neretnieks, and L. Moreno. 2018. "Solute Transport along a Single Fracture with a Finite Extent of Matrix: A New Simple Solution and Temporal Moment Analysis." *Journal of Hydrology* 562(1): 290–304.

Natarajan, N. 2014. "Effect of Time Varying Fracture-Skin Thickness on Contaminant Transport in Fracture-Matrix Coupled System." *KSCE Journal of Civil Engineering* 18(1): 124–31.

Ngo, Tri Dat, André Fourno, and Benoit Noetinger. 2017. "Modeling of Transport Processes through Large-Scale Discrete Fracture Networks Using Conforming Meshes and Open-Source Software." *Journal of Hydrology* 554(1): 66–79.

National Research Council. 1996. "Rock Fractures and Fluid Flow: Contemporary Understanding and Applications". Washington, D.C.: The National Academies Press.

National Academies of Sciences, Engineering, and Medicine. 2015. "Characterization, Modeling, Monitoring, and Remediation of Fractured Rock". Washington, D.C: The National Academies Press.

Persaud, Elisha, Jana Levison, Peeter Pehme, Kentner Novakowski, and Beth Parker. 2018. "Cross-Hole Fracture Connectivity Assessed Using Hydraulic Responses during Liner Installations in Crystalline Bedrock Boreholes." *Journal of Hydrology* 556: 233–46.

Quiroga, R. Quian, A. Kraskov, T. Kreuz, and P. Grassberger. 2002. "Performance of Different Synchronization Measures in Real Data: A Case Study on Electroencephalographic Signals." *Physical Review E* 65(4): 041903.

Rausch, Randolf, Wolfgang Schafer, Rene Therrien, and Christian Wagner. 2005. *Solute Transport Modelling: An Introduction to Models and Solution Strategies*. Berlin. Stuttgart: Gebr. Borntraeger Verlagsbuchhandlung.

Ren, Shuangpo, Samuel Gragg, Ye Zhang, Bradley J. Carr, and Guangqing Yao. 2018. "Borehole Characterization of Hydraulic Properties and Groundwater Flow in a Crystalline Fractured Aquifer of a Headwater Mountain Watershed, Laramie Range, Wyoming." *Journal of Hydrology* 561: 780–95.

Schreiber, S., J.M. Fellous, D. Whitmer, P. Tiesinga, and T.J. Sejnowski. 2003. "A New Correlation-Based Measure of Spike Timing Reliability." *Neurocomputing* 52–54: 925–31.

Shakas, A., N. Linde, T. Le Borgne, and O. Bour. 2018. "Probabilistic Inference of Fracture-Scale Flow Paths and Aperture Distribution from Hydrogeophysically-Monitored Tracer Tests." *Journal of Hydrology* 567: 305–19.

Shakas, Alexis, Niklas Linde, Ludovic Baron, Olivier Bochet, Olivier Bour, and Tanguy Le Borgne. 2016. "Hydrogeophysical Characterization of Transport Processes in

Fractured Rock by Combining Push-Pull and Single-Hole Ground Penetrating Radar Experiments." *Water Resources Research* 52: 938–53.

Shapiro, A M. 2002. "Fractured-Rock Aquifers; Understanding an Increasingly Important Source of Water. " *USGS Fact Sheet 112-02*.

Singhal, B. B. S., and R. P. Gupta. 2010. Applied Hydrogeology of Fractured Rocks. 2nd ed. Springer Netherlands.

Somogyvári, Márk, Mohammadreza Jalali, Santos Jimenez Parras, and Peter Bayer. 2017. "Synthetic Fracture Network Characterization with Transdimensional Inversion." *Water Resources Research* 53(6): 5104–23.

Sudicky, E. A., and E. O. Frind. 1982. "Contaminant Transport in Fractured Porous Media: Analytical Solutions for a System of Parallel Fractures." *Water Resources Research* 18(6): 1634–42.

Suzuki, Anna, Sergei Fomin, Vladimir Chugunov, and Toshiyuki Hashida. 2018. "Mathematical Modeling of Non-Fickian Diffusional Mass Exchange of Radioactive Contaminants in Geological Disposal Formations." *Water* 10(2): 1–11.

Tang, D. H., E. O. Frind, and E. A. Sudicky. 1981. "Contaminant Transport in Fractured Porous Media: Analytical Solution for a Single Fracture." *Water Resources Research* 17(3): 555–64.

Tsang, Chin-fu, Ernest Orlando, and Lawrence Berkeley. 1998. "Flow Rocks in Heterogeneous Study Transport." *Rev. Geophys* 36: 275–98.

Vitale, Sarah A., Gary A. Robbins, and Edwin Romanowicz. 2019. “Identifying Cross-Well Fracture Connections Using the Dissolved Oxygen Alteration Method.” *Journal of Hydrology* 572: 781–89.

Chapter 3

A GENETIC PROGRAMMING–BASED MODEL FOR COLLOID RETENTION IN FRACTURES

ABSTRACT

Understanding the behavior of colloids in groundwater is critical as some are pathogenic while others may facilitate or inhibit the transport of dissolved contaminants. Colloid behavior in saturated fractured aquifers is governed by the physical and chemical properties of the groundwater-particle-fracture system. The interaction between these properties is nonlinear, and there is a need for a mathematical model describing the relationship between them to advance the mechanistic understanding of colloid transport in fractures and facilitate modeling in fractured environments. This paper coupled genetic programming and linear regression within a multigene genetic programming framework to develop a robust mathematical model describing the relationship between colloid retention in fractures and the physical and chemical parameters that describe the system. The data employed for model development and validation were collected from a series of 75 laboratory-scale colloid tracer experiments conducted under a range of conditions in three laboratory-induced discrete dolomite fractures and their epoxy replicas. The model sufficiently reproduced the observed data with coefficients of determination (R^2) of 0.92 and 0.80 for model development and validation, respectively. A cross-validation demonstrated the model generality to more than

86% of the observed data. A variance-based global sensitivity analysis confirmed that attachment is the primary retention mechanism in the systems employed in this work. The model developed in this study provides a tool describing colloid retention in factures, which furthers the understanding of groundwater-particle-fracture system conditions contributing to the retention of colloids and can aid in the design of groundwater remediation strategies and development of groundwater management plans.

Keywords: Genetic Programming, Colloid transport, Fractured aquifer

3.1. INTRODUCTION

Groundwater represents the primary water resource in many regions globally, and is required for human health, well-being, and development (Rivera 2017). Increasing reliance on groundwater due to population growth and industrialization has accelerated aquifer depletion (Tang et al. 2017; Castellazzi et al. 2018), necessitating the extraction of water from increasing depths where the likelihood of encountering a fractured bedrock aquifer is high. The Geological Survey of Canada identified the characterization of fractured aquifers as a major knowledge gap (Rivera 2005), yet 70% of Canada's regional aquifers exist in fractured formations (Rivera 2005). Fractures represent only a minor portion of the porosity in these aquifers; however, they are the main conduits for groundwater flow and contaminant transport. Colloids represent a class of contaminants that, within the field of hydrogeology, are typically defined as particles ranging in size from one nanometer to 10 micrometers (Buddemeier and Hunt 1988; Hunter 2001; Bekhit and Hassan 2005; Delleur 2007). Examples include inorganic mineral grains (i.e., fine silt and clay), organic particles, microorganisms and other cells, and anthropogenic particles (e.g., microplastics). Microorganisms may be pathogenic (Hunt and Johnson 2016), and chronic exposure to engineered particles can also be harmful to human and environmental health (Karlsson et al. 2015). While most colloids are benign, they may facilitate or inhibit the transport of dissolved contaminants depending on colloid-fracture, colloid-solute, colloid-matrix, and hydro-dynamic interactions (Abdel-salam and Chrysikopoulos 1995; Ibaraki and

Sudicky 1995). Colloid transport and retention have been studied extensively in porous media aquifers (e.g., Sun et al. 2015; Lehoux et al. 2017; Kam-rani et al. 2018), fractured rock aquifers (e.g., Rodrigues and Dickson 2015; Bagalkot and Kumar 2018; Neukum 2018), and karst aquifers (e.g., Göppert and Goldscheider 2008; Flynn and Sinreich 2010; Schiperski et al. 2016). Colloids normally carry a negative charge under natural groundwater conditions (Zvikelsky and Weisbrod 2006; Hunt and Johnson 2016), and the combination of their size and charge causes them to behave differently than dissolved contaminants in groundwater. Specifically, colloids move faster than solutes due to size exclusion, charge exclusion, and Taylor dispersion (Ryan and Elimelech 1996). Within a fracture, colloids are excluded from slow moving portions of the Poiseuille velocity profile due to their finite size, thereby increasing their effective velocity and decreasing their overall dispersion (James and Chrysikopoulos 2003). As the size increases, even beyond that of a colloid, particles are forced into faster streamlines within the velocity profile resulting in increased effective velocity. Additionally, irregular fracture walls cause a three-dimensional, nonuniform, tortuous flow fields to develop (Brush and Thomson 2003), and the resulting hydrodynamic forces lead to changes in particle flow path directions (Zhang et al. 2012).

The behavior of colloids in fractured groundwater systems has become an increasingly active research area over the past two decades. Advection is the primary mechanism responsible for colloid transport in fractures, while attachment, sedimentation, physical straining, and diffusion into the rock matrix are responsible

for retention (Zhang et al. 2012; Weisbrod et al. 2013; Cohen and Weisbrod 2018). Attachment is a two-step process: the colloid must first contact a fracture wall and subsequently attach (Abdel-salam and Chrysikopoulos 1994). For attachment to occur, the attractive van der Waals forces must overcome the repulsive forces within the electric double layer (O'Melia and Stumm 1967). As size increases, the particle may be excluded from contacting the fracture wall, thereby decreasing the likelihood of retention through attachment. Sedimentation typically affects larger/more dense particles (Vilks et al. 2008; Stoll et al. 2017), and aggregated colloids (Swanton 1995), as their weight may exceed the buoyant force. Larger particles may also be excluded from main flow pathways due to physical straining or charge exclusion in smaller aperture regions (McCarthy and Zachara 1989). In contrast, small colloids are more likely to be retained by diffusion into the rock matrix in regions where the groundwater velocity is low and matrix porosity is high (Zhang et al. 2012).

It is generally accepted that colloid retention mechanisms in fractures are governed by the physical and chemical properties of the groundwater, groundwater flow conditions, surface chemistry of the fracture matrix, aperture field geometry, and the physical and surface properties of the colloid (Zhang et al. 2012). Groundwater chemistry (pH and ionic strength) affects retention by enhancing or deteriorating the particle-fracture wall interaction. While lower ionic strength reduces the likelihood of attachment by strengthening the particle-fracture wall repulsion forces (Mondal and Sleep 2012; Neukum 2018), reducing the solution pH

enhances the attractive Van der Waal forces providing favorable attachment conditions (Zhang et al. 2012). Groundwater hydraulics also affect colloid retention as turbulence may facilitate contact with fracture walls, which increases the likelihood of colloid-fracture wall interaction, and high velocity strengthens the shear force between attached colloids and fracture walls (Zhang et al. 2012). Detachment will occur when these forces are large enough to overcome the attractive Van der Waal forces (Lin et al. 2014). The combination of aperture variability and particle size can result in retention via straining when the aperture is too small for a colloid to pass through (Fahim and Wakao 1982; Carstens et al. 2017). Particle size and surface charge affect transport and retention through size and/or charge exclusion from specific aperture regions (Tufenkji 2007; Alaskar et al. 2015). These mechanisms force larger/highly charged colloids into higher velocity streamlines closer to the center of a fracture (Weisbrod et al. 2013), rendering these particles less susceptible to retention. Based on this mechanistic description of colloid retention in fractures, factors affecting the fraction of particles retained (F_r) along a fracture can be grouped into: (1) physical (e.g., fracture geometry and specific discharge) and (2) chemical (e.g., ionic strength of the groundwater and the surface charges of fracture walls and particles) characteristics.

Despite the extensive research that has been conducted to understand the behavior of colloids in fractures, sufficiently accurate mathematical relationship between F_r and the factors that influence it has not been developed to the best of the authors' knowledge. Rodrigues and Dickson (2014) worked toward obtaining

such a mathematical representation through a series of colloid tracer experiments incorporating the effects of particle properties (size, diffusion coefficient, and surface charge), fracture characteristics (length, width, aperture size, and surface charge), solution ionic strength, and specific discharge. A stepwise multiple linear regression was adopted in their study and the resulting model was able to predict Fr in a single saturated fracture with a coefficient of determination (R^2) of 0.64. The relatively large errors in their model can be attributed to the complex nonlinear relationship between F_r and the parameters influencing it, and the interaction between these parameters. The study by Rodrigues and Dickson (2014) represents a baseline for simulating the behavior of colloids in fractures under a range of physical and chemical conditions, and highlights the need for a more robust technique that can effectively obtain the desired relationship.

Genetic programming (GP) is an evolutionary algorithm that provides the ability to uncover complex mathematical relationships between a set of inputs and an output that is difficult to identify via classic mathematical or statistical techniques (Koza 1994). It has been widely applied in the field of water resources engineering to identify rainfall-runoff relationships (Savic et al. 1999; Chadalawada et al. 2017), predict stream flow (Ravansalar et al. 2017), obtain suitable reservoir operation rules (Ashofteh et al. 2017), model sea-level rise and the propagation of algae blooms (Muttil and Chau 2006; Ghorbani et al. 2010), and estimate saturated hydraulic conductivity (Parasuraman et al. 2007).

The goal of this work is to improve our understanding of the major physical and chemical parameters, and their confounding effects, that influence colloid retention in fractures. GP was applied to an experimental dataset describing colloid retention under a range of physical and chemical groundwater-colloid-fracture system parameters, as reported by Rodrigues and Dickson (2014), to obtain a sufficiently accurate relationship between F_r and these parameters. Such a relationship will provide an understanding of how modification of these parameters may either: 1) mobilize colloids, thereby facilitating various remediation strategies (e.g., bioremediation, nanoparticle-based remediation technologies); or, 2) enhance the retention of colloids that may be harmful to human and environmental health (e.g., pathogens, enteric viruses, microplastics).

3.2. COLLOID RETENTION MODEL

3.2.1. DATASET

The dataset utilized in this study includes the results from 75 laboratory-scale colloid tracer experiments conducted in laboratory-induced dolomite fractures and their epoxy replicates (Rodrigues and Dickson 2014). The experiments were designed to examine the effect of a range of physical and chemical parameters on F_r in single, saturated laboratory-scale fractures fitted within plexiglass flow cells. The reader is referred to Rodrigues et al. (2013) for a detailed description of the experimental setup and procedures. Of the 75 laboratory experiments, seven were conducted in triplicate to ensure reproducibility between experiments. The current

study utilizes the arithmetic mean of F_r from the repeated experiments, thus reducing the dataset from 75 to 54 observations. Of the 54 remaining observations, 41 are chosen randomly for the model development (training dataset) while the remaining 13 are used for the model validation.

The parameters used by Rodrigues and Dickson (2014) were: 1) fracture characteristics including length (L_f), width (W), hydraulic aperture (b_c), mass balance aperture (b_m), friction loss aperture (b_f), and surface charge (Q_m); 2) physiochemical and hydraulic water properties including ionic strength (I) and specific discharge (q); and, 3) particle properties including diameter (d_p), surface area (A_p), volume (V_p), density (ρ_p), diffusion coefficient (D), and surface charge (Q_p). These parameters are combined iteratively, in the current study, into seven variables describing various physical and chemical aspects of the system to reduce the size of the problem exported to GP. Table 3-1 lists the formulation, physical representation, and experimental range for each of these seven variables. The relationships between these variables and the observed F_r are shown in Figure 3-1. It is noteworthy that the fracture aperture variability was implicitly considered by incorporating b_m, b_f, and b_c, which are sensitive to the largest, smallest, and mean apertures, respectively. It is also noteworthy that fracture surface charge heterogeneity was not considered as Rodrigues and Dickson (2014) reported only two different values for Q_m depending on whether the fracture was dolomite or epoxy.

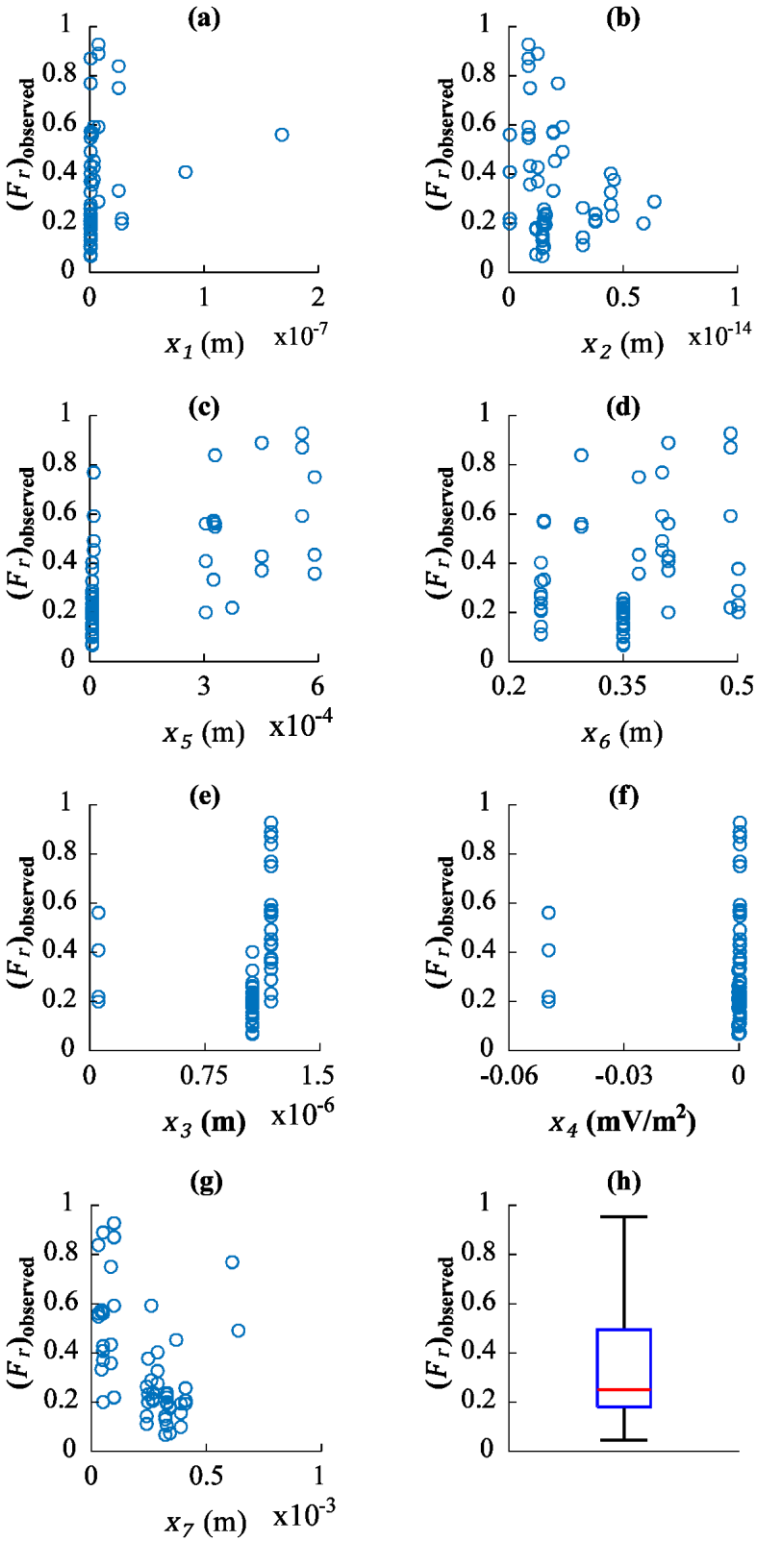

Figure 3-1: (a to g) represent the relationship between the observed F_r and the variables x_1 to x_7 respectively, and (h) shows a box plot for the observed F_r

Table 3-1: Variables used in the current study

Variable **{Formulation}**	**[Experimental Range]** **Physical Representation**
x_1 **(m)** $\left\{D/q\right\}$	**[**$2.5\text{x}10^{-10}$, $1.7\text{x}10^{-7}$] Ratio between diffusive and advective forces on the particle represented by the diffusion coefficient (D) and the specific discharge (q) respectively
x_2 **(m)** $\left\{V_p/(b_m \times W)\right\}$	**[**$7\text{x}10^{-20}$, $6.3\text{x}10^{-15}$] Degree of fracture clogging represented by the ratio of particle volume (V_p) to fracture area perpendicular to flow direction expressed through the multiplication of fracture width (W) and the mass balance aperture (b_m)
x_3 **(m)** $\left\{\left(\rho_p/\rho_w\right) \times d_p\right\}$	**[**$5.3\text{x}10^{-8}$, $1.2\text{x}10^{-6}$] Effect of buoyant force on the particle represented by the ratio between the particle (ρ_p) and water (ρ_w) densities where d_p is the particle diameter
x_4 **(mV/m^2)** $\left\{Q_m/(A_r \times I \times A_p)\right\}$	**[**$-1.3\text{x}10^{-13}$, $-4.95\text{x}10^{-2}$] Ratio between the effect of fracture surface charge (Q_m) to the effect of groundwater ionic strength (I) employing Avogadro's number (A_{vr}) and the particle surface area (A_p)
x_5 **(m)** $\left\{\left(Q_m/Q_p\right) \times b_c\right\}$	**[**$4.73\text{x}10^{-6}$, $5.9\text{x}10^{-4}$] Effect of fracture surface potential to particle surface potential/charge (Q_p) in a distance equals the fracture hydraulic aperture (b_c)

Variable {Formulation}	[Experimental Range] Physical Representation
x_6 (m) $\{L_f\}$	[0.241, 0.5] Fracture length
x_7 (m) $\{b_f\}$	[3.3×10^{-5}, 6.4×10^{-4}] Friction loss aperture size to represent the small regions in the fracture

3.2.2. GENETIC PROGRAMMING

GP is a class of evolutionary algorithms, inspired by Darwin's theory of natural selection, that depends on the survival of the most adapted solution (Koza 1994). Being an evolutionary search technique, GP adopts special operations to prevent the solution from being trapped in local minima and maxima. Thus, GP solutions are considered to be near-optimal because of the errors that may be presented in the inputs or the actual output especially for experimental datasets. In addition to optimizing the relationship between a group of inputs and an output, GP produces optimum values for the constants that may be included in the solution.

GP is initialized by randomly generating hundreds to thousands of mathematical expressions (solutions) describing the relationship between the inputs and output. Each solution generated is referred to as an individual or a candidate and contains a combination of functions (mathematical or logical operators) and terminals (input variables and constants). Each individual is assigned a fitness value according to a predefined objective function, and genetic operations (elitism,

crossover, and mutation) are applied to reproduce new generations. Individuals with high fitness values are reproduced directly to the next generation (elitism). The remaining individuals are combined and changed randomly using crossover and mutation to produce offspring. Crossover is an operation in which two individuals are selected either randomly (tournament) or according to their fitness values (roulette in which the section of the wheel is proportional to the fitness value), and subsequently mixed to produce new ones. Mutation is the process in which each individual is changed randomly by adding/removing or replacing part(s) of it. The process of reproduction is repeated until a termination criterion is met. The termination criterion might, for example, be a specified maximum number of generations, a value of the objective function, or a computation time. A flowchart describing the application of GP is shown in Figure 3-2.

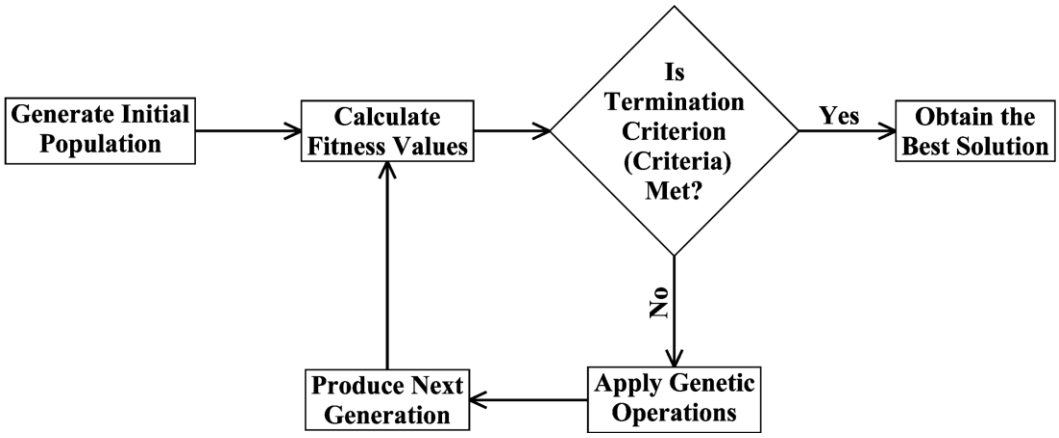

Figure 3-2: Flowchart for the application of GP

GP typically results in a single, near optimal solution that can be represented by a tree with a certain depth. The solution, however, is highly dependent on the GP parameters employed (i.e., function set, size of initial population, percentage of

elite individuals, crossover rate, and mutation rate). Thus, a different set of GP parameters applied to the same inputs and target output may result in a different solution. Since the most adapted solution may not necessarily account for all input variables, the current study forces the GP technique to include all inputs.

Multigene Genetic Programming (MGGP) is an improvement over classic GP, that combines several GP solutions through linear regression. MGGP aims to develop a linear combination of short trees with low complexity rather than a single complex mathematical expression that is typically produced by classic GP when the number of inputs is large (Searson et al. 2010). Each tree/gene obtained by the MGGP is weighted through a linear regression analysis aimed at minimizing the least squared error against the target output. This results in a so-called pseudo-linear model that embeds the nonlinear behavior of the system (Searson et al. 2010).

This study adopted MGGP through the MATLAB© toolbox GPTIPS developed by Searson et al. (2010). The MGGP parameters used in the current study are summarized in Table 3-2. The genes obtained using MGGP are referred to as the MGGP solution, while the linear combination of these genes is referred to as the model. In evolutionary algorithms, the choice of the maximum number of generations and the population size is vital as they significantly affect the computation time and the results. A large number of generations are typically employed to ensure that evolutionary algorithms produce the best results. However, the current study uses a relatively small number of generations (50) but combines it with a large population (4000) to provide a wide search space for the MGGP,

thereby increasing the likelihood of obtaining a satisfactory solution within an acceptable computation time.

Table 3-2: MGGP parameters used in the current study

Parameter	Value	Parameter	Value
Terminal Set	Variables (x_1, …, x_7) Constants range between [-10^3, 10^3]	Function Set	+, -, *, /, square root, power, exp, sin, cos
Number of Genes	2	Maximum Tree Depth	14
Termination Criteria	Specified fitness value	Desired Objective Function's Value	1.10
Genetic Operations Ratios**	Elitism = 0.05 Cross Over*** = 0.80 Mutation = 0.15	Selection Criteria for Cross-Over	Tournament Selection

**Probability of reproducing an individual through a certain genetic operation
***Two points crossover is used

A near optimal MGGP solution requires a well-defined objective function, reflective of the objective of the model, in order to measure the fitness of each individual in the population. Typically, the goal is to minimize the error between the estimated values and the actual output. The current study utilizes a combination of a linear correlation measure with an error estimator as follows:

$$F = RMSE + \frac{1}{R^2} \qquad (3-1)$$

where F is the objective function, RMSE is the root mean squared error, and R^2 is the coefficient of determination between the estimated and actual values. Combining R^2 and RMSE results in the value of F being equal to or larger than 1.0. When F is minimized to 1.0 (i.e., RMSE = 0, R^2 = 1), a model that can replicate the actual output is guaranteed. To obtain a perfect model using GP (i.e., minimizing F to its absolute minimum which is 1.0) within acceptable computational time, large population together with large number of data points for training are essential. Given the limited computational resources available for the current study, a slightly larger value for F (i.e., 1.10) is adopted as shown in Table 3-2.

3.2.3. MODEL PERFORMANCE ASSESSMENT

The defined objective function is used to assess the ability of the developed model to reproduce the validation part of the experimental dataset while reproducing the training part is inherently achieved during the model development. Applying the MGGP technique requires combining different genes through linear regression. Thus, a residual analysis is conducted to assure the validity of the linear regression assumptions. This is achieved by ensuring that the errors between the observed and estimated outputs closely follow normal distribution with a mean of zero, and there are no observable trends between these errors and the observed or estimated output.

The termination criteria adopted in the MGGP guarantees a high fitness value for the training part used in the model development. Large errors produced by a

small portion of the training dataset would typically not affect the overall model performance. Thus, there is a need for a cross-validation (CV) process to assess the generality of a model to an independent dataset (Rohani et al. 2018). A range of CV techniques have been developed such as holdout, *k*-fold, and bootstrap, each with its own set of limitations, biases, and computational costs (Kohavi 1995). The current study utilizes the *k*-fold CV as its performance has been confirmed (Kohavi 1995; Borra and Di Ciaccio 2010). Thus, the experimental data (including training and validation sets) were divided into nine folds. Eight of these folds were used for calibration while the remaining fold was kept for testing, with the data included in each fold chosen randomly. The CV was repeated 1,000 times to ensure model robustness, and to minimize the individual effects of random data assignment to folds. Ensemble averages of R^2 and RMSE were then calculated using the results from the 1,000 CV runs for all folds.

3.2.4. MODEL SENSITIVITY ANALYSIS

The purpose of a sensitivity analysis (SA) is to provide insight into the effects of input variables (i.e., physical and chemical parameters) on the variability of the model output (i.e., F_r), and they can be assessed either locally or globally. Local SA assesses the impact of an input, sampled from a particular part of its range, on the model output which can be misleading in case of non-linear responses. A global sensitivity analysis (GSA) is preferred over the local SA as it utilizes the input parameters sampled from their entire range and can also consider the nonlinearity

embedded in the system. The variance-based GSA is used to estimate the direct (*S*) and total (*ST*) sensitivity indices of each input following the procedures described by Saltelli et al. (2008). Large *S* value indicates that the model output is directly sensitive to the corresponding input, while large *ST* value indicates that the direct effect of an input together with its interaction with other inputs contribute to the output variability. The variance-based method is preferred over other GSA approaches as it is model-free and captures the interaction between the inputs (Saltelli et al. 2008). The current study utilizes the variance-based GSA by generating 10,000 quasi-random samples of the physiochemical parameters defined by Rodrigues and Dickson (2014) using their fitted statistical distributions (Table 3-3). Subsequently, the corresponding variables, x_1 through x_7, are estimated according to Table 3-1. A Monte-Carlo framework is adopted by repeating this process 1,000 times and the ensemble averages of *S* and *ST* are calculated for each variable.

Table 3-3: Fitted statistical distributions of the parameters defined by Rodrigues and Dickson (2014)

Parameter	Fitted Statistical Distribution	Parameter	Fitted Statistical Distribution
L	LN¥ (-1.06, 0.23)	I	U [$1x10^{-7}$, 0.64]
W	U¥¥ [0.15, 0.31]	d_p	U [$5x10^{-8}$, $1.2x10^{-6}$]
b_m	LN (-6.41, 0.56)	Q_p	U [-18, -12.1]
b_c	U [0.17, 0.69]	ρ_p	U [1020, 1055]

Parameter	Fitted Statistical Distribution	Parameter	Fitted Statistical Distribution
b_f	LN (-8.65, 0.89)	Q_m	U [-23.43, -0.213]
D	U [$4.2\text{x}10^{-13}$, $9.7\text{x}10^{-12}$]	q	U [$1.7\text{x}10^{-5}$, $1.7\text{x}10^{-3}$]

¥ lognormal distribution
¥¥ Uniform distribution

3.3. RESULTS AND DISCUSSION

3.3.1. MODEL STRUCTURE

The application of the MGGP technique resulted in two genes (*G1* and *G2*) shown in tree representations in Figure 3-3. In addition to the variables considered in the current study (Table 3-1), the MGGP employed constants to match the model predictions to corresponding observations. The quantities T_1 through T_9 combine the variables (x_1 through x_7) and constants, and are developed in the current study to facilitate estimating *G1* and *G2*. The model developed to estimate F_r is a linear combination of *G1* and *G2* as follows:

$$F_r = 26.66 - 3.51 \times (G1) - 0.07 \times (G2) \qquad (3-2)$$

The constants in Equation (3-2) resulted from regressing *G1* and *G2* with the corresponding observations during model development. The relationship developed (Equation (3-2)) expresses the nonlinear nature of the groundwater-particle-fracture system through *G1* and *G2*, which contain nonlinear functions. The complexity of the developed model is attributed to the interaction between the physical and

chemical parameters influencing particulate transport and retention in fractures, expressed by the quantities T_1 through T_9.

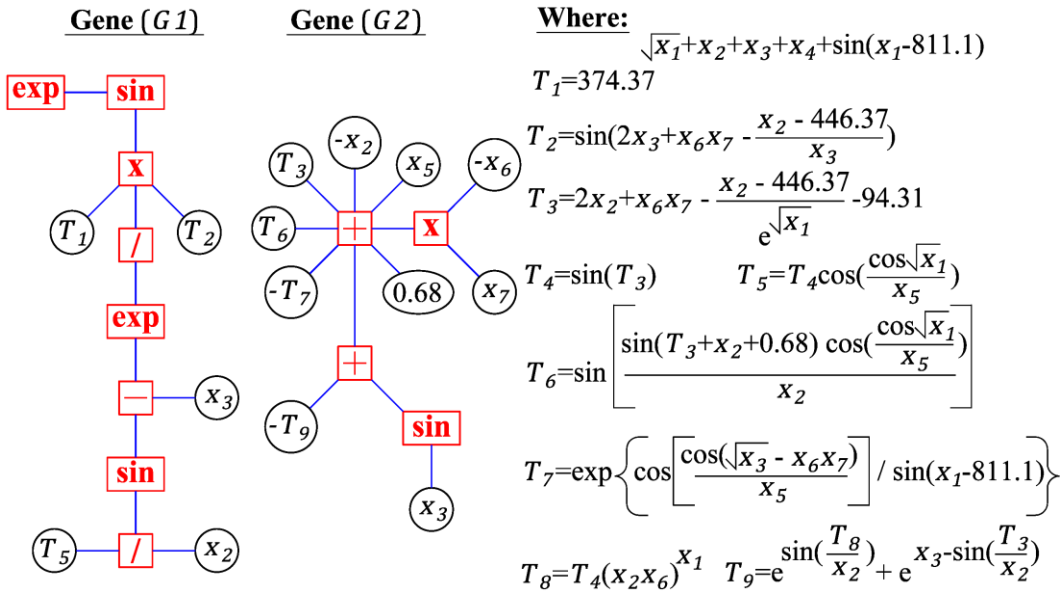

Figure 3-3: Tree representation for the MGGP-obtained genes (i.e., *G1* and *G2*) with the quantities (i.e., T_1 through T_9) developed in the current study to facilitate calculating *G1* and *G2*

3.3.2. MODEL PERFORMANCE

As discussed above, the experimental data were partitioned into training and validation sets. F_r is predicted separately for each dataset using Equation (3-2), and is compared to the corresponding observed values. Figure 3-4 shows scatterplots of the predicted vs. the observed F_r for both the training and validation datasets, which indicates that the developed model can adequately predict the observed data. This qualitative assessment of the data in Figure 3-4 was augmented by calculating the RMSE and R^2 between the observed and predicted values of F_r. R^2 and RMSE are 0.92 and 0.06, respectively for the training dataset, and 0.80 and 0.13, respectively,

for the validation dataset. These values, for both the training and validation datasets, demonstrate the adequacy of the model developed in predicting F_r in single saturated fractures within the ranges of x_1 through x_7 specified in Table 3-1. It is noteworthy that even when the physical and chemical parameters employed in the calculation of x_1 through x_7 follow the distributions given in Table 3-3, they may lead to values of x_1 through x_7 that fall outside their specified ranges (Table 3-1), resulting in predictions of F_r that are below zero or larger than 1.0.

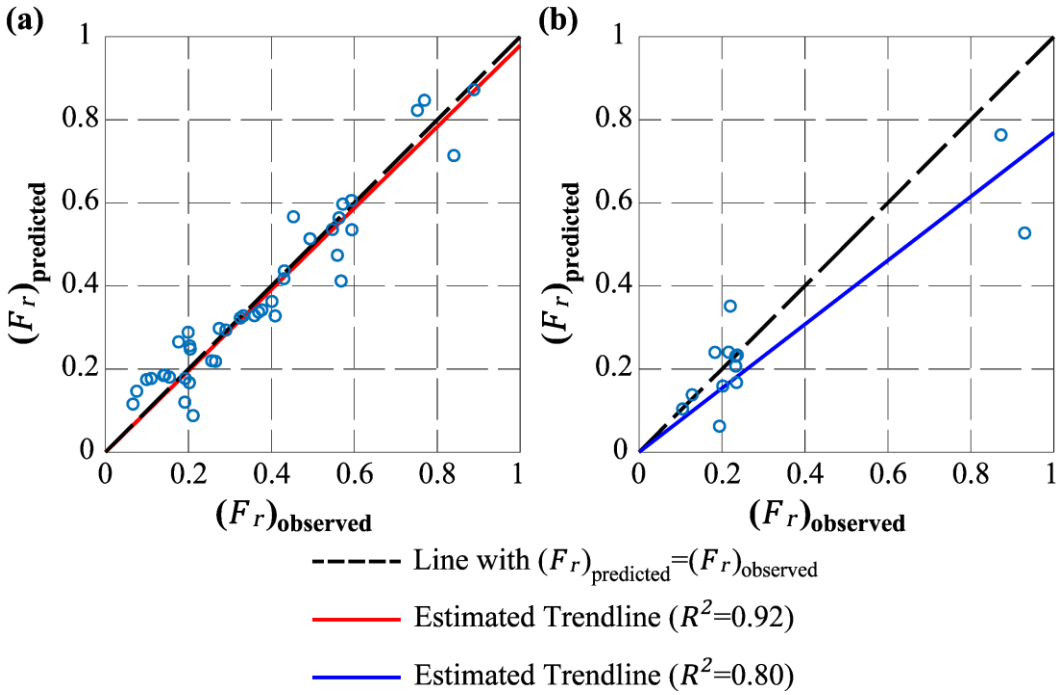

Figure 3-4: Predicted vs. observed values of F_r for (a) the training dataset and (b) the validation dataset

A residual analysis was employed to ensure the assumptions invoked by linear regression within the MGGP technique are satisfied. Indeed, the errors from the application of the developed model to the training dataset are identically distributed as supported by the normal probability plot shown in Figure 3-5. This

plot also shows that the points are clustered around zero, and the error dispersion is relatively small. These errors are attributed to additional factors that may affect particulate transport in fractures that were not accounted for explicitly in the input variables such as aperture field variability, surface charge heterogeneity, and micro-scale roughness.

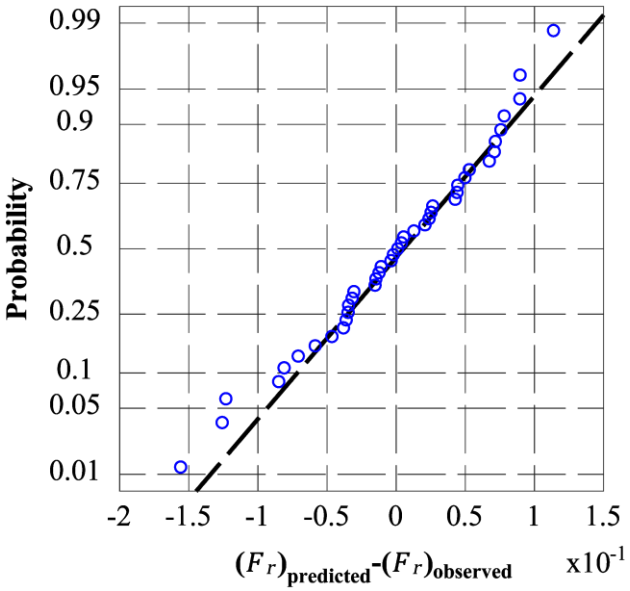

Figure 3-5: Normal probability plot of the estimated errors for the training dataset

The model robustness has been demonstrated through CV. Figure 3-6 shows a box plot based on the ensemble averages of the calibration and testing folds for R^2 and RMSE. The dataset used for model calibration clearly exhibited less variability for both R^2 and RMSE, which is attributed to the larger number of observations employed for calibration vs. testing. However, despite their higher variability, the testing datasets show higher mean R^2 (87 %) and lower mean RMSE (7.4 %) than the calibration datasets.

Although the efficacy of the colloid retention model was confirmed through conducting residual and CV analyses, and comparing model predictions to experimental observations, the use of this model is limited to the variable ranges defined in the current study (Table 3-1). Additional limitation is that the aperture field variability is not incorporated explicitly, and surface charge heterogeneity and micro-scale roughness are not considered in this model.

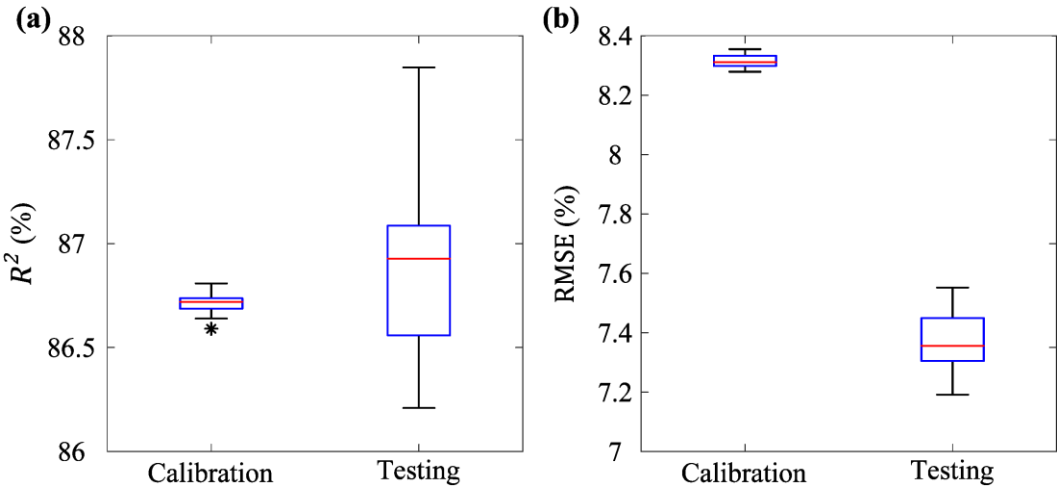

Figure 3-6: Boxplot of (a) R^2 and (b) RMSE for both calibration and testing datasets based on ensemble averages from 1,000 CV runs.

3.3.3. MODEL SENSITIVITY

The variance-based GSA employed in the current study resulted in *S* and *ST* sensitivity indices, shown in Figure 3-7, that reflect the direct and total contributions of x_1 through x_7 to the variability of F_r predicted using the developed model.

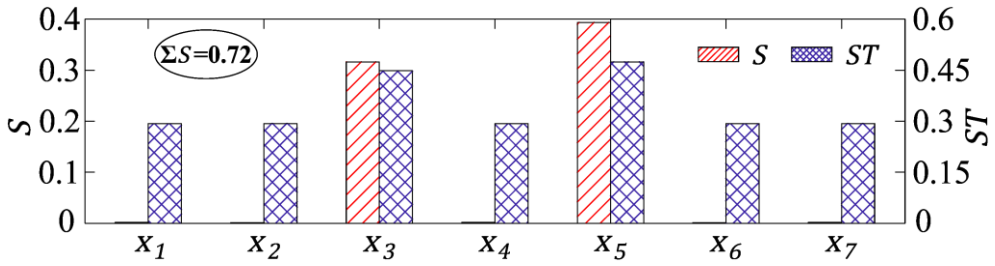

Figure 3-7: Sensitivity indices (*S* and *ST*) estimated using the employed variance-based GSA

The variability of F_r is largely attributed to the interaction between all variables rather than their direct effects as supported by the difference between *ST* and *S* values. However, a major portion of the variability in F_r results from x_3 and x_5, and particularly x_5 as indicated by its larger *S* and *ST* values. The variable x_3 reflects the effects of particle size and relative weight while x_5 measures the contribution of particle and fracture wall surface charges, as described in Table 3-1. This suggests that attachment is the dominant colloid retention mechanism in the water-colloid-fracture systems considered in this work. This finding supports those from several other studies conducted under different water-colloid-fracture system conditions (e.g., Rodrigues and Dickson 2015; Stoll et al. 2017; Cohen and Weisbrod 2018).

3.4. CONCLUSIONS

Classic mathematical and statistical techniques are insufficient to develop robust models describing colloid retention in fractures which is controlled by a large number of physical and chemical parameters describing the groundwater-particle-fracture system, many of which are confounding. This highlights the need for

alternative techniques. The current study combines GP with linear regression in a MGGP framework to develop a model describing the fraction of colloids retained in a single, saturated fracture based on the physical and chemical parameters of the groundwater-particle-fracture system. The model reproduced the experimental observations with R^2 of 0.92 and 0.80, and RMSE of 0.06 and 0.13, for the training and validation datasets, respectively. A cross validation process was applied and confirmed the generality of the model to more than 86% of the experimental dataset. Model performance is confirmed for the range of the variables defined within the current study, and therefore its applicability is limited to these ranges. Additional model limitations are that aperture field variability is not incorporated explicitly, and surface charge heterogeneity and micro-scale roughness are not considered. A variance-based GSA confirmed the role of attachment as the primary mechanism governing colloid retention in the fracture-water-colloid systems investigated. The SA also demonstrated that careful attention must be paid to obtaining the surface properties of both the colloids and fractures, as they are the largest contributors to the variability of F_r under the conditions employed. The model developed provides a better understanding of colloid retention in single, saturated fractures within the specified range of physical and chemical parameters. This model can be applied to aid in the design of groundwater remediation strategies, or the development of groundwater management plans, through determining how to modify the groundwater-colloid-fracture system properties to enhance the mobilization or retention of colloids.

3.5. ACKNOWLEDGEMENT

This research was supported by NSERC through the Canadian Nuclear Energy Infrastructure Resilience under Systemic Risk (CaNRisk) – Collaborative Research and Training Experience (CREATE) and Discovery Grant programs. The authors would like to thank the four reviewers for their constructive feedback which improved the manuscript discussed in this chapter.

3.6. NOTATIONS

A_p:	Particle surface area	q:	specific discharge
b_c:	Hydraulic aperture	Q_m:	fracture surface charge
b_f:	Friction loss aperture	Q_p:	particle surface charge
b_m:	Mass balance aperture	R^2:	Coefficient of determination
D:	Diffusion coefficient	S:	direct sensitivity index
d_p:	Particle diameter	SA:	sensitivity analysis
F:	The objective function	ST:	total sensitivity index

F_r: Fraction of particles retained along a fracture

$G1$: The first gene resulted from applying the MGGP technique

$G2$: The second gene resulted from applying the MGGP technique

I:	Groundwater ionic strength	V_p:	particle volume
L_f:	Fracture length	W:	Fracture width

Greek Letters:

ρ_p: particle density

3.7. ACRONYMS

CV: Cross-validation

GP: Genetic programming

GSA: Global sensitivity analysis

MGGP: Multigene genetic programming

RMSE: the root mean squared error

3.8. REFERENCES

Abdel-salam, Assem, and Constantinos V Chrysikopoulos. 1994. “Analytical Solutions for One-Dimensional Colloid Transport in Saturated Fractures.” *Advances in Water Resources* 17(5): 283–296.

Abdel-salam, Assem, and Constantinos V Chrysikopoulos. 1995. “Analysis of a Model for Contaminant Transport in Fractured Media in the Presence of Colloids.” *Journal of Hydrology* 165(1–4): 261–281.

Alaskar, Mohammed, Kewen Li, and Roland Horne. 2015. “Silica Particles Mobility Through Fractured Rock.” *Arab J Sci Eng* 40(4): 1205–1222.

Ali Ghorbani, Mohammad et al. 2010. “Sea Water Level Forecasting Using Genetic Programming and Comparing the Performance with Artificial Neural Networks.” *Computers and Geosciences* 36(5): 620–627.

Ashofteh, Parisa Sadat, Omid Bozorg-Haddad, and Hugo A. Loáiciga. 2017. “Logical Genetic Programming (LGP) Development for Irrigation Water Supply Hedging Under Climate Change Conditions.” *Irrigation and Drainage* 66(4): 530–541.

Bagalkot, Nikhil, and G. Kumar. 2018. “Colloid Transport in a Single Fracture–Matrix System: Gravity Effects, Influence of Colloid Size and Density.” *Water* 10(11): 1531.

Bekhit, Hesham M., and Ahmed E. Hassan. 2005. “Stochastic Modeling of Colloid-Contaminant Transport in Physically and Geochemically Heterogeneous Porous Media.” *Water Resources Research* 41(2).

Borra, Simone, and Agostino Di Ciaccio. 2010. "Measuring the Prediction Error. A Comparison of Cross-Validation, Bootstrap and Covariance Penalty Methods." *Computational Statistics and Data Analysis* 54(12): 2976–2989.

Brush, David J., and Neil R. Thomson. 2003. "Fluid Flow in Synthetic Rough-Walled Fractures: Navier-Stokes, Stokes, and Local Cubic Law Simulations." *Water Resources Research* 39(4): 1085.

Buddemeier, Robert W., and James R. Hunt. 1988. "Transport of Colloidal Contaminants in Groundwater: Radionuclide Migration at the Nevada Test Site." *Applied Geochemistry* 3(5): 535–548.

Carstens, Jannis F., Jörg Bachmann, and Insa Neuweiler. 2017. "Effects of Flow Interruption on Transport and Retention of Iron Oxide Colloids in Quartz Sand." *Colloids and Surfaces A: Physicochemical and Engineering Aspects* 520(1): 532–543.

Castellazzi, Pascal et al. 2018. "Quantitative Mapping of Groundwater Depletion at the Water Management Scale Using a Combined GRACE/InSAR Approach." *Remote Sensing of Environment* 205(1): 408–418.

Chadalawada, Jayashree, Vojtech Havlicek, and Vladan Babovic. 2017. "A Genetic Programming Approach to System Identification of Rainfall-Runoff Models." *Water Resources Management* 31(12): 3975–3992.

Cohen, Meirav, and Noam Weisbrod. 2018. "Transport of Iron Nanoparticles through Natural Discrete Fractures." *Water Research* 129(1): 375–383.

Delleur, Jacques W. 2007. *The Handbook of Groundwater Engineering*. 2nd ed. Boca Raton, FL: Taylor & Francis Group, LLC.

Fahim, M A, and N Wakao. 1982. "Parameter Estimation from Tracer Response Measurements." *The Chemical Engineering Journal* 25(1): 1–8.

Flynn, Raymond M., and Michael Sinreich. 2010. "Characterisation of Virus Transport and Attenuation in Epikarst Using Short Pulse and Prolonged Injection Multi-Tracer Testing." *Water Research* 44(4): 1138–1149.

Göppert, Nadine, and Nico Goldscheider. 2008. "Solute and Colloid Transport in Karst Conduits under Low- and High-Flow Conditions." *Groundwater* 46(1): 61–68.

Hunt, Randall J, and William P Johnson. 2016. "Pathogen Transport in Groundwater Systems: Contrasts with Traditional Solute Transport." *Hydrogeology Journal* 25(4): 921–930.

Hunter, Robert J. 2001. Foundation of Colloid Science. Second Edi. New York.

Ibaraki, M, and E A Sudicky. 1995. "Colloid-Facilitated Transport in Discretely Fractured Porous Medium: 1. Numerical Formulation and Sensitivity Analysis." *Water Resources Research* 31(12): 2945–2960.

James, Scott C., and Constantinos V. Chrysikopoulos. 2003. "Effective Velocity and Effective Dispersion Coefficient for Finite-Sized Particles Flowing in a Uniform Fracture." *Journal of Colloid and Interface Science* 263(1): 288–295.

Kamrani, Salahaddin, Mohsen Rezaei, Mehdi Kord, and Mohammed Baalousha. 2018. "Transport and Retention of Carbon Dots (CDs) in Saturated and Unsaturated Porous

Media: Role of Ionic Strength, PH, and Collector Grain Size." *Water Research* 133(1): 338–347.

Karlsson, Hanna L., Muhammet S. Toprak, and Bengt Fadeel. 2015. "Toxicity of Metal and Metal Oxide Nanoparticles." *In Handbook on the Toxicology of Metals*, eds. Gunnar F. Nordberg, Bruce A. Fowler, and Monica Nordberg. Academic Press, 75–112.

Kohavi, Ron. 1995. "A Study of Cross-Validation and Bootstrap for Accuracy Estimation and Model Selection." *In IJCAI-95*, ed. C.S. Mellish. Montreal, Que.: Morgan Kaufmann, Los Altos, CA, 1137–1143.

Koza, John R. 1994. "Genetic Programming as a Means for Programming Computers by Natural Selection." *Statistics and Computing* 4(2): 87–112.

Lehoux, Alizée P. et al. 2017. "Combined Time-Lapse Magnetic Resonance Imaging and Modeling to Investigate Colloid Deposition and Transport in Porous Media." *Water Research* 123(1): 12–20.

Lin, Jianfeng et al. 2014. "Goethite Colloid Enhanced Pu Transport through a Single Saturated Fracture in Granite." *Journal of Contaminant Hydrology* 164(1): 251–258.

McCarthy, John F, and John M. Zachara. 1989. "Subsurface Transport of Contaminants." *Environmental Science and Technology* 23(5): 496–502.

Mondal, Pulin K, and Brent E Sleep. 2012. "Colloid Transport in Dolomite Rock Fractures: Effects of Fracture Characteristics, Specific Discharge, and Ionic Strength." *Environmental Science and Technology* 46(18): 9987–9994.

Muttil, Nitin, and Kwok-Wing Chau. 2006. "Neural Network and Genetic Programming for Modelling Coastal Algal Blooms." *Int. J. Environment and Pollution* 284(34): 223–238.

Neukum, Christoph. 2018. "Transport of Silver Nanoparticles in Single Fractured Sandstone." *Journal of Contaminant Hydrology* 209(1): 61–67.

O'Melia, Charles R., and Werner Stumm. 1967. "Theory of Water Filtration." *Journal (American Water Works Association)* 59(11): 1393–1412.

Parasuraman, Kamban, Amin Elshorbagy, and Bing Cheng Si. 2007. "Estimating Saturated Hydraulic Conductivity Using Genetic Programming." *Soil Science Society of America Journal* 71(6): 1676–1684.

Ravansalar, Masoud, Taher Rajaee, and Ozgur Kisi. 2017. "Wavelet-Linear Genetic Programming: A New Approach for Modeling Monthly Streamflow." *Journal of Hydrology* 549(1): 461–475.

Rivera, Alfonso. 2005. How Well Do We Understand Groundwater in Canada? A Science Case Study. Toronto, Canada. Natural Resources Canada and Geologic Survey of Canada.

Rivera, Alfonso. 2017. "The State of Ground Water in Canada." Ground Water Canada. https://www.groundwatercanada.com/education/the-state-of-ground-water-what-we-know-and-dont-know-about-ground-water-in-canada-3584 (accessed September 2017).

Rodrigues, S., and S. Dickson. 2015. "The Effect of Matrix Properties and Preferential Pathways on the Transport of Escherichia Coli RS2-GFP in Single, Saturated,

Variable- Aperture Fractures." *Environmental Science and Technology* 49(14): 8425–8431.

Rodrigues, S., S. Dickson, and J. Qu. 2013. "Colloid Retention Mechanisms in Single, Saturated, Variable-Aperture Fractures." *Water research* 47(1): 31–42.

Rodrigues, Sandrina, and Sarah Dickson. 2014. "A Phenomenological Model for Particle Retention in Single, Saturated Fractures." *Groundwater* 52(2): 277–283.

Rohani, Abbas, Morteza Taki, and Masoumeh Abdollahpour. 2018. "A Novel Soft Computing Model (Gaussian Process Regression with K-Fold Cross Validation) for Daily and Monthly Solar Radiation Forecasting (Part: I)." *Renewable Energy* 115(1): 411–422.

Ryan, Joseph N., and Menachem Elimelech. 1996. "Colloid Mobilization and Transport in Groundwater." *Colloids and Surfaces A* 107(95): 1–56.

Saltelli, A et al. 2008. *Global Sensitivity Analysis*. The Primer. West Sussex, England: John Wiley & Sons Ltd.

Savic, Dragan A., Godfrey A.Walters, and Jamesw. Davidson. 1999. "A Genetic Programming Approach to Rainfall-Runoff Modelling." *Water Resources Management* 13(3): 219–231.

Schiperski, Ferry, Johannes Zirlewagen, and Traugott Scheytt. 2016. "Transport and Attenuation of Particles of Different Density and Surface Charge: A Karst Aquifer Field Study." *Environmental Science and Technology* 50(15): 8028–8035.

Searson, Dp, De Leahy, and Mj Willis. 2010. "GPTIPS: An Open Source Genetic Programming Toolbox for Multigene Symbolic Regression." *In Proceedings of the*

International of the MultiConference of Engineers and Computer Scientists Vol I. Hong Kong.

Stoll, M., F. M. Huber, E. Schill, and T. Schäfer. 2017. "Parallel-Plate Fracture Transport Experiments of Nanoparticulate Illite in the Ultra-Trace Concentration Range Investigated by Laser-Induced Breakdown Detection (LIBD)." *Colloids and Surfaces A: Physicochemical and Engineering Aspects* 529(1): 222–230.

Sun, Yuanyuan et al. 2015. "Transport, Retention, and Size Perturbation of Graphene Oxide in Saturated Porous Media: Effects of Input Concentration and Grain Size." *Water Research* 68(1): 24–33.

Swanton, Stephen W. 1995. "Modelling Colloid Transport in Groundwater; the Prediction of Colloid Stability and Retention Behaviour." *Advances in Colloid and Interface Science* 54(1): 129–208.

Tang, Yin et al. 2017. "Reconstructing Annual Groundwater Storage Changes in a Large-Scale Irrigation Region Using GRACE Data and Budyko Model." *Journal of Hydrology* 551(1): 397–406.

Tufenkji, Nathalie. 2007. "Modeling Microbial Transport in Porous Media: Traditional Approaches and Recent Developments." *Advances in Water Resources* 30(6-7): 1455–1469.

Vilks, P, N H Miller, and A Vorauer. 2008. "Laboratory Bentonite Colloid Migration Experiments to Support the Äspö Colloid Project." *Physics and Chemistry of the Earth* 33(14-16): 1035–1041.

Weisbrod, Noam, Hanan Meron, Sharon Walker, and Vitaly Gitis. 2013. “Virus Transport in a Discrete Fracture.” *Water Research* 47(5): 1888–1898.

Zhang, Wei, Xiangyu Tang, Noam Weisbrod, and Zhuo Guan. 2012. “A Review of Colloid Transport in Fractured Rocks.” *Journal of Mountain Science* 9(6): 770–787.

Zvikelsky, Ori, and Noam Weisbrod. 2006. “Impact of Particle Size on Colloid Transport in Discrete Fractures.” *Water Resources Research* 42(12): 1–12.

Chapter 4

ANALYTICAL DESCRIPTION OF COLLOID BEHAVIOR IN SINGLE FRACTURES UNDER IRREVERSIBLE DEPOSITION

ABSTRACT

Understanding colloid transport and retention in groundwater is crucial for management and remediation purposes, as some colloids are pathogenic whereas others may influence the transport of dissolved contaminants. Colloid behavior in fractures is governed by the interplay between physical and chemical properties of the groundwater-colloid-fracture system. Irreversible deposition is the primary retention mechanism for colloids in fractures with an impermeable matrix and is typically modeled using a lumped deposition coefficient that reflects the system's physical and chemical conditions. For a single fracture under an instantaneous injection at the inlet, colloid behavior has not yet been described analytically; thus, a solution for the mathematical relationship between the deposition coefficient and the fraction of colloids retained within a fracture is unknown. The present study developed that solution/model through conceptualizing irreversible deposition as first-order decay. The model facilitates the prediction of colloid deposition in single fractures under various physical and chemical conditions. A variance-based global sensitivity analysis revealed that fracture length, aperture, and deposition coefficient are the main contributors to the variability of the fraction of colloids retained; therefore, attention must be paid when measuring or estimating these

parameters. The model developed can be integrated with readily available relationships between the fraction of colloids retained along a fracture and the groundwater-colloid-fracture system's physical and chemical properties. Therefore, this model can be employed to determine how system's physical and chemical properties may be modified to control the deposition coefficient for the purpose of enhancing or inhibiting colloid deposition for water quality management purposes.

Keywords: Analytical solution, Colloid deposition, Fractures, Instantaneous injection

4.1. INTRODUCTION

Many regions around the world depend on groundwater systems for water supply, health and wellbeing, food security, economic development, and the environment preservation (Schuster-Wallace and Dickson 2017), and contamination of this critical resource impacts the security of those who depend on it. Population growth and industrialization have increased reliance on groundwater. This has led to accelerated aquifer depletion (Tang et al. 2017; Castellazzi et al. 2018), and resulted in the extraction of water from increasing depths where fractured systems are more likely to be encountered. Fractured aquifers represent a class of groundwater systems in which open, connected fractures convey water together with any contaminants that are present. Contaminants may be dissolved, particulate, or non-aqueous in phase, each of which is subject to different fate and transport mechanisms. Colloids represent a subset of particulates that range in size from nanometers to 10 micrometers (Zhang et al. 2012), and they can pose risk to human health and the environment (e.g., pathogenic microorganisms, nanoparticles, heavy metals). While many colloids are benign (i.e., clay and fine silt particles), they can nonetheless alter hydraulic conductivity (Grolimund et al. 2007; Chuang et al. 2018) or enhance or inhibit the migration of more harmful contaminants (Walshe et al. 2010; Wolfsberg et al. 2017). The coupled colloid-contaminant behavior is governed by the colloid-fracture, colloid-contaminant, and hydrodynamic interactions (Abdel-salam and Chrysikopoulos 1995; Ibaraki and Sudicky 1995). It is generally accepted that colloid behavior in fractures differs

from that of solutes (e.g., Ryan and Elimelech, 1996; Stoll et al. 2016) as the combination of colloid size and charge subjects it to several forces (i.e., drag, gravity, Van der Waals, and electric double layer forces).

While advection is the primary transport mechanism for colloids in fractures, their retention is attributed to attachment/deposition, sedimentation, physical straining, charge exclusion, and matrix diffusion (Swanton 1995; Cohen and Weisbrod 2018). Understanding colloid behavior in fractured aquifers requires adequate characterization of the aforementioned transport and retention mechanisms, which are governed by numerous physical/hydraulic (e.g., fracture geometry and specific discharge) and chemical (e.g., groundwater ionic strength and the surface charges of fracture walls and colloids) properties of the groundwater-colloid-fracture system (Zhang et al. 2012). Extensive descriptions of the relationship between these physical and chemical properties and colloid retention mechanisms in fractures have been presented in several studies (e.g., Zhang et al. 2012; Hunt and Johnson, 2016), albeit without mathematically identifying the dependence between colloid retention and the parameters characterizing the groundwater-colloid-fracture system properties. A phenomenological model describing the relationship between these parameters and the fraction of colloids retained (F_r) within laboratory-scale dolomite fractures and their epoxy replicas was originally developed by Rodrigues and Dickson (2014), and was enhanced by Yosri et al. (2019) who developed a multigene genetic

programming-based colloid retention model using the dataset of Rodrigues and Dickson (2014).

Deposition has been identified as the primary retention mechanism for colloids in fractures (Rodrigues and Dickson 2014; Stoll et al. 2017; Cohen and Weisbrod 2018) as: *i*) matrix diffusion is relatively insignificant for colloids due to their size (Zhang et al. 2012); and, *ii*) sedimentation and physical straining are of less importance unless chemical conditions favor coagulation (Swanton 1995). Colloid deposition is typically assumed to be an irreversible process as the release of deposited colloids has been observed to be negligible (Bowen and Epstein 1979), and/or requires physical/chemical perturbation of the groundwater-colloid-fracture system (e.g., Nocito-gobel and Tobiason, 1996; Mondal and Sleep, 2012; Masciopinto and Visino, 2017). Irreversible deposition of colloids in fractures has been mathematically described using a deposition coefficient (κ), which is effectively a fitting parameter that is typically determined through laboratory or field experiments (Abdel-Salam and Chrysikopoulos 1994). Although colloid retention is governed by the forces acting on it, it is prohibitive to implement models based on these forces beyond the microscale. Thus, the lumped coefficient, κ, has been employed beyond the microscale to analytically describe colloid deposition (Abdel-salam and Chrysikopoulos 1994). An analytical relationship between F_r and κ can then be developed in single fractures under relevant initial and boundary conditions.

Several boundary conditions can be adopted at the inlet when simulating colloid behavior in a single fracture (e.g., constant concentration, constant flux, instantaneous injection), each of which affects the solution (obtained analytically or numerically). Abdel-Salam and Chrysikopoulos (1994) developed analytical solutions for colloid transport in a semi-infinite, parallel plate fracture considering advection, longitudinal dispersion, and matrix diffusion under: *i*) constant concentration; and, *ii*) constant flux boundary conditions at the inlet. Although analytical solutions do not exist for an instantaneous injection boundary condition in this colloid-fracture system, the following approximations have been suggested: a solution in the Laplacian domain (e.g., Yan, 1996); the use of numerical techniques (e.g., James and Chrysikopoulos, 1999; Natarajan and Kumar, 2014); and, the assumption of quasi-steady laminar flow conditions (e.g., James and Chrysikopoulos, 2003). Nonetheless, the use of approximations can yield inaccurate predictions of F_r, and subsequently an inaccurate relationship between F_r and κ, highlighting the need for more accurate approaches.

Bodin et al. (2003) reported an analytical solution describing solute transport in a single fracture with an impermeable matrix under an instantaneous injection at the inlet considering advection, hydrodynamic dispersion, and first-order decay. Solute decay and irreversible deposition both result in permanent mass loss; thus, irreversible deposition can be conceptually represented by first-order decay. A relationship between the deposition and first-order decay coefficients (κ and λ,

respectively) can be then established, and subsequently applied to develop an analytical relationship between F_r and κ.

The objective of the present study is to develop an analytical model describing the relationship between F_r and κ in a semi-infinite, parallel-plate, saturated fracture with an impermeable matrix under an instantaneous colloid injection at the inlet and irreversible deposition. This model will serve as a predictive tool for F_r in laboratory- and field- scale fractures under similar conditions, and can be coupled with available relationships between F_r and the parameters describing the groundwater-colloid-fracture system's physical and chemical properties (i.e., the multigene genetic programming-based model presented in Chapter 3) to enhance the prediction of colloid behavior under different physical and chemical conditions. The model developed can also be employed to determine how κ may be modified to enhance or inhibit colloid deposition for water quality management purposes.

4.2. METHODOLOGY

4.2.1. COLLOID BEHAVIOR IN SINGLE FRACTURES

Colloid behavior in a single fracture with an impermeable matrix is described mathematically by the classical advection-dispersion equation (ADE) coupled with irreversible deposition. The irreversible deposition mechanism leads particles to be partitioned into aqueous (i.e., mobile) and solid (i.e., deposited) phases. The classical ADE coupled with irreversible colloid deposition in a saturated fracture

with walls idealized as parallel plates, under steady-state flow conditions, can be written as (Abdel-Salam and Chrysikopoulos 1994):

$$\frac{\partial C}{\partial t} + \frac{2\kappa U}{b^2} C = D\frac{\partial^2 C}{\partial x^2} - u\frac{\partial C}{\partial x} \qquad (4-1)$$

where C is the concentration of aqueous colloids, x is the distance along the fracture from the inlet, t is the time, u is the average steady state groundwater velocity, b is the aperture, $D = D_e + {U^2 b^2}/{210 D_e}$ is the longitudinal Taylor dispersion coefficient that accounts for molecular diffusion and velocity variations across the fracture, and D_e is the diffusion coefficient. Equation (4-1) describes uniaxial colloid transport along a fracture with an impervious matrix under irreversible deposition conditions without accounting for previously deposited colloids (Figure 4-1). The last expression on the left-hand-side of Equation (4-1) (i.e., ${2\kappa U}/{b^2} \times C$) represents a sink process induced by irreversible deposition and results in an attenuated breakthrough curve (BTC) as shown in Figure 4-2. When irreversible deposition is considered, the mass of colloids exiting the fracture (M') is smaller than the mass injected (M_o) and the difference ($M_o - M'$) is referred to as the mass retained, recognizing that retention in Equation (4-1) is solely due to irreversible deposition. Subsequently, F_r can be defined as the ratio between ($M_o - M'$) and M_o. To the best of the authors' knowledge, an analytical solution for Equation (4-1) under an instantaneous injection at the fracture inlet has not yet been developed, and thus approximations (e.g., Yan, 1996; James and Chrysikopoulos, 1999) can be adopted to estimate M' and F_r.

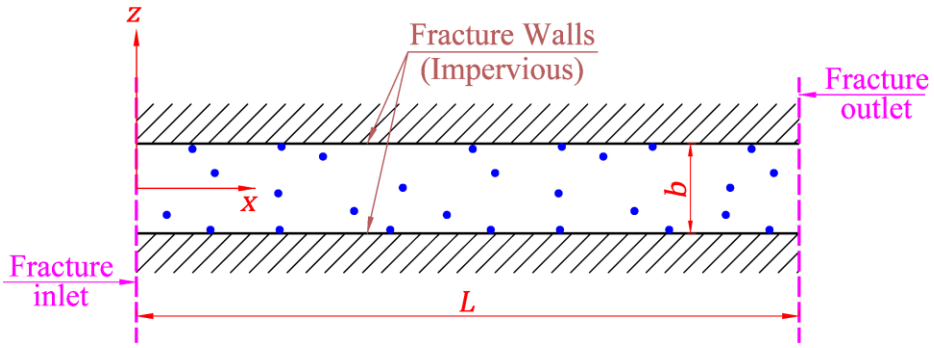

Figure 4-1: Schematic of colloid transport in a single fracture with an impermeable matrix under irreversible deposition where the flow is assumed to be steady and in the *x*-direction only

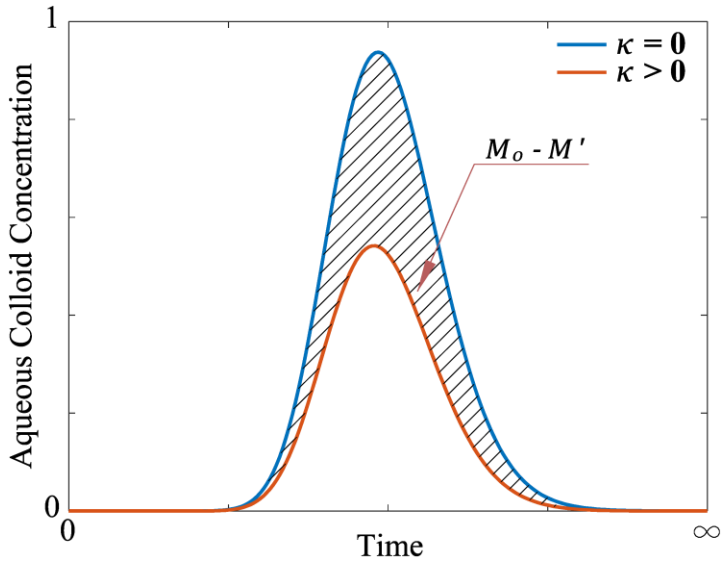

Figure 4-2: Typical BTCs of aqueous phase colloids at the outlet of a single fracture under an instantaneous injection at the inlet, where the hatched area indicates the mass of colloids retained

4.2.2. SOLUTE TRANSPORT IN SINGLE FRACTURES

The relationship describing uniaxial transport of a solute in a saturated fracture with an impermeable matrix considering advection, dispersion, and first-order decay is given by:

$$\frac{\partial C}{\partial t} + \lambda C = D_s \frac{\partial^2 C}{\partial x^2} - u \frac{\partial C}{\partial x} \qquad (4-2)$$

where $D_s = D_e + \alpha U$ is the hydrodynamic dispersion coefficient, which couples the effects of diffusion (expressed through D_e) and mechanical dispersion (expressed through αU), where α is the dispersivity. Equations (4-1) and (4-2) are of the same form except: *i*) the last expression on the left-hand-side of Equations (4-1) and (4-2) simulates the mass lost due to irreversible deposition and first-order decay, respectively; and, *ii*) longitudinal dispersion of colloids and solutes are described by different coefficients. For both colloids and solutes, longitudinal dispersion is independent of diffusion at high Peclet numbers $\left(P_e = {Ub}/{D}\right)$. Thus, a single value of dispersivity can be used to describe the dispersion of colloids and solutes (i.e., $D = D_s$) (Abdel-Salam and Chrysikopoulos 1994). Under these conditions, a comparison between Equations (4-1) and (4-2) shows that, in a saturated fracture with an impermeable matrix, when deposition is irreversible, colloid deposition is mathematically equivalent to first-order decay with λ given by:

$$\lambda = \frac{2\kappa U}{b^2} \qquad (4-3)$$

4.2.3. FRACTION OF COLLOIDS RETAINED ALONG A SINGLE FRACTURE

Bodin et al. (2003) reported an analytical solution for Equation (4-2) at the fracture outlet (i.e., $x = L$, where L is the fracture length), for an instantaneous injection at the fracture inlet:

$$C(L,t) = \frac{M_o L}{Q\sqrt{4\pi D t^3}} exp\left[-\frac{(L-Ut)^2}{4Dt}\right] exp[-\lambda t] \qquad (4-4)$$

where Q is the steady state volumetric flow rate. Combining Equations (4-3) and (4-4) provides an analytical solution for Equation (4-1) under the same injection scheme. Therefore, the effluent concentration of aqueous colloids (under irreversible deposition conditions) is given as:

$$C(L,t) = \frac{M_o L}{Q\sqrt{4\pi D t^3}} exp\left[-\frac{(L-Ut)^2}{4Dt}\right] exp\left[-\frac{2\kappa U}{b^2} t\right] \qquad (4-5)$$

It is noteworthy that Equation (4-5) can also be developed by applying the transformation introduced by Danckwerts (1953) to the analytical solution developed by Abdel-Salam and Chrysikopoulos (1994) describing colloid behavior in a fracture under irreversible deposition with a constant concentration at the inlet boundary. The colloid mass exiting the fracture under an instantaneous injection at the inlet boundary (i.e., *M'*) can subsequently be evaluated by:

$$M' = \int_0^\infty Q \cdot C(L,t) dt \qquad (4-6)$$

where *C(L, t)* is described by Equation (4-5). When κ = 0 (i.e., colloids are conservative), *M'* must equal M_o, and F_r (i.e., the ratio between $M_o - M'$ and M_o) is zero. When $\kappa > 0$, F_r can be calculated as:

$$F_r = \frac{L}{\sqrt{4\pi D}} \int_0^\infty t^{-3/2} exp\left[-\frac{(L-Ut)^2}{4Dt}\right]\left[1 - exp\left(-\frac{2\kappa U}{b^2} t\right)\right] dt \qquad (4-7)$$

The integration in Equation (4-7) was evaluated analytically to establish the relationship between F_r and κ (see Appendix - A for details) as follows:

$$F_r = 1 - exp\left[\frac{1}{2}(P_e)_g\left(1 - \sqrt{1 + KI}\right)\right] \qquad (4-8)$$

where $(P_e)_g = {UL}/{D}$ is the general form of Peclet number, and $KI = {8\kappa D}/{Ub^2}$ is a dimensionless number introduced in the present study and hereafter referred to as the deposition index.

4.2.4. MODEL VERIFICATION

The model developed in the present study to estimate F_r (i.e., Equation (4-8)) was verified by comparing its predictions to F_r observations reported by Rodrigues and Dickson (2014), who conducted a series of laboratory-scale colloid tracer experiments in laboratory-induced dolomite fractures and their epoxy replicas. Their experimental fractures were fitted in plexiglass flow cells, and a colloid suspension was introduced instantaneously at the inlet of each fracture under a range of physical (fracture geometry, groundwater velocity, colloid size and density) and chemical (ionic strength, surface charge of matrix and particle) conditions to investigate their coupled effects on F_r. The reader is referred to Rodrigues et al. (2013) for further details of the experimental setup and procedures. As these experiments were conducted at high values of P_e (4.8×10^3 - 6.1×10^6), Equation (4-8) can be applied as D can be assumed to be independent of D_e, and therefore it can be replaced by D_s, which is dependent on α. It should be mentioned

that Rodrigues and Dickson (2014) did not report *D* values in their work, and thus *D* was optimized by minimizing the root mean squared error (RMSE) between the F_r predictions (Equations (4-7) and (4-8)) and the corresponding experimental observations (Figure 4-3). Additionally, Rodrigues and Dickson (2014) reported hydraulic, mass balance, and friction loss apertures rather than a direct measure of *b*. Therefore, rather than calculating κ and *b* from the experimental data, the present study utilized the ratio κ/b^2 as a lumped quantity.

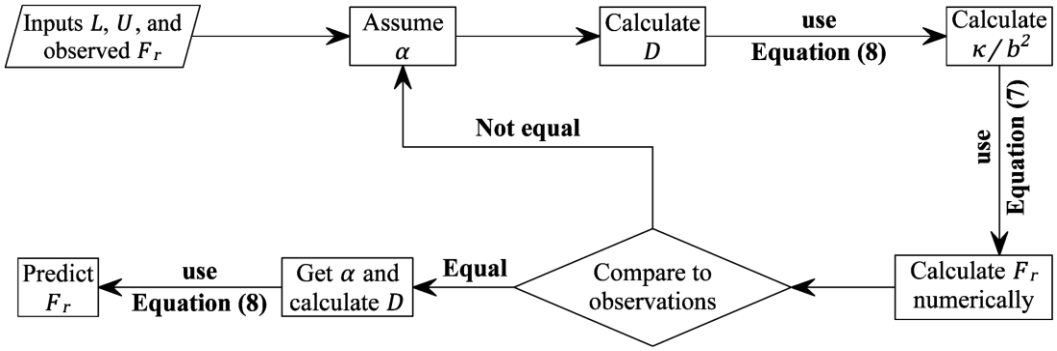

Figure 4-3: Flowchart for optimizing the Taylor dispersion coefficient (*D*) in the fractures examined by Rodrigues and Dickson (2014)

4.3. RESULTS AND DISCUSSION

4.3.1. ANALYTICAL DESCRIPTION OF F_r

Equation (4-8) represents an analytical relationship between F_r and κ in a single, saturated, parallel-plate fracture with an impermeable matrix under an instantaneous colloid injection at the inlet boundary. The values of $(P_e)_g$ and *KI* in Equation (4-8) must be positive, as they are calculated based on physical quantities that cannot be negative (i.e., *u*, *D*, *L*, *b*, and κ). Equation (4-8) shows that F_r ranges

between 0 and 1 as the quantity $(P_e)_g\left(1-\sqrt{1+KI}\right)/2$ is typically negative when $\kappa > 0$. At higher values of $(P_e)_g$ and KI, the exponential term in Equation (4-8) approaches 0 (i.e., F_r approaches 1), indicating that the mass retained within the fracture approaches the mass injected. The enhanced particle-fracture wall interactions that lead to F_r approaching 1 are referred to as favourable deposition conditions. In contrast, very low values of both $(P_e)_g$ and KI yield very small or negligible values of F_r, representing unfavorable deposition conditions. Figure 4-4 shows a graphical representation of Equation (4-8) as a predictive tool for κ in a saturated, parallel-plate, fracture with an impermeable matrix under an instantaneous colloid release and a specified F_r. This predictive tool can also be employed to determine how κ may be modified to enhance or inhibit colloid deposition for water quality management purposes.

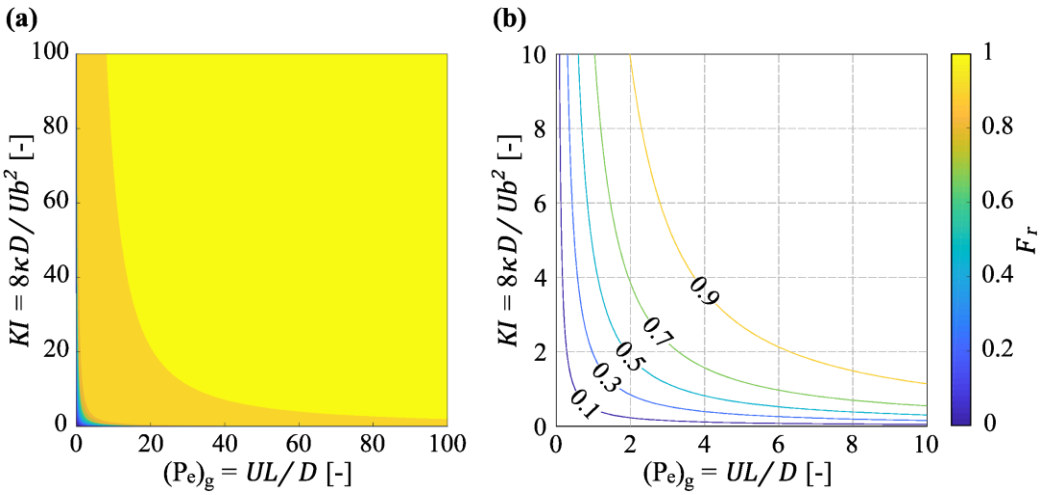

Figure 4-4: Graphical representation of the F_r - κ analytical relationship: (a) for a large range of $(P_e)_g$ and KI; and, (b) zoomed to $(P_e)_g$ and KI between 0 and 10

4.3.2. VERIFICATION OF THE MODEL DEVELOPED

Figure 4-5a shows the RMSE between the observed and predicted F_r calculated based on all fractures examined by Rodrigues and Dickson (2014) for different values of D. The value of D is expressed through α (i.e., $D = D_e + \alpha U$) which was assumed to be a fraction of the fracture length, and the same for all fractures. The optimum ratio of α/L (i.e., RMSE minimized) was approximately 0.05, and the corresponding D values ranged from $2\text{x}10^{-7}$ to $3\text{x}10^{-5}$ m^2/sec. This range represents 0.004% to 21% of the corresponding Taylor dispersion coefficient in the fractures examined, which violates the velocity distribution assumption (Zheng et al. 2009) and therefore justifies the use of D_s to represent colloid dispersion for the experimental fractures. Figure 4-5b shows the relationship between the predicted (Equation (4-8)) and observed values of F_r for the optimum α/L ratio. The line of best fit has a unit slope and zero-intercept demonstrating the ability of Equation (4-8) to replicate the experimental observations of F_r.

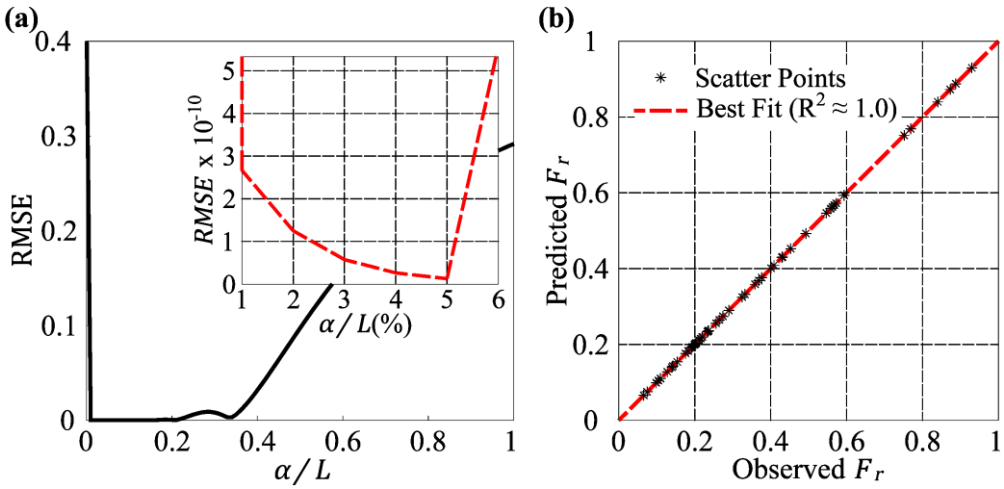

Figure 4-5: RMSE between observed and predicted values of F_r for different α/L and, (b) predicted vs. observed values of F_r at the optimum value of α/L

4.3.3. SENSITIVITY ANALYSIS

To investigate the impact of individual model parameters (i.e., u, L, D, b, and κ) and their confounding effects on the model output, F_r was calculated using Equation (4-8) for different values of each parameter. The effect of each parameter on F_r was investigated first individually (i.e., interaction with other parameters was neglected) by sampling the parameter of interest from a uniform distribution, with mean = μ and coefficient of variation = 50%, while setting all other parameters to their mean values. The μ values employed for u, L, D, and κ/b^2 were 1.0 m/year, 5.0 m, 0.25 m^2/year, and 6.98×10^{-2} m^{-1}, respectively, and were based on those of Abdel-Salam and Chrysikopoulos (1994). The Latin hyper cubed technique was used to generate 1,000 realizations of each parameter to ensure that its entire range was represented. As shown in Figure 4-6, when the parameters are considered independently (i.e., do not interact together), F_r is highly sensitive to L and κ/b^2, with minor or negligible sensitivity to u and D. Increasing L enhanced colloid deposition, which is expected as the fracture length determines the surface area available for deposition. Additionally, increasing the κ/b^2 ratio also enhanced colloid deposition (i.e., larger F_r) as: *i*) larger κ with constant b increases the fraction of colloids subject to deposition; and, *ii*) smaller b with constant κ enhances colloid-fracture wall interactions, increasing the likelihood of colloid deposition. It is noteworthy that F_r increases slightly at lower u (Figure 4-6) due to the increased particle residence time, which increases the likelihood of colloid-fracture wall interactions.

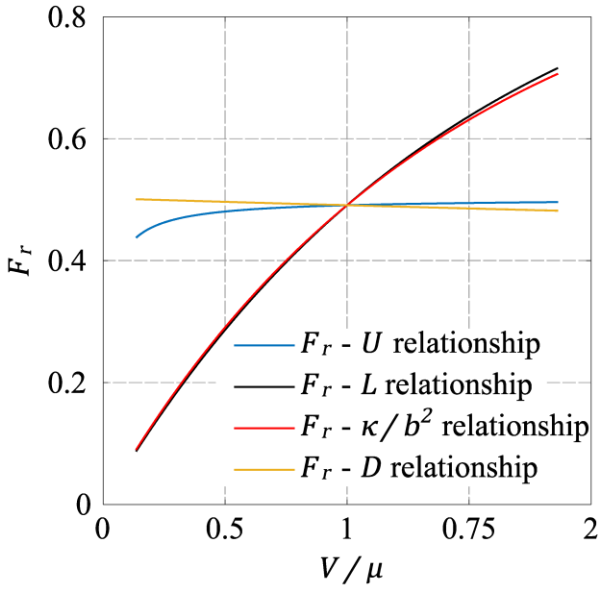

Figure 4-6: The effect of non-interacting parameters (*U*, *L*, *D*, *b*, and κ) on F_r, where *V* represents any parameter, and μ is the corresponding mean value of the parameter

The results presented in Figure 4-6 were augmented by applying a variance-based global sensitivity analysis (GSA), as described by Saltelli et al. (2008), to investigate the primary contributors to the variability of F_r considering the interaction between all parameters. Variance-based GSA was adopted by generating 1,000 realizations of all parameters simultaneously using the same procedures described above, and assuming that the parameters are independent. Figure 4-7 shows the direct (*S*) and total (*ST*) sensitivity indices estimated based on the variance-based GSA. The variability of F_r is attributed to the interaction between all parameters as supported by non-zero *ST* values; however, the direct effects of *L* and κ/b^2 on the variability of F_r were dominant over those of others (i.e., *u* and *D*) as indicated by their larger *S* values. The results of the variance-based GSA are consistent with the previous assessment of F_r response to the change of

each individual parameter (Figure 4-6). It is noteworthy that all parameters were assumed to be independent from each other; however, other sensitivity analysis methods (e.g., the modified Fourier Amplitude Sensitivity Test) can be used when the correlation between dependent inputs is known.

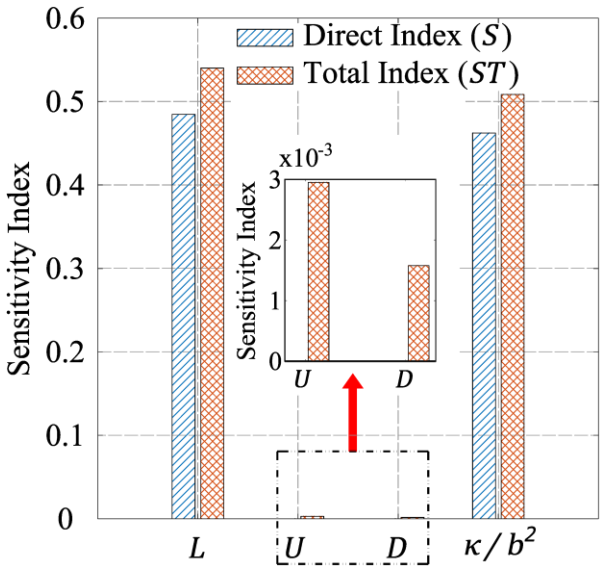

Figure 4-7: *S* and *ST* for *L*, *U*, *D*, and κ/b^2 estimated using the variance-based GSA

4.4. CONCLUSIONS

The present study developed an analytical relationship between the fraction of colloids retained and the deposition coefficient in a semi-infinite, saturated fracture with an impermeable matrix under an instantaneous injection considering advection, dispersion, and irreversible deposition. The relationship was developed by conceptualizing irreversible colloid deposition as first-order decay. The analytical relationship developed, together with its graphical representation, enable the prediction of the fraction of colloids retained along a laboratory- or field-scale

fracture under different physical and chemical conditions. A sensitivity analysis revealed that colloid deposition is most impacted by changes in the fracture length, aperture, and deposition coefficient. The relationship developed can be coupled with readily available models that relate the fraction of colloids retained to physical and chemical parameters describing the groundwater-colloid-fracture system properties (e.g., the multigene genetic programming presented in Chapter 3 of this dissertation) to: *i*) enhance the prediction of colloid behavior under different physical and chemical conditions; and, *ii*) determine how these properties may be modified to enhance or inhibit colloid deposition for water quality management purposes.

4.5. ACKNOWLEDGEMENT

This research was supported by NSERC through the Canadian Nuclear Energy Infrastructure Resilience under Systemic Risk (CaNRisk) – Collaborative Research and Training Experience (CREATE) and Discovery Grant programs.

4.6. NOTATIONS

b: Fracture aperture

C: Concentration of aqueous colloids

D: Longitudinal Taylor dispersion

D_e: Diffusion coefficient

D_s: Hydrodynamic dispersion coefficient

F_r: Fraction of colloids retained along a fracture

KI: Deposition index

L: Fracture length

M': Mass of colloids exiting the fracture

M_o: Injected mass of colloids

P_e: Peclet number in fractures

$(P_e)_g$: General form of Peclet number

Q: Steady state volumetric flow rate

R^2: Coefficient of determination

S: Direct senstivity index

ST: Total senstivity index

t: Time

u: Average steady state groundwater velocity

x: Distance along the fracture from the inlet

Greek Letters:

α: Dispersivity (m)

κ: Deposition coefficient

λ: First ordre decay coefficient

μ: Mean of uniform distribution

4.7. ACRONYMS

ADE: Advection dispersion equation

BTC: Concentration breakthrough curve

GSA: Global sensitivity analysis

RMSE: Root mean squared error

4.8. REFERENCES

Abdel-salam, Assem, and Constantinos V Chrysikopoulos. 1994. “Analytical Solutions for One-Dimensional Colloid Transport in Saturated Fractures.” *Advances in Water Resources* 17(5): 283–96.

Abdel-salam, Assem, and Constantinos V Chrysikopoulos. 1995. “Analysis of a Model for Contaminant Transport in Fractured Media in the Presence of Colloids.” *Journal of Hydrology* 165(1–4): 261–81.

Bagalkot, Nikhil, and G. Kumar. 2018. “Colloid Transport in a Single Fracture–Matrix System: Gravity Effects, Influence of Colloid Size and Density.” *Water* 10(11): 1531.

Bodin, Jacques, Gilles Porel, and Fred Delay. 2003. “Simulation of Solute Transport in Discrete Fracture Networks Using the Time Domain Random Walk Method.” *Earth and Planetary Science Letters* 208(3–4): 297–304.

Bowen, Bruce D., and Norman Epstein. 1979. “Fine Particle Deposition in Smooth Parallel-Plate Channels.” *Journal of Colloid and Interface Science* 72(1): 81–97.

Castellazzi, Pascal, Laurent Longuevergne, Richard Martel, Alfonso Rivera, Charles Brouard, and Estelle Chaussard. 2018. “Quantitative Mapping of Groundwater Depletion at the Water Management Scale Using a Combined GRACE/InSAR Approach.” *Remote Sensing of Environment* 205(1): 408–18.

Chuang, Po-Yu, Yeeping Chia, Yung-Chia Chiu, Mao-Hua Teng, and Sofia Ya Hsuan Liou. 2018. “Mapping Fracture Flow Paths with a Nanoscale Zero-Valent Iron Tracer Test and a Flowmeter Test.” *Hydrogeology Journal* 26(1): 321–31.

Cohen, Meirav, and Noam Weisbrod. 2018. "Transport of Iron Nanoparticles through Natural Discrete Fractures." *Water Research* 129(1): 375–83.

Danckwerts, P.V. 1953. "Continuous Flow Systems Distribution of Residence Times." *Chemical Engineering Science* 2(1): 1–13.

Flynn, Raymond M., and Michael Sinreich. 2010. "Characterisation of Virus Transport and Attenuation in Epikarst Using Short Pulse and Prolonged Injection Multi-Tracer Testing." *Water Research* 44(4): 1138–49.

Göppert, Nadine, and Nico Goldscheider. 2008. "Solute and Colloid Transport in Karst Conduits under Low- and High-Flow Conditions." *Groundwater* 46(1): 61–68.

Grolimund, Daniel, Kurt Barmettler, and Michal Borkovec. 2007. "Colloid Facilitated Transport in Natural Porous Media: Fundamental Phenomena and Modelling." *In Colloidal Transport in Porous Media*, eds. Fritz H. Frimmel, Frank von der Kammer, and Hans-Curt Flemming. Springer, Berlin, Heidelberg, 3–24.

Hunt, Randall J, and William P Johnson. 2016. "Pathogen Transport in Groundwater Systems: Contrasts with Traditional Solute Transport." *Hydrogeology Journal* 25(4): 921–930.

Ibaraki, M, and E A Sudicky. 1995. "Colloid-Facilitated Transport in Discretely Fractured Porous Medium: 1. Numerical Formulation and Sensitivity Analysis." *Water Resources Research* 31(12): 2945–60.

James, Scott C., and Constantinos V. Chrysikopoulos. 2003. "Analytical Solutions for Monodisperse and Polydisperse Colloid Transport in Uniform Fractures." *Colloids and Surfaces A: Physicochemical and Engineering Aspects* 226(1–3): 101–18.

James, Scott C, and V Chrysikopoulos. 1999. "Transport of Polydisperse Colloid Suspensions in a Single Fracture." *Water Resources Research* 35(3): 707–18.

Kamrani, Salahaddin, Mohsen Rezaei, Mehdi Kord, and Mohammed Baalousha. 2018. "Transport and Retention of Carbon Dots (CDs) in Saturated and Unsaturated Porous Media: Role of Ionic Strength, PH, and Collector Grain Size." *Water Research* 133(1): 338–47.

Lehoux, Alizée P., Pamela Faure, François Lafolie, Stéphane Rodts, Denis Courtier-Murias, Philippe Coussot, and Eric Michel. 2017. "Combined Time-Lapse Magnetic Resonance Imaging and Modeling to Investigate Colloid Deposition and Transport in Porous Media." *Water Research* 123(1): 12–20.

Masciopinto, Costantino, and Fabrizio Visino. 2017. "Strong Release of Viruses in Fracture Flow in Response to a Perturbation in Ionic Strength: Filtration/Retention Tests and Modeling." *Water Research* 126: 240–51.

Mondal, Pulin K, and Brent E Sleep. 2012. "Colloid Transport in Dolomite Rock Fractures: Effects of Fracture Characteristics, Specific Discharge, and Ionic Strength." *Environmental Science and Technology* 46(18): 9987–94.

Natarajan, N., and G. Suresh Kumar. 2014. "Numerical Modelling of Colloidal Transport in Fractured Porous Media with Double Layered." *Journal of Geo-Engineering Sciences* 1(2): 83–94.

Neukum, Christoph. 2018. "Transport of Silver Nanoparticles in Single Fractured Sandstone." *Journal of Contaminant Hydrology* 209(1): 61–67.

Nocito-gobel, Jean, and John E. Tobiason. 1996. “Effects of Ionic Strength on Colloid Deposition and Release.” *Colloids and Surfaces A* 107: 223–31.

Rodrigues, S N, and S E Dickson. 2015. “The Effect of Matrix Properties and Preferential Pathways on the Transport of Escherichia Coli RS2-GFP in Single, Saturated, Variable- Aperture Fractures.” *Environmental Science and Technology* 49(14): 8425–31.

Rodrigues, S N, S E Dickson, and J Qu. 2013. “Colloid Retention Mechanisms in Single, Saturated, Variable-Aperture Fractures.” *Water Research* 47(1): 31–42.

Rodrigues, Sandrina, and Sarah Dickson. 2014. “A Phenomenological Model for Particle Retention in Single, Saturated Fractures.” *Groundwater* 52(2): 277–83.

Ryan, Joseph N., and Menachem Elimelech. 1996. “Colloid Mobilization and Transport in Groundwater.” *Colloids and Surfaces A* 107(95): 1–56.

Saltelli, A, M Ratto, T Andres, F Campolongo, J Cariboni, D Gatelli, M Saisana, and S Tarantola. 2008. *Global Sensitivity Analysis*. The Primer. West Sussex, England: John Wiley & Sons Ltd.

Schiperski, Ferry, Johannes Zirlewagen, and Traugott Scheytt. 2016. “Transport and Attenuation of Particles of Different Density and Surface Charge: A Karst Aquifer Field Study.” *Environmental Science and Technology* 50(15): 8028–35.

Schuster-Wallace, Corinne J., and Sarah E. Dickson. 2017. “Pathways to a Water Secure Community.” *In The Human Face of Water Security*, eds. David Devlaeminck, Zafar Adeel, and Robert Sandford. Springer Nature, 197–216.

Stoll, M., F. M. Huber, E. Schill, and T. Schäfer. 2017. "Parallel-Plate Fracture Transport Experiments of Nanoparticulate illite in the Ultra-Trace Concentration Range Investigated by Laser-Induced Breakdown Detection (LIBD)." *Colloids and Surfaces A: Physicochemical and Engineering Aspects* 529(1): 222–30.

Sun, Yuanyuan, Bin Gao, Scott A. Bradford, Lei Wu, Hao Chen, Xiaoqing Shi, and Jichun Wu. 2015. "Transport, Retention, and Size Perturbation of Graphene Oxide in Saturated Porous Media: Effects of Input Concentration and Grain Size." *Water Research* 68(1): 24–33.

Swanton, Stephen W. 1995. "Modelling Colloid Transport in Groundwater; the Prediction of Colloid Stability and Retention Behaviour." *Advances in Colloid and Interface Science* 54(1): 129–208.

Tang, Yin, Milad Hooshyar, Tingju Zhu, Claudia Ringler, Alexander Y. Sun, Di Long, and Dingbao Wang. 2017. "Reconstructing Annual Groundwater Storage Changes in a Large-Scale Irrigation Region Using GRACE Data and Budyko Model." *Journal of Hydrology* 551(1): 397–406.

Walshe, Gillian E., Liping Pang, Markus Flury, Murray E. Close, and Mark Flintoft. 2010. "Effects of PH, Ionic Strength, Dissolved Organic Matter, and Flow Rate on the Co-Transport of MS2 Bacteriophages with Kaolinite in Gravel Aquifer Media." *Water Research* 44(4): 1255–69.

Wolfsberg, Andrew, Zhenxue Dai, Lin Zhu, Paul Reimus, Ting Xiao, and Doug Ware. 2017. "Colloid-Facilitated Plutonium Transport in Fractured Tuffaceous Rock." *Environmental Science and Technology* 51(10): 5582–90.

Yan, Y D. 1996. “Pulse-Injection Chromatographic Determination of the Deposition and Release Rate Constants of Colloidal Particles in Porous Media.” *Langmuir* 12(14): 3383–88.

Yosri, Ahmed, Ahmad Siam, Wael El-Dakhakhni, and Sarah Dickson-Anderson. 2019. “A Genetic Programming–Based Model for Colloid Retention in Fractures.” *Groundwater* 57(5): 693-703.

Zhang, Wei, Xiangyu Tang, Noam Weisbrod, and Zhuo Guan. 2012. “A Review of Colloid Transport in Fractured Rocks.” *Journal of Mountain Science* 9(6): 770–87.

Zheng, Q, S E Dickson, and Y Guo. 2009. “Differential Transport and Dispersion of Colloids Relative to Solutes in Single Fractures.” *Journal of Colloid and Interface Science* 339(1): 140–51.

Chapter 5

A MODIFIED TIME DOMAIN RANDOM WALK APPROACH FOR SIMULATING COLLOID BEHAVIOR IN FRACTURES: METHOD DEVELOPMENT AND VERIFICATION

ABSTRACT

Colloids are ubiquitous in groundwater systems and, as they can pose a threat to human and environmental health, understanding their behavior is of critical importance. Extensive research has been conducted to model colloid behavior in fractures leading to the development of a number of analytical solutions, albeit for individual fractures. However, the application of such solutions at the network-scale has not yet been established; and thus, fracture networks are typically modeled using numerical techniques that are verified first in single fractures. Time domain random walk (TDRW) is a Lagrangian-based approach originally designed to simulate solute transport in single fractures considering advection, dispersion, and matrix diffusion. Although TDRW usually yields higher accuracy at a lower computational cost compared to other approaches, its application to colloid transport has not yet been verified. The present study overcomes this drawback through developing a modified TDRW approach (MTDRW) based on the analytical solution of colloid transport in single fractures. The MTDRW approach was validated through simulating the behavior of: *i*) monodisperse colloids in a synthetic, single fracture with- and without- matrix diffusion; *ii*) polydisperse

colloids in a synthetic, single fracture with impermeable matrix; and *iii*) monodisperse colloids in a synthetic impermeable fracture network. In all three cases, the MTDRW approach effectively replicated the results of analytical solutions in single fractures and the semi-analytical solution in fracture networks. The developed MTDRW approach is expected to enhance the reliability of colloid transport modelling due to its computational efficiency, and capability of simulating the physiochemical heterogeneity over the network.

Keywords: Time domain random walk, colloid deposition, polydisperse colloids, fracture networks.

5.1. INTRODUCTION

More than 50% of the global population uses groundwater as a source of drinking water, and 35% depend solely on groundwater for their domestic water supply (WWAP 2015). Demands on groundwater are increasing for domestic, agriculture, and industrial purposes, and this increasing reliance on groundwater has accelerated aquifer depletion (Y. Tang et al. 2017; Castellazzi et al. 2018), necessitating the extraction of water from increasing depths where fractured systems most often exist. Fractured systems represent 20% of groundwater aquifers around the globe (Chandra et al. 2019), thereby they provide water for different activities and represent locations for waste isolation in the regions where they exist (Shapiro 2002). In these aquifers, open fractures are the primary conduits for groundwater and contaminants despite representing only a minor portion of the aquifer porosity. Understanding colloid behavior in fractured aquifers has emerged as a critical environmental issue over the past few decades as some colloids are pathogenic (Hunt and Johnson 2016), and others can facilitate or inhibit the transport of dissolved contaminants (Abdel-salam and Chrysikopoulos 1995; Ibaraki and Sudicky 1995; James et al. 2018). Fractures are often connected such that they form a network; however, conclusions about the behavior of colloids at the network-scale has been drawn based on the understanding of their behavior in single fractures (Abdel-salam and Chrysikopoulos 1995). Colloids (e.g., inorganic mineral grains, organic particles, microorganisms, anthropogenic particles) represent a class of contaminants that range in size from a nanometers to 10

micrometers (Buddemeier and Hunt 1988; Hunter 2001; Bekhit and Hassan 2005; Delleur 2007), and are negatively charged under normal groundwater conditions (Zvikelsky and Weisbrod 2006; Hunt and Johnson 2016). The combination of size and surface charge causes colloids to behave differently when compared to dissolved contaminants in groundwater; specifically, colloids can migrate faster and over significant distances due to size and charge exclusion and Taylor dispersion (Ryan and Elimelech 1996). Furthermore, colloids are subject to different forces (e.g., weight, buoyant force, drag force, lift force, Van der Wall attractive forces, repulsive forces, short range repulsive forces) that control their behavior (Ibaraki and Sudicky 1995; Reimus 1995).

While colloid transport in fractures is due to advection and longitudinal dispersion, colloid retention mechnisms include matrix diffusion, physical straining, sedimentation, and deposition (Zhang et al. 2012). Irreversible deposition has been observed as the primary colloid retention mechanism in fractures (Rodrigues and Dickson 2015; Stoll et al. 2017; Cohen and Weisbrod 2018), as: *i*) matrix diffusion is insignificant for colloids in contrast to solutes, especially when the presence of matrix micro-fissures can be neglected (Stoll et al. 2017); *ii*) sedimentation and physical straining are of secondary importance unless the chemical conditions favor coagulation of colloids (Swanton 1995); and, *iii*) remobilization requires perturbing the groundwater-colloid-fracture system physically and/or chemically (Nocito-gobel and Tobiason 1996; Masciopinto and Visino 2017), and was observed to be negligible (Bowen and Epstein 1979; Abdel-

salam and Chrysikopoulos 1994; Elimelech et al. 1995). The DLVO (Derjaguin and Landau 1941; Verwey and Overbeek 1984) and extended DLVO theories have been suggested to describe the combined effect of the different forces acting on a colloid in a flowing suspension, and has been extensively employed to conceptualize colloid-collector interfacial interactions (i.e., colloid deposition) in porous media (Torkzaban et al. 2008; Mondal and Sleep 2013; Zhang et al. 2016; Kamrani et al. 2018b; Shan et al. 2018; Wu et al. 2018; Carstens et al. 2019). However, the assumptions of these theories (e.g., homogenous surface characteristics and flat surfaces) are violated in fractures (Christenson 1988; Degueldre et al. 1996; An et al. 2000), restricting the modelling of colloid deposition based on the forces acting on it. Instead, irreversible colloid deposition has been described macroscopically in fractures through a deposition coefficient (κ) that reflects the system's physical and chemical conditions, and is a fitting parameter typically estimated from laboratory or field investigations (Abdel-salam and Chrysikopoulos 1994).

Contaminant transport in groundwater has been an active research area for many decades. While the classic advection-dispersion equation (ADE) is typically used to describe Fickian transport in homogenous geological formations, several alternatives have been suggested to simulate the non-Fickain transport typically observed in heterogenous media. Such alternatives include: the local ADE approach (Fiori et al. 2013); the multi-rate mass transfer model (Haggerty and Gorelick 1995); time fractional-derivative models (Metzler and Klafter 2000); and the continuous time random walk approach (Berkowitz et al. 2006). However, the ADE

can still be adopted for transport simulations at scales where heterogeneity is negligible. In fractures with surfaces idealized as parallel plates and with a constant dispersion coefficient, coupling the ADE and irreversible colloid deposition results in the advection-dispersion-irreversible deposition equation (ADIDE) that can be utilized to describe colloid behavior. Different studies have been carried out to solve the ADIDE for monodisperse and polydisperse colloids under different boundary and matrix conditions, both numerically (e.g., James et al., 2018; James and Chrysikopoulos, 1999; Natarajan and Kumar, 2014) and analytically (i.e., Abdel-Salam and Chrysikopoulos, 1994; James and Chrysikopoulos, 2003). Despite the accuracy of such analytical solutions, their application has been limited to single fractures; and subsequently, colloid behavior in fracture networks is most often modeled using numerical techniques that are verified first at the single-fracture scale.

Numerical techniques used for colloid transport modeling in fractures are generally classified into: *i*) Eulerian-based (e.g., finite difference, finite elements); and *ii*) Lagrangian-based (random walk) approaches. Eulerian-based approaches rely on converting the ADIDE into a system of algebraic equations at the grid nodes resulting from discretizing the space-time domain (Rausch et al. 2005). Attention must be then paid when discretizing the space-time domain such that Eulerian-based solutions are accurate and free of numerical dispersion. On the other hand, Lagrangian-based approaches depend on replacing the dispersion portion of the transport problem by its equivalent stochastic process (Rausch et al. 2005); and

thereby, do not exhibit numerical issues associated with Eulerian-based approaches. While Eulerian-based approaches are designed to solve the equations describing the underlying physical system directly, Lagrangian-based approaches aim at estimating the behavior of the physical system stochastically. Lagrangian-based approaches include: random walk particle tracking (Prickett et al. 1981), continuous time random walk (Berkowitz and Scher 1997; Berkowitz et al. 2006), and time domain random walk (Banton et al. 1997; Bodin and Delay 2001).

Within Lagrangian-based approaches, time domain random walk (TDRW) is preferred over others in fractures because of its accuracy and computational efficiency, suitability for parallel computing, and extendibility to the network scale. TDRW was first introduced by Banton et al. (1997) to simulate the transport of conservative contaminants in single fractures. In the TDRW approach, the contaminant mass is replaced by a cloud of particles, and the breakthrough curve (BTC) at a downstream location is estimated based on the probability density function (PDF) of particle travel time. A lognormal distribution is typically assumed for particle travel time when TDRW is employed, and the statistics of that distribution are obtained from the Fokker-Planck formalism of the ADE (Banton et al. 1997; Bodin and Delay 2001). When irreversible colloid deposition is introduced, the statistics of the colloid travel time distribution cannot be inferred from the Fokker-Planck formalism of the ADIDE. Therefore, the classic TDRW approach becomes inapplicable.

The objective of the present study is to develop a modified TDRW approach (MTDRW) that can effectively simulate colloid behavior in single fractures considering advection, longitudinal dispersion, matrix diffusion, and irreversible deposition. MTDRW will provide a more flexible tool for simulating colloid behavior in fractured systems as this approach is extendible to the network-scale. Additionally, the MTDRW-based solution adopts κ to simulate colloid deposition; and thus, the MTDRW approach is able to capture physical and chemical heterogeneity across the fracture network. Overall, the MTDRW approach is expected to enhance the reliability of colloid transport models in fractures, and significantly reduce the extensive computation time typically required to simulate colloid behavior in fracture networks.

5.2. MODEL DEVELOPMENT

5.2.1. COLLOID BEHAVIOR IN SINGLE FRACTURES

The two primary mechanisms governing colloid behavior in fractures are advection and irreversible deposition; they are also affected by longitudinal dispersion and matrix diffusion (Figure 5-1). Coupling these mechanisms through the ADIDE provides a mathematical description of colloid behavior in fractures under the assumptions that: *i*) the dispersion coefficient is constant along the fracture; *ii*) the irreversible deposition is dominant over sedimentation and physical straining; *iii*) macroscopic modelling of colloid deposition is achieved using a deposition coefficient that combines the different influencing factors; *iv*) the

chemical and physical characteristics of the groundwater-colloid-fracture system are constant along the fracture (i.e., κ is constant); *v*) colloid deposition inside the matrix is negligible; and, *vi*) the ADE can be applied when colloid deposition is neglected. Subsequently, colloid behavior in a semi-infinite fracture with a permeable matrix and with surfaces idealized as two parallel plates under a uniaxial steady flow can be described mathematically (Abdel-Salam and Chrysikopoulos 1994) as:

$$\frac{\partial C}{\partial t} = D\frac{\partial^2 C}{\partial x^2} - u\frac{\partial C}{\partial x} - \frac{2\kappa u}{b^2}C + \frac{2\theta D_e}{b}\frac{\partial C_m}{\partial z} \qquad (5-1)$$

$$\frac{\partial C_m}{\partial t} = D_e\frac{\partial^2 C_m}{\partial z^2} \qquad (5-2)$$

where C is the concentration of undeposited (i.e., moving) colloids in the fracture, C_m is the colloid concentration in the matrix, D is the longitudinal Taylor dispersion coefficient that combines the effects of molecular diffusion and velocity variation across the fracture, u is the steady-state groundwater velocity, b is the fracture aperture (i.e., the distance between the idealized fracture surfaces), θ is the matrix porosity, D_e is the effective diffusion coefficient, x is the distance along the fracture, z is the distance perpendicular to the fracture axis (measured from the fracture centerline), and t is the time. The expression $\left({}^{2\kappa u}/_{b^2}\, C\right)$ in Equation (5-1) simulates the colloid mass flux eliminated due to irreversible deposition under the assumptions: *i*) previously deposited colloids are not considered; and, *ii*) colloid size is significantly small such that aperture reduction caused by colloids deposited

is negligible. Similar formulae are suggested for that term to describe colloid filtration in porous media (e.g., Harvey and Garabedian, 2005).

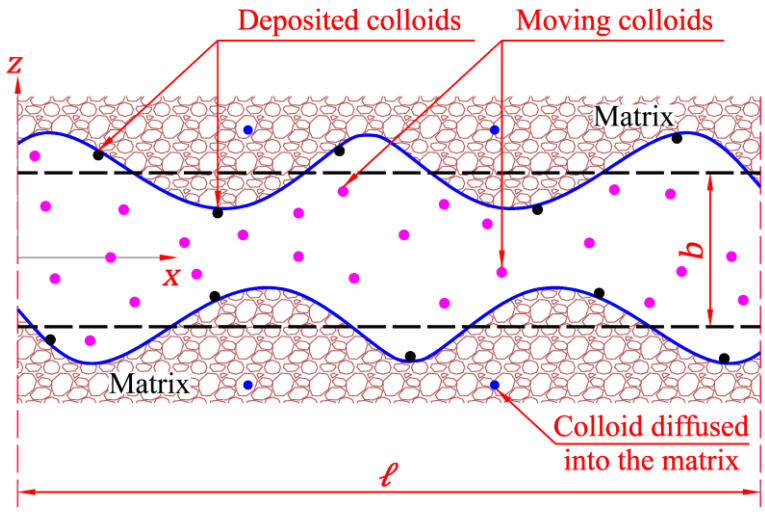

Figure 5-1: Schematic of colloid behavior in a single fracture with surfaces idealized as two parallel plates under irreversible deposition

As the objective of the present study is to develop a modified TDRW approach, MTDRW, to simulate colloid behavior in fractures with different matrix configurations, matrix diffusion is neglected at this stage and will be accounted for later. Abdel-Salam and Chrysikopoulos (1994) solved the system of Equations (5-1 and 5-2) analytically under a constant concentration at the fracture inlet, with- and without- matrix diffusion. This analytical solution for a fracture with an impermeable matrix (i.e., without matrix diffusion) can be written as:

$$C(x,t) = \frac{C_o}{2}\left\{exp\left[\frac{ux}{2D}(1-\xi)\right] erfc\left[\frac{x-ut\xi}{\sqrt{4Dt}}\right] + exp\left[\frac{ux}{2D}(1+\xi)\right] erfc\left[\frac{x+ut\xi}{\sqrt{4Dt}}\right]\right\} \quad (5-3)$$

where C_o is the concentration at the inlet, and ξ is calculated as $\sqrt{1 + {8\kappa D}/{ub^2}}$. Kreft and Zuber (1978) reported several transformation formulae to convert a solution for a constant concentration at the inlet to a corresponding solution under instantaneous injection, depending on whether the flux concentration or the resident concentration is of interest. As Equation (5-3) was originally developed by Abdel-Salam and Chrysikopoulos (1994) for a flux concentration, applying the transformation developed by Danckwerts (1953), and reported in Kreft and Zuber (1978), yields an analytical description of colloid behavior in the same fracture with an instantaneous injection at the inlet:

$$C(x,t) = \frac{M_o x}{Q\sqrt{4\pi D t^3}} exp\left[-\frac{(x-ut)^2}{4Dt}\right] exp\left[-\frac{2\kappa u}{b^2}t\right] \qquad (5-4)$$

where M_o is the mass of colloids injected instantaneously at the inlet, and Q is the volumetric steady-state flow rate in the fracture. At a distance x from the fracture inlet, Equation (5-4) yields a concentration breakthrough curve (BTC) for which the infinite time integral is an indication of the total mass of undeposited colloids arriving at that location. In is noteworthy that Equation (5-4) can also be developed by conceptualizing the irreversible deposition of colloids as a first-order decay, within the same fracture-matrix configuration.

5.2.2. MATRIX DIFFUSION

Matrix diffusion is a very slow process that results in heavy-tailed BTCs. It is influenced by the groundwater velocity, the size of matrix-micro fissures as

compared to particle size, the concentration gradient across the fracture surface, and the pore connectivity within the matrix. As numerical techniques can be employed for contaminant transport modelling at single-fracture and fracture-network scales, efficient numerical representation of matrix diffusion is essential. For solutes, several alternatives have been suggested to simulate their transport in a single fracture when matrix diffusion is considered. These include: *i*) convolution between the solution when matrix diffusion is neglected, and an analytical representation of the fracture-matrix system response to the inlet boundary condition when longitudinal dispersion is neglected (Liu et al. 2017; Shuo Meng et al. 2018); and, *ii*) using a retardation factor (*R*) that accounts for the delay caused by matrix diffusion as compared to pure advection (Bodin and Delay 2001). While the efficacy of both alternatives has been demonstrated, the retardation factor-based approach is preferred as the fracture-matrix system response is difficult to obtain analytically in fracture networks. Bodin and Delay (2001) developed an analytical description for *R* based on the ratio between the characteristic times of advection-matrix diffusion (t_{ad}) and pure advection (t_o):

$$R = 1 + \Omega \left(\frac{8D\ell}{u^3}\right)^{1/4} \left[\frac{exp(-\eta^2)}{\sqrt{\eta}\, erfc(\eta)} - \eta\right] \qquad (5-5)$$

where $\Omega = \sqrt{\theta D_e}/b$, and $\eta = \Omega\ell/u \times \left(2u^3/D\ell\right)^{1/4}$. It is worth noting that *R* tends to 1.0 when matrix diffusion is neglected (i.e., when $\Omega = 0$); and therefore, t_{ad} and t_o are identical. It is also noteworthy that *R* can be calculated for colloids in a

fracture-matrix system using Equation (5-5) with $\Omega = {\theta\sqrt{D_e}}/{b}$ (see Appendix - B for details).

5.2.3. TIME DOMAIN RANDOM WALK APPROACH

Several numerical techniques have been used to simulate contaminant transport in single fractures. Among these approaches, the TDRW approach showed higher accuracy and greater computational efficacy in estimating BTCs for solutes in fractures with and without matrix diffusion (e.g., Bodin and Delay, 2001; Bodin et al., 2003, 2007; Painter et al., 2008). The TDRW approach relies on the fact that a BTC estimated using Equation (5-4) when κ = 0 shows similar behavior to a lognormal PDF at high Peclet numbers (P_e); therefore, the BTC can be recalculated using a lognormal PDF that describes the particle travel time distribution (Bodin and Delay 2001). For lower values of P_e, the accuracy of the TDRW approach can be preserved by modifying the statistics of the lognormal PDF assumed for particle travel time using an empirical correction factor of $\left(1 - {1}/{33P_e}\right)$ (Bodin et al. 2003). When TDRW is employed in a fracture with an impermeable matrix, the solute mass injected is replaced by a cloud of particles for which the travel time follows a lognormal distribution with a mean of ${x}/{u}$ and a variance of ${2Dx}/{u^3}$, as estimated from the Fokker-Planck formalism of the ADE (Banton et al. 1997; Bodin and Delay 2001). The BTC at a distance *x* from the inlet is subsequently estimated as the ratio between the mass flux (expressed as a function of the travel time PDF,

or equivalently the travel time histogram) and *Q*. When matrix diffusion is considered to be reversible, particle travel time is the summation of: *i*) a lognormal random variable (t'_p) with a mean of x/uR and a variance of $2Dx/u^3$ to represent the travel time through the open fracture; and *ii*) a random variable representing the particle residence time within the matrix (Bodin and Delay 2001). The total particle travel time is then expressed as:

$$t_p = t'_p + \left[\frac{\Omega x}{u\, erfc^{-1}(U_{01})}\right]^2 \qquad (5-6)$$

where U_{01} is a uniform random number between 0 and 1. It should be mentioned that when matrix diffusion is considered, solute particles are assumed to migrate with an average apparent velocity of *uR* instead of the groundwater velocity (i.e., *u*). Subsequently, *D* should be calculated based on this apparent velocity when solute dispersion is velocity dependent. It is also noteworthy that TDRW should either be applied with a large number of particles (typically hundreds of thousands) or be embedded within a Monte-Carlo framework to eliminate the random noise existing in the estimated BTC as a result of the stochastic nature of this approach.

5.2.4. MODIFIED TIME DOMAIN RANDOM WALK APPROACH

While the classical TDRW approach is efficient for simulating solute transport at the single fracture and fracture network scales, its application to colloid behavior has not yet been established. As discussed above, the classic TDRW approach was developed based on the comparison between solute BTCs and

particle travel time distributions in single fractures, where a lognormal PDF is typically employed. Therefore, the MTDRW approach is based on the determination of an appropriate PDF to effectively describe colloid travel time in fractures. Since it is possible to develop an exact travel time PDF using the analytical description of colloid behavior (Equation (5-4)), this approach was chosen over comparing colloid BTCs to theoretical PDFs. This exact PDF is based on the total number of particles travelling a distance *x* from the inlet at time *t*, obtained by integrating the BTC, derived from Equation (5-4). Similar procedures have been used to estimate particle travel time and mass recovery in porous media for one- two- and three-dimensional transport (Bodin 2015). While the infinite time integral of a colloid BTC at a distance *x* from the inlet of a fracture with an impermeable matrix yields M_o/Q when deposition is neglected (i.e., κ = 0 in Equation (5-4)), the corresponding integral when deposition is considered yields $M'(x)/Q$, where *M'(x)* is the total colloid mass arriving at that distance *x*. The mass *M'(x)*, the cumulative distribution function (CDF) of colloid travel time (F_t), and the corresponding PDF (f_t) at that location can be calculated, respectively:

$$M'(x) = M_o \, exp\left[\frac{ux}{2D}(1-\xi)\right] \qquad (5-7)$$

$$F_t(x,t) = \frac{1}{2}\left[erfc\left(\frac{x-ut\xi}{\sqrt{4Dt}}\right) + exp\left(\frac{ux}{D}\xi\right) erfc\left(\frac{x+ut\xi}{\sqrt{4Dt}}\right)\right] \qquad (5-8)$$

$$f_t(x,t) = \frac{x}{2\sqrt{\pi D t^3}} \exp\left[-\frac{(x-ut\xi)^2}{4Dt}\right] \qquad (5-9)$$

where F_t is calculated as the ratio between the colloid mass travelling a distance x up to time t $\left(\int_0^t QC(x,t)dt\right)$ and the total colloid mass travelling the same distance over infinite time $\left(\int_0^\infty QC(x,t)dt\right)$; and f_t is the time derivative of F_t, with C is calculated using Equation (5-4). While f_t and F_t differ from those of any well-known statistical distribution, the colloid travel time PDF can still be approximated by a lognormal PDF (f_t') with the same first and second moments as those of f_t (Table 5-1), and a corresponding CDF (F_t'). Although higher moments of f_t' deviate from those of f_t for $P_e\xi$ < 10 (Table 5-1), a correction factor of $\left(1 - {}^{1}/_{33P_e\xi}\right)$, similar to that introduced by Bodin and Delay (2001) for the classic TDRW approach, can be employed to reduce this deviation. The first two moments of both f_t and f_t' (Table 5-1) support the faster migration and lower effective dispersion of colloids over solutes as ξ is always greater than 1.0. This has also been reported by others who used different approaches (e.g., Cohen and Weisbrod, 2018; James and Chrysikopoulos, 2003a; Mckay et al., 1993; Zvikelsky and Weisbrod, 2006). This supports the ability of the MTDRW approach to replicate the main features of colloid behavior reported in other studies.

The MTDRW approach relies on assigning a travel time t_{pm} to each colloid, where t_{pm} follows either f_t or f_t' with moments shown in Table 5-1. While the former (i.e., using f_t) is more accurate, the latter (i.e., using f_t') is more computationally efficient in fracture networks where colloids move through multiple fractures and the total colloid travel time is the summation of t_{pm} in each fracture. As t_{pm} in each

fracture is independent from that in others, and when f_t' is used to describe the distribution of t_{pm}, the total colloid travel time through a series of fractures can also be approximated by a lognormal distribution with equivalent statistics (Fenton 1960; Schwartz and Yeh 1982; Beaulieu and Xie 2004; Mehta et al. 2007). Therefore, colloid behavior at the network-scale can be efficiently described without loss of accuracy when f_t' is utilized to approximate the colloid travel time distribution through each single fracture within the network.

Table 5-1: Comparison between the first four moments of the exact colloid travel time distribution and the lognormal distribution approximation

	Travel time PDF $f_t(x,t)$	**Lognormal distribution PDF** $f_t'(x,t)$
Mean (μ)	$\frac{x}{u\xi}$	$\frac{x}{u\xi}$
Variance (σ^2)	$\frac{2Dx}{u^3\xi^3}$	$\frac{2Dx}{u^3\xi^3}$
Skewness (γ_1)	$\sqrt{\frac{18}{P_e\xi}}$	$\sqrt{\frac{18}{P_e\xi}}+\sqrt{\frac{8}{P_e^3\xi^3}}$
Kurtosis (γ_2)	$\frac{30}{P_e\xi}$	$\frac{32}{P_e\xi}+\frac{60}{P_e^2\xi^2}+\frac{48}{P_e^3\xi^3}+\frac{16}{P_e^4\xi^4}$

If colloid diffusion into the matrix is considered, Equation (5-6) can still be applied within the MTDRW approach to generate colloid travel time with t_p' replaced by a modified version of t_{pm}. This modified travel time, t_{pm}', is also

lognormally distributed with a mean of $x/u\xi R$ and a variance of $2Dx/u^3\xi^3$, where R is the retardation factor estimated using Equation (5-5) with $\Omega = \theta\sqrt{D_e}/b$. As matrix diffusion is a very slow process, the total mass recovery occurs after very long time that might be beyond the time frame of interest; and therefore, Equation (5-6) may result in t_p equals to ∞ when large values of U_{01} are generated. A truncated travel time distribution can then be adopted through removing the outliers of t_p, resulting in a maximum colloid travel time of t_{max}. The particles with travel time larger than t_{max} are then eliminated; thereby, $M'(x)$ is modified to be:

$$M'(x) = M_o \, exp\left[\frac{ux}{2D}(1-\xi)\right] erfc\left[\frac{\theta\sqrt{D_e}x}{u\sqrt{t_{max} - x/u}}\right] \qquad (5-10)$$

where $1 - erfc\left[\frac{\theta\sqrt{D_e}x}{u\sqrt{t_{max}-x/u}}\right]$ represents the ratio of colloid mass eliminated due to the slow nature of matrix diffusion (i.e., colloids with infinite residence time in the matrix such that their travel time is larger than t_{max}).

It is worth noting that colloids were assumed to be monodisperse in the analytical solution by Abdel-Salam and Chrysikopoulos (1994); however, naturally-occurring colloid suspensions typically contains polydisperse particles with diameters following a lognormal distribution (Ledin et al. 1994). Analytical solutions for the transport of polydisperse colloids in single fractures with impermeable matrix exist under different boundary conditions (James and Chrysikopoulos 2003a). The MTDRW approach is also capable of simulating the

behavior of polydisperse colloids through assigning a different dispersion coefficient to each particle based on the dispersion–diffusion–particle size relationship. Multiple CDFs are then adopted, each of which is used to assign a t_{pm} to the corresponding particle. Figure 5-2 shows an example, based on five diameters, of F_t and F_t' for polydisperse colloids calculated at the end of a fracture with characteristics obtained from the study by James and Chrysikopoulos (1999); colloid diameter is assumed to follow lognormal distribution with a mean of 1 μm and a standard deviation of $\sqrt{0.9}$ μm.

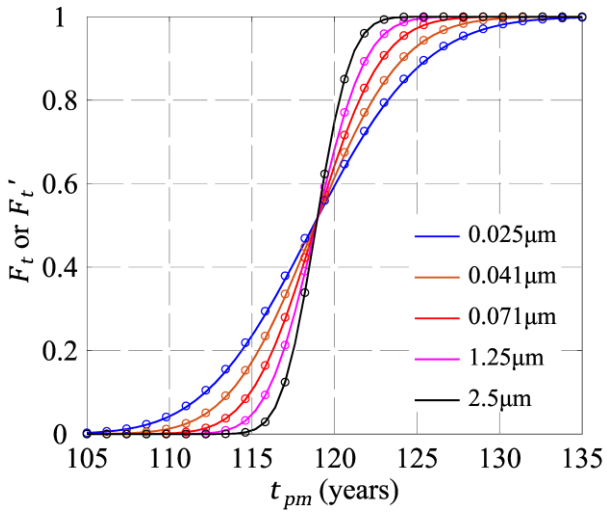

Figure 5-2: Exact travel time CDF, F_t, and the lognormal CDF approximating it (F_t') for polydisperse colloids. Solid lines and open circles represent F_t and F_t', respectively

5.3. METHOD VERIFICATION

Three different cases were chosen to demonstrate the efficacy of the MTDRW approach in simulating colloid behavior: *i*) monodisperse colloids in a synthetic, parallel-plate, single fracture with a constant concentration at the inlet under both

impermeable and permeable matrix conditions; *ii*) polydisperse colloids in a synthetic, parallel-plate, single fracture with a constant concentration at the inlet and an impermeable matrix; and, *iii*) monodisperse colloids in an impermeable, synthetic fracture network within a 10,000 m^2 square domain (Figure 5-3) under an instantaneous injection at the inlet boundary. The fracture and colloid characteristics as well as the boundary conditions for each of these cases are given in Table 5-2. For case *ii*, colloid deposition was represented through the dimensionless Damköhler number (D_a) defined in James and Chrysikopoulos (2003a) and is related to κ through $D_a = 12\kappa u/(12D_e - 2\kappa u)$. A single value of D_a was assigned to all particles to represent colloid deposition, which implicitly implies that κ varies among the colloids according to their diameter. In addition, D was related to colloid diameter and D_a as described by James and Chrysikopoulos (2003a).

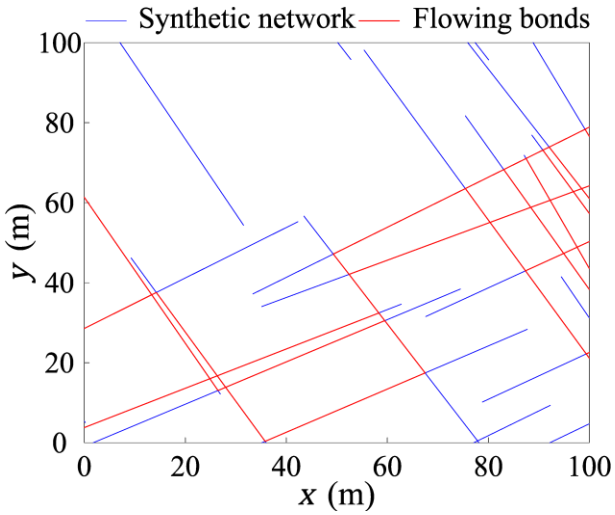

Figure 5-3: The synthetic impermeable fracture network employed within the MTDRW approach in the verification case *iii*

Table 5-2: Fracture characteristics, colloid characteristics, and boundary conditions employed in the different verification cases of the MTDRW approach

- **Case *i***
  - Fracture characteristics: (Abdel-Salam and Chrysikopoulos 1994)
    ℓ = 5 m b = 125 μm u = 1 m/year
    κ/b^2 = 6.4x10^{-3} m^{-1}, 3.2x10^{-2} m^{-1}, and 1.6x10^{-1} m^{-1} θ = 1 %.
  - Colloid characteristics: (Abdel-Salam and Chrysikopoulos 1994)
    Monodisperse Diameter = 1 μm
    D = 0.25 m^2/year D_e = 1.29x10^{-5} m^2/year
  - Transport boundary condition at the inlet: Constant concentration at the fracture inlet
- **Case *ii***
  - Fracture characteristics: (Abdel-Salam and Chrysikopoulos 1994)
    ℓ = 5 m b = 125 μm u = 1 m/year
    D_a = 1x10^{-6}, 1x10$^{-4.5}$, and 1x10^{-4} θ = 0 %.
  - Colloid characteristics: (James and Chrysikopoulos 1999)
    Polydisperse with diameter following lognormal distribution with a mean of 1 μm and a standard deviation of 0.9 μm
    D_e is related to the diameter D is related to the diameter and D_a
  - Transport boundary condition at the inlet: Constant concentration at the fracture inlet
- **Case *iii***
  - Fracture characteristics:
    b = 100 μm κ/b^2 = 6.4x10^{-3} m^{-1}, 3.2x10^{-2} m^{-1}, and 1.6x10^{-1} m^{-1}
  - Colloid characteristics:
    Monodisperse Diameter = 1 μm
    D = 0.25 m^2/year D_e = 1.29x10^{-5} m^2/year
  - Flow boundary conditions:
    North: no-flow South: no-flow
    East: specified head = 100 m West: specified head = 90 m
  - Transport boundary conditions at the inlet: Instantaneous injection along the West boundary

A cloud of 10,000 colloidal particles was injected at the inlet in all three cases, and each particle was assigned a t_{pm} or t_p value depending on whether a permeable or impermeable matrix is assumed. The MTDRW approach was also embedded within a Monte-Carlo framework with 500 realizations to reduce the expected noise in the resulting BTCs. The ensemble average BTC was estimated at the outlet boundary through: 1) estimating the histogram of colloid travel time; 2) calculating the corresponding travel time PDF (*ft'*); and, 3) calculating $C_{out}(t) = {M' f'(t)}/{Q\Delta t}$ where C_{out} is the effluent concentration, *M'* is the total effluent mass (mass exiting the fracture in cases *i* and *ii*, and mass exiting the network in case *iii*), and Δt is the histogram bin width. The results from the application of MTDRW for the first two cases were compared to those obtained from the analytical solutions developed by Abdel-Salam and Chrysikopoulos (1994) and by James and Chrysikopoulos (2003a), respectively. On the other hand, a semi-analytical solution similar to that developed by Bodin et al. (2003) for solute transport in fracture networks was adopted to assess the efficacy of the MTDRW approach in case *iii*. This semi-analytical solution relies on converting the fracture network into a set of elementary paths, each of which represents a possible path that a colloid may follow, and can be written as (Bodin et al. 2003):

$$C(t) = \frac{M_o}{Q_{tot}} \sum_{k=1}^{Np} \left[\left(\prod_{j=2}^{Nj-1} \varepsilon_{kj} \right) f_{eq}^{k}(t) \right] \qquad (5-11)$$

where k is the elementary path index (k = 1, 2, …, N_p) with N_p is the number of elementary paths, Q_{tot} is the summation of the volumetric flow rate over all elementary paths, j is the junction index along each path, N_j is the number of junctions along the elementary path k, ε_{kj} is the mass sharing ratio at the junction j in the elementary path k, and f_{eq}^{k} is the colloid's equivalent travel time PDF through the elementary path k. Each elementary path, with index k, consists of $N_j - 1$ fractures (with an index of w = 1, 2, …, $N_j - 1$) connected in series, and the equivalent characteristics of an elementary path can be obtained from those of the fracture series. As t_{pm} is a lognormal random variable, the total colloid travel time through an impermeable elementary path can be approximated by a lognormal random variable (Fenton 1960; Schwartz and Yeh 1982; Beaulieu and Xie 2004; Mehta et al. 2007). Subsequently, f_{eq} is estimated for each elementary path k as:

$$f_{eq}(t) = \frac{\ell_{eq}}{2\sqrt{\pi D_{eq} t^3}} exp\left[-\frac{\left(\ell_{eq} - u_{eq} t \xi_{eq}\right)^2}{4 D_{eq} t}\right] \qquad (5-12)$$

where the equivalent characteristics (ℓ_{eq}, u_{eq}, D_{eq}, and ξ_{eq}) are estimated based on the mass conservation for groundwater and colloids within both systems (i.e., the elementary path and the corresponding fracture series), and can be written as:

$$u_{eq} = \sqrt[3]{\frac{2 D_{eq} \ell_{eq}}{\xi_{eq}^3}} \left(\sum_{w=1}^{N_j - 1} \frac{2 D_w \ell_w}{u_w^3 \xi_w^3}\right)^{-1/3} \qquad (5-13)$$

$$\ell_{eq} = \frac{1}{u_{eq}^3} \sum_{w=1}^{N_j-1} \ell_w u_w^3 \qquad (5-14)$$

$$\xi_{eq} = \frac{\ell_{eq}}{u_{eq}} \left(\sum_{w=1}^{N_j-1} \frac{\ell_w}{u_w \xi_w} \right)^{-1} \qquad (5-15)$$

$$D_{eq} = \frac{1}{2} \ell_{eq} u_{eq} (1-\xi_{eq}) \left[\sum_{w=1}^{N_j-1} \frac{u_w \ell_w}{2D_w} (1-\xi_w) \right]^{-1} \qquad (5-16)$$

As MTDRW generally yields BTCs corresponding to an instantaneous injection at the inlet whereas the analytical solutions by Abdel-Salam and Chrysikopoulos (1994) and James and Chrysikopoulos (2003a) were developed for a constant concentration at the inlet, the transformation rule $\left({}^{C_o Q}/_{M_o} \times \int_0^t C_{out}(t)dt \right)$ developed by Danckwerts (1953) was applied to the MTDRW-based BTCs in cases *i* and *ii* for comparison. In contrast, the semi-analytical solution for fracture networks is corresponding to an instantaneous injection at the inlet. However, the transformation rule was also applied to the MTDRW-based and semi-analytical BTCs in case *iii* for consistency.

5.4. RESULTS AND DISCUSSION

The MTDRW approach efficiently replicates the analytical BTCs for cases (*i* and *ii*) and the semi-analytical BTCs for case *iii* at the different deposition levels as shown in Figure 5-4. As expected, increasing deposition level enhances the colloid-

fracture wall interaction leading to a decrease in the peak concentration (Figure 5-4). In addition, the presence of matrix diffusion in case *i* reduces the peak concentration (see the vertical axis in Figure 5-4a and Figure 5-4b) as the matrix behaves as a reservoir that stores some colloids for an extended period of time. It is noteworthy that nearly steady state concentrations are achieved in case *i* after longer times when matrix diffusion is considered (80 to 100 years compared to 8 to 10 years when matrix diffusion is neglected) supporting the fact that matrix diffusion is a very slow process. The results from all three cases support the efficacy of the MTDRW approach in simulating colloid behavior at single fracture and fracture network scales; therefore, enhance the reliability of colloid transport modelling in fractured systems. Furthermore, utilizing κ or D_a to simulate colloid deposition enable the MTDRW approach to incorporate the physical and chemical heterogeneity over a fracture network, and even in a single fracture by discretizing it into segments with homogenous physical and chemical properties

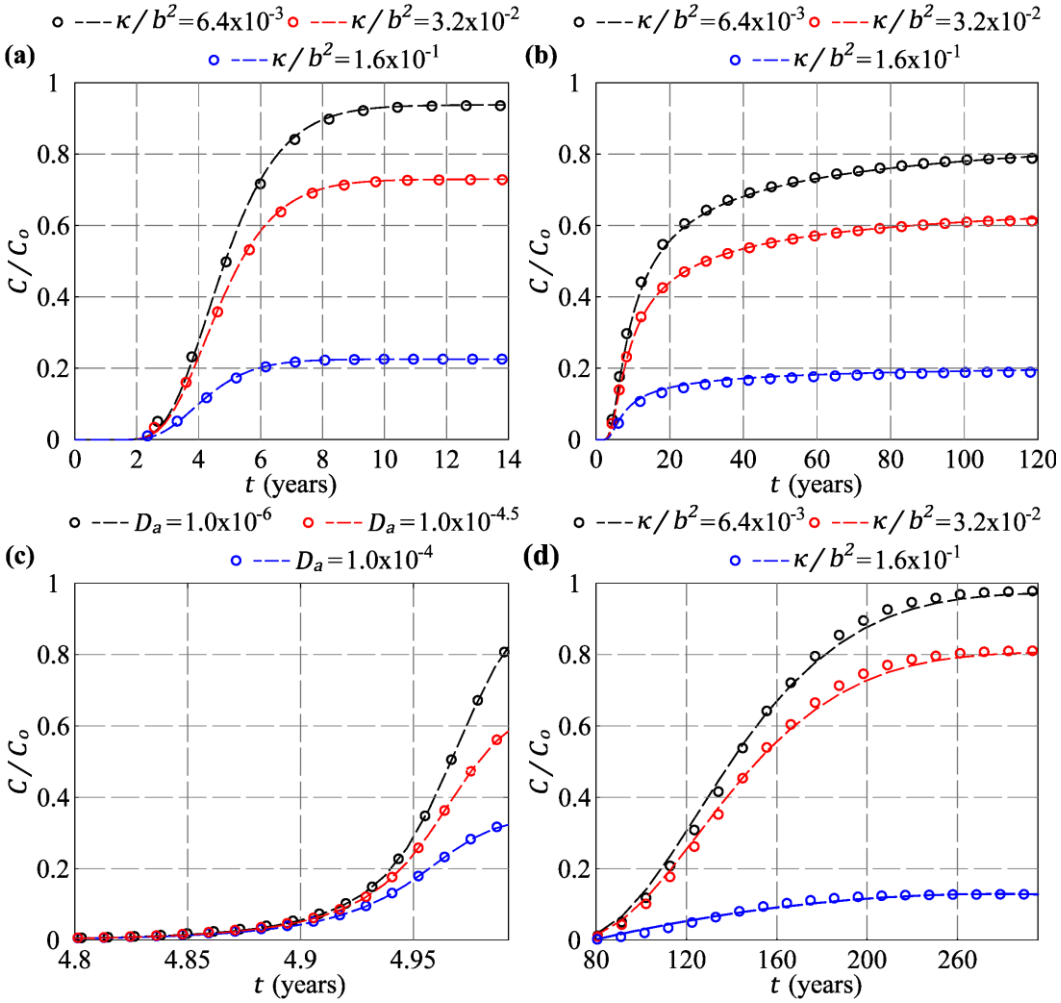

Figure 5-4: Comparison between MTDRW-based BTCs and (a) analytical BTCs in case *i* when matrix diffusion is neglected; (b) analytical BTCs in case *i* when matrix diffusion is considered; (c) analytical BTCs for case *ii*; and, (d) semi-analytical BTCs in case *iii*. Dashed lines represent analytical and semi-analytical BTCs, and scatter points represent the corresponding MTDRW-based BTCs

5.5. CONCLUSIONS

The equivalence between colloid BTCs in a single fracture and the travel time PDF enabled the development of the MTDRW approach that can effectively simulate the behavior of monodisperse and polydisperse colloids in fractures. The developed MTDRW approach is capable of simulating colloid advection,

longitudinal dispersion, matrix diffusion, and irreversible deposition. The efficacy of MTDRW was demonstrated through its ability to simulate the behavior of: *i*) monodisperse colloids in a synthetic, parallel-plate, single fracture with impermeable and permeable matrix and under a constant concentration at the inlet; *ii*) polydisperse colloids in a synthetic, parallel-plate, single fracture with impermeable matrix under constant concentration at the inlet; and *iii*) monodisperse colloids in a synthetic impermeable fracture network under an instantaneous injection at the inlet boundary. The MTDRW-based BTCs were compared to the corresponding estimates of analytical solutions in single fractures, and a semi-analytical solution for impermeable fracture networks. The verification results of the present study support the efficacy of the MTDRW approach in simulating colloid behavior in fractured systems with different matrix conditions and under multiple deposition levels. Overall, MTDRW is expected to enhance the reliability of colloid transport models as it is more computationally efficient and can also capture the chemical and physical heterogeneity of the groundwater-colloid-fracture system through using a deposition coefficient that varies within the aquifer.

5.6. ACKNOWLEDGEMENT

This research was supported by NSERC through the Canadian Nuclear Energy Infrastructure Resilience under Systemic Risk (CaNRisk) – Collaborative Research and Training Experience (CREATE) and Discovery Grant programs.

5.7. NOTATIONS

b:	Fracture aperture
C:	Concentration of undeposited colloids
C_m:	Colloid concentration in the matrix
C_{out}:	Effluent colloid concentration
D:	Longitudinal Taylor dispersion coefficient
D_e:	Effective diffusion coefficient
D_{eq}:	Equivalent dispersion coefficient in an elementary path
f_{eq}^{k}:	Colloid's equivalent travel time PDF through the elementary path k
f_t:	PDF of colloid travel time
F_t:	CDF of colloid travel time
f_t':	Lognormal PDF approximating f_t
F_t':	Lognormal CDF approximating F_t
j:	Junction index along each elementary path
k:	Elementary path index
ℓ:	Fracture length
ℓ_{eq}:	Equivalent length of an elementary path
$M'(x)$:	Total colloid mass arriving at a distance x

M':	Total effluent mass
M_o:	Injected mass of colloids
N_j:	Number of junctions along the elementary path k
N_p:	Number of elementary paths
P_e:	Peclet number
Q:	Steady state volumetric flow rate
Q_{tot}:	Summation of the volumetric flow rate over all elementary paths
R:	Retardation factor caused by matrix diffusion
t:	Time
t_{ad}:	Characteristic time of advection-matrix diffusion
t_o:	Characteristic time of pure advection
t_p:	Total particle travel time in a fracture-matrix system when matrix diffusion is considered
t'_p:	Travel time of a solute particle through the open fracture when matrix diffusion is considered
t_{pm}:	Travel time of a colloid through the open fracture when matrix diffusion is neglected
t'_{pm}:	Travel time of a colloid through the open fracture when matrix diffusion is considered
u:	Steady-state groundwater velocity

U_{01}: Uniform random number between 0 and 1

u_{eq}: Equivalent steady-state groundwater velocity in an elementary path

w: Fracture index within an elementary path k

x: Distance along the fracture

z: Distance perpendicular to the fracture axis

Δt: Bin width of the travel time histogram

Greek Letters:

γ_1: Skewness of colloid travel time distribution

γ_2: Kurtosis of colloid travel time distribution

θ: Matrix porosity

κ: Deposition coefficient

μ: Mean of colloid travel time distribution

σ^2: Variance of colloid travel time distribution

ε_{kj}: Mass sharing ratio at the junction j in the elementary path k

5.8. ACRONYMS

ADE: Advection-dispersion equation

ADIDE: Advection-dispersion-irreversible deposition equation

BTC: Concentration breakthrough curve

CDF: Cumulative distribution function

MTDRW: Modified time domain random walk approach

PDF: Probability density function

TDRW: Time domain random walk

5.9. REFERENCES

Abdel-salam, Assem, and Constantinos V Chrysikopoulos. 1994. “Analytical Solutions for One-Dimensional Colloid Transport in Saturated Fractures.” *Advances in Water Resources* 17(5): 283–96.

Abdel-salam, Assem, and Constantinos V Chrysikopoulos. 1995. “Analysis of a Model for Contaminant Transport in Fractured Media in the Presence of Colloids.” *Journal of Hydrology* 165(1–4): 261–81.

An, Yuehuei H., Richard B. Dickinson, and Ronald J. Doyle. 2000. “Mechanisms of Bacterial Adhesion and Pathogenesis of Implant and Tissue Infections.” *In Handbook of Bacterial Adhesion,* eds. Y.H. An and R.J. Friedman. Totowa, NJ: Humana Press, 1–27.

Banton, Olivier, Frédérick Delay, and Gilles Porel. 1997. “A New Time Domain Random Walk Method for Solute Transport in 1-D Heterogenous Media.” *Groundwater* 35(6): 1008–13.

Beaulieu, Norman C., and Qiong Xie. 2004. “An Optimal Lognormal Approximation to Lognormal Sum Distributions*.” IEEE Transactions on Vehicular Technology* 53(2): 479–89.

Bekhit, Hesham M., and Ahmed E. Hassan. 2005. “Stochastic Modeling of Colloid-Contaminant Transport in Physically and Geochemically Heterogeneous Porous Media.” *Water Resources Research* 41(2).

Berkowitz, Brian, Andrea Cortis, Marco Dentz, and Harvey Scher. 2006. "Modeling Non-Fickian Transport in Geological Formations as a Continuous Time Random Walk." *Reviews of Geophysics* 44(2): 1–49.

Berkowitz, Brian, and Harvey Scher. 1997. "Anomalous Transport in Random Fracture Networks." *Physical Review Letters* 79(20).

Bodin, Jacques. 2015. "From Analytical Solutions of Solute Transport Equations to Multidimensional Time-Domain Random Walk (TDRW) Algorithms." *Water Resources Research* 51(1): 1860–71.

Bodin, Jacques, and Frederick Delay. 2001. "Time Domain Random Walk Method to Simulate Transport by Advection-Dispersion and Matrix Diffusion in Fracture Networks." *Geophysical Research Letters* 28(21): 4051–54.

Bodin, Jacques, Gilles Porel, and Fred Delay. 2003. "Simulation of Solute Transport in Discrete Fracture Networks Using the Time Domain Random Walk Method." *Earth and Planetary Science Letters* 208(3–4): 297–304.

Bodin, Jacques, Gilles Porel, Fred Delay, Fabrice Ubertosi, Stéphane Bernard, and Jean Raynald de Dreuzy. 2007. "Simulation and Analysis of Solute Transport in 2D Fracture/Pipe Networks: The SOLFRAC Program." *Journal of Contaminant Hydrology* 89(1–2): 1–28.

Bowen, Bruce D., and Norman Epstein. 1979. "Fine Particle Deposition in Smooth Parallel-Plate Channels." *Journal of Colloid and Interface Science* 72(1): 81–97.

Buddemeier, Robert W., and James R. Hunt. 1988. "Transport of Colloidal Contaminants in Groundwater: Radionuclide Migration at the Nevada Test Site." *Applied Geochemistry* 3(5): 535–48.

Carstens, Jannis F., Jörg Bachmann, and Insa Neuweiler. 2019. "A New Approach to Determine the Relative Importance of DLVO and Non-DLVO Colloid Retention Mechanisms in Porous Media." *Colloids and Surfaces A: Physicochemical and Engineering Aspects* 560: 330–35.

Castellazzi, Pascal, Laurent Longuevergne, Richard Martel, Alfonso Rivera, Charles Brouard, and Estelle Chaussard. 2018. "Quantitative Mapping of Groundwater Depletion at the Water Management Scale Using a Combined GRACE/InSAR Approach." *Remote Sensing of Environment* 205(1): 408–18.

Chandra, Subash, Esben Auken, Pradip K. Maurya, Shakeel Ahmed, and Saurabh K. Verma. 2019. "Large Scale Mapping of Fractures and Groundwater Pathways in Crystalline Hardrock by AEM." *Scientific Reports* 9(1): 1–11.

Christenson, H. K. 1988. "Non-DLVO Forces between Surfaces - Solvation, Hydration and Capillary Effects" *Journal of Dispersion Science and Technology* 9(2): 171–206.

Cohen, Meirav, and Noam Weisbrod. 2018. "Transport of Iron Nanoparticles through Natural Discrete Fractures." *Water Research* 129(1): 375–83.

Danckwerts, P.V. 1953. "Continuous Flow Systems Distribution of Residence Times." *Chemical Engineering Science* 2(1): 1–13.

Degueldre, C, R Grauer, A Laube, A Oess, and H Silby. 1996. "Colloid Properties in Granitic Groundwater Systems. II: Stability and Transport Study." *Applied Geochemistry* 11(5): 697–710.

Delleur, Jacques W. 2007. *The Handbook of Groundwater Engineering*. 2nd ed. Boca Raton, FL: Taylor & Francis Group, LLC.

Derjaguin, B., and L. D. Landau. 1941. "Theory of the Stability of Strongly Charged Lyophobic Sols and of the Adhesion of Strongly Charged Particles in Solutions of Electrolytes." *Acta Physicochimica* U.R.S.S. 14: 633–62.

Elimelech, M., J. Gregory, X. Jia, and R.A. Williams. 1995. *Particle Deposition and Aggregation: Measurement, Modeling and Simulation*. Oxford: Butterworth-Heinemann.

Fenton, Lawrence F. 1960. "The Sum of Log-Normal Probability Distributions in Scatter Transmission Systems." *IRE Transactions on Communications Systems* 8(1): 57–67.

Fiori, A., G. Dagan, I. Jankovic, and A. Zarlenga. 2013. "The Plume Spreading in the MADE Transport Experiment: Could It Be Predicted by Stochastic Models?" *Water Resources Research* 49(5): 2497–2507.

Haggerty, Roy, and Steven M. Gorelick. 1995. "Multiple-Rate Mass Transfer for Modeling Diffusion and Surface Reactions in Media with Pore-Scale Heterogeneity." *Water Resources Research* 31(10): 2383–2400.

Harvey, Ronald W., and Stephen P. Garabedian. 2005. "Use of Colloid Filtration Theory in Modeling Movement of Bacteria through a Contaminated Sandy Aquifer." *Environmental Science and Technology* 25(1): 178–85.

Hunt, Randall J, and William P Johnson. 2016. "Pathogen Transport in Groundwater Systems: Contrasts with Traditional Solute Transport." *Hydrogeology Journal* 25(4): 921–930.

Hunter, Robert J. 2001. *Foundation of Colloid Science*. 2nd Edition. New York.

Ibaraki, M, and E A Sudicky. 1995. "Colloid-Facilitated Transport in Discretely Fractured Porous Medium: 1. Numerical Formulation and Sensitivity Analysis." *Water Resources Research* 31(12): 2945–60.

James, Scott C., and Constantinos V. Chrysikopoulos. 2003a. "Analytical Solutions for Monodisperse and Polydisperse Colloid Transport in Uniform Fractures." *Colloids and Surfaces A: Physicochemical and Engineering Aspects* 226: 101–18.

James, Scott C., and Constantinos V. Chrysikopoulos. 2003b. "Effective Velocity and Effective Dispersion Coefficient for Finite-Sized Particles Flowing in a Uniform Fracture." *Journal of Colloid and Interface Science* 263(1-3): 288–95.

James, Scott C., Lichun Wang, and Constantinos V. Chrysikopoulos. 2018. "Modeling Colloid Transport in Fractures with Spatially Variable Aperture and Surface Attachment." *Journal of Hydrology* 566: 735–42.

James, Scott C, and V Chrysikopoulos. 1999. "Transport of Polydisperse Colloid Suspensions in a Single Fracture." *Water Resources Research* 35(3): 707–18.

Kamrani, Salahaddin, Mohsen Rezaei, Mehdi Kord, and Mohammed Baalousha. 2018. "Transport and Retention of Carbon Dots (CDs) in Saturated and Unsaturated Porous Media: Role of Ionic Strength, PH, and Collector Grain Size." *Water Research* 133: 338–47.

Kreft, A, and A Zuber. 1978. “On the Physical Meaning of the Dispersion Equation and Its Solutions for Different Initial and Boundary Conditions.” *Chemical Engineering Science* 33(11): 1471–80.

Ledin, Anna, Stefan Karlsson, Anders Düker, and Bert Allard. 1994. “Measurements in Situ of Concentration and Size Distribution of Colloidal Matter in Deep Groundwaters by Photon Correlation Spectroscopy.” *Water Research* 28(7): 1539–45.

Liu, Longcheng, Ivars Neretnieks, Pirouz Shahkarami, Shuo Meng, and Luis Moreno. 2017. “Solute Transport along a Single Fracture in a Porous Rock: A Simple Analytical Solution and Its Extension for Modeling Velocity Dispersion.” *Hydrogeology Journal* 26(1): 297–320.

Masciopinto, Costantino, and Fabrizio Visino. 2017. “Strong Release of Viruses in Fracture Flow in Response to a Perturbation in Ionic Strength: Filtration/Retention Tests and Modeling.” *Water Research* 126: 240–51.

Mckay, Larry D, W Gillham, and John A Cherry. 1993. “Field Experiments in a Fractured Clay Till: 2. Solute and Colloid Transport.” *Water Resources Research* 29(12): 3879–90.

Mehta, Neelesh B., Jingxian Wu, Andreas F. Molisch, and Jin Zhang. 2007. “Approximating a Sum of Random Variables with a Lognormal.” *IEEE Transactions on Wireless Communications* 6(7): 2690–99.

Meng, Shuo, Longcheng Liu, Batoul Mahmoudzadeh, Ivars Neretnieks, and Luis Moreno. 2018. “Solute Transport along a Single Fracture with a Finite Extent of Matrix: A

New Simple Solution and Temporal Moment Analysis." *Journal of Hydrology* 562: 290–304.

Metzler, Ralf, and Joseph Klafter. 2000. "The Random Walk's Guide to Anomalous Diffusion: A Fractional Dynamics Approach." *Physics Report* 339(1): 1–77.

Mondal, Pulin K., and Brent E. Sleep. 2013. "Virus and Virus-Sized Microsphere Transport in a Dolomite Rock Fracture." *Water Resources Research* 49: 808–24.

Natarajan, N., and G. Suresh Kumar. 2014. "Numerical Modelling of Colloidal Transport in Fractured Porous Media with Double Layered." *Journal of Geo-Engineering Sciences* 1(2): 83–94.

Nocito-gobel, Jean, and John E. Tobiason. 1996. "Effects of Ionic Strength on Colloid Deposition and Release." *Colloids and Surfaces A* 107: 223–31.

Painter, Scott, Vladimir Cvetkovic, James Mancillas, and Osvaldo Pensado. 2008. "Time Domain Particle Tracking Methods for Simulating Transport with Retention and First-Order Transformation." *Water Resources Research* 44(1): 1–11.

Prickett, T. A, C. G Lonnquist, and T. G Naymik. 1981. *A "Random-Walk" Solute Transport Model for Selected Groundwater Quality Evaluations*. Champaign: Illinois State Water Survey Bulletin.

Rausch, Randolf, Wolfgang Schafer, Rene Therrien, and Christian Wagner. 2005. *Solute Transport Modelling: An Introduction to Models and Solution Strategies*. Berlin. Stuttgart: Gebr. Borntraeger Verlagsbuchhandlung.

Reimus, Paul W. 1995. Transport of Synthetic Colloids through Single Saturated Fractures: A Literature Review. New Mexico.

https://digital.library.unt.edu/ark:/67531/metadc793343/.

Rodrigues, S N, and S E Dickson. 2015. "The Effect of Matrix Properties and Preferential Pathways on the Transport of Escherichia Coli RS2-GFP in Single, Saturated, Variable- Aperture Fractures." *Environmental Science and Technology* 49(14): 8425–31.

Ryan, Joseph N., and Menachem Elimelech. 1996. "Colloid Mobilization and Transport in Groundwater." *Colloids and Surfaces A* 107(95): 1–56.

Schwartz, S. C., and Y. S. Yeh. 1982. "On the Distribution Function and Moments of Power Sums.Pdf." *Bell System Technical Journal* 61(7): 1441–62.

Shan, Yongping, Hauke Harms, and Lukas Y. Wick. 2018. "Electric Field Effects on Bacterial Deposition and Transport in Porous Media." *Environmental Science and Technology* 52(24): 14294–301.

Shapiro, A M. 2002. Fractured-Rock Aquifers; Understanding an Increasingly Important Source of Water. *USGS Fact Sheet 112-02*.

Stoll, M., F. M. Huber, E. Schill, and T. Schäfer. 2017. "Parallel-Plate Fracture Transport Experiments of Nanoparticulate illite in the Ultra-Trace Concentration Range Investigated by Laser-Induced Breakdown Detection (LIBD)." *Colloids and Surfaces A: Physicochemical and Engineering Aspects* 529(1): 222–30.

Swanton, Stephen W. 1995. "Modelling Colloid Transport in Groundwater; the Prediction of Colloid Stability and Retention Behaviour." *Advances in Colloid and Interface Science* 54(1): 129–208.

Tang, D. H., E. O. Frind, and E. A. Sudicky. 1981. "Contaminant Transport in Fractured Porous Media: Analytical Solution for a Single Fracture." *Water Resources Research* 17(3): 555–64.

Tang, Yin, Milad Hooshyar, Tingju Zhu, Claudia Ringler, Alexander Y. Sun, Di Long, and Dingbao Wang. 2017. "Reconstructing Annual Groundwater Storage Changes in a Large-Scale Irrigation Region Using GRACE Data and Budyko Model." *Journal of Hydrology* 551(1): 397–406.

Torkzaban, Saeed, Shiva S. Tazehkand, Sharon L. Walker, and Scott A. Bradford. 2008. "Transport and Fate of Bacteria in Porous Media: Coupled Effects of Chemical Conditions and Pore Space Geometry." *Water Resources Research* 44(4): 1–12.

Verwey, E. J. W., and J. TH. G. Overbeek. 1984. *Theory of Stability of Lyophobic Colloids*. Elsevier, Amsterdam.

Wu, Dan, Lei He, Zhi Ge, Meiping Tong, and Hyunjung Kim. 2018. "Different Electrically Charged Proteins Result in Diverse Bacterial Transport Behaviors in Porous Media." *Water Research* 143: 425–35.

WWAP (*United Nations World Water Assessment Programme*). 2015. The United Nations World Water Development Report 2015: Water for a Sustainable World. Paris, *UNESCO.*

Yosri, Ahmed, Ahmad Siam, Wael El-Dakhakhni, and Sarah Dickson-Anderson. 2019. "A Genetic Programming–Based Model for Colloid Retention in Fractures." *Groundwater* 57(5): 693-703.

Zhang, Huixin, Hongbo Zeng, Ania C. Ulrich, and Yang Liu. 2016. “Comparison of the Transport and Deposition of Pseudomonas Aeruginosa under Aerobic and Anaerobic Conditions.” *Water Resources Research* 52(2): 1127–39.

Zhang, Wei, Xiangyu Tang, Noam Weisbrod, and Zhuo Guan. 2012. “A Review of Colloid Transport in Fractured Rocks.” *Journal of Mountain Science* 9(6): 770–87.

Zvikelsky, Ori, and Noam Weisbrod. 2006. “Impact of Particle Size on Colloid Transport in Discrete Fractures.” *Water Resources Research* 42(12): 1–12.

Chapter 6

SUMMARY, CONCLUSIONS, AND RECOMMENDATIONS

6.1. SUMMARY

The research presented in this dissertation aims at enhancing the reliability of modelling colloid behavior in fractured systems through: *i*) developing a framework to identify the hydraulic connection between two locations within a fractured aquifer, which was achieved through applying the stochastic event synchrony (SES) technique to solute concentrations acquired from these locations; *ii*) obtaining a mathematical relationship between the fraction of colloids retained along a fracture (F_r) and the parameters describing the physical and chemical properties of the groundwater-colloid-fracture system, where multigene genetic programming was applied to the dataset collected by an earlier study from multiple laboratory-scale colloid tracer experiments; *iii*) developing an analytical relationship between the fraction of colloids retained along a fracture and the deposition coefficient (κ), which is based on conceptualizing irreversible colloid deposition as first-order decay; and, *iv*) designing an efficient time domain-based numerical technique to simulate colloid behavior at the single-fracture and fracture network scales, under different physical and chemical conditions, based on the correspondence between breakthrough curves and colloid travel time in single fractures.

6.2. CONCLUSIONS AND CONTRIBUTIONS

The research in the present study introduces efficient tools to describe and simulate the behavior of colloids, and colloid-behaving contaminants (i.e., radionuclides), in fractured systems. The developed multigene genetic programming-based model and F_r–κ relationship represent accurate predictive models for colloid deposition in single fractures under a range of physical and chemical conditions. These conditions are considered either explicitly in the multigene genetic programming-based model or implicitly through the deposition coefficient in the F_r–κ relationship. The modified time domain random walk approach, also developed in the present study, represents an accurate and a computationally efficient simulation tool for colloid behavior in single fractures and fracture networks. This approach enables predicting colloid behavior in fracture networks considering the physical and chemical heterogeneity over the network, and even within each single fracture. Coupling the multigene genetic programming-based model, F_r–κ relationship, and the modified time domain random walk approach, and applying them to fracture networks constrained to SES-based hydraulic connections enables the reliable prediction of colloid behavior in fractured systems under actual field conditions. Therefore, these tools can aid in the design of effective water quality and remediation strategies through understanding how to modify the system's physical and chemical properties in order to enhance or inhibit colloid migration.

6.2.1. CONCLUSIONS AND CONTRIBUTIONS FROM CHAPTER 2

The coherence between solute transport in a saturated fracture and time series synchronization enabled the development of a SES-based framework that can effectively identify the hydraulic connection between two locations within a fractured aquifer.

- The framework provides a cost-effective alternative to obtain the hydrogeological properties within the connections identified.
- The SES-based hydraulic connections can be employed as an additional constraint when generating fracture networks stochastically, which is essential for the development of reliable flow and transport models in fractured aquifers.

6.2.2. CONCLUSIONS AND CONTRIBUTIONS FROM CHAPTER 3

An accurate mathematical relationship between F_r and the parameters describing the groundwater-colloid-fracture system's physical and chemical properties was developed using multigene genetic programming, and was validated for a subset of the observations of laboratory-scale colloid tracer experiments collected by an earlier study.

- The multigene genetic programming-based model can effectively predict F_r for a specified range of the parameters describing the system's physical and chemical properties.

- Attachment was found to be the primary retention mechanism for colloids in the fractures examined, which is consistent with conclusions from earlier studies.
- Surface charges of the colloid and fracture are the primary contributors to the variability of F_r; therefore, attention must be paid when measuring such properties.
- The multigene genetic programming-based model enhances the current understanding of colloid retention in single fractures and provides guidance about how to control the system's physical and chemical conditions for the effective management of groundwater quality in fractures.

6.2.3. CONCLUSIONS AND CONTRIBUTIONS FROM CHAPTER 4

The conceptualization of irreversible colloid deposition and first-order decay enabled simulating colloid behavior using the analytical solution describing the migration of decaying conservative solutes in single fractures; and therefore, developing an analytical relationship between F_r and κ in the same fracture-matrix configuration under an instantaneous colloid release at the inlet boundary. In addition, a graphical representation for F_r–κ relationship was developed.

- The F_r–κ relationship, together with its graphical representation, can be employed to predict F_r along a laboratory- or field-scale single fracture with an impermeable matrix under different deposition levels defined by κ.

- The fracture length, aperture, and κ are the primary contributors to the variability of F_r; therefore, attention must be paid when measuring or estimating these parameters.
- The F_r–κ relationship can be coupled with the multigene genetic programming-based model to develop a mathematical relationship between κ and the parameters describing the system's physical and chemical properties, which enables the prediction of colloid behavior under heterogeneous physical and chemical conditions.

6.2.4. CONCLUSIONS AND CONTRIBUTIONS FROM CHAPTER 5

A modified time domain random walk approach was designed to simulate colloid behavior in fractures considering advection, longitudinal dispersion, matrix diffusion, and irreversible deposition. This approach was developed at the single-fracture scale based on the equivalence between colloid breakthrough curves and the probability density function of colloid travel time, and its efficiency was then verified in an impermeable fracture network.

- The modified time domain random walk approach can efficiently simulate colloid behavior in single fractures with and without matrix diffusion, and also in impermeable fracture networks.
- The modified time domain random walk approach was developed for the case of an instantaneous colloid release at the inlet; however, this approach can

effectively simulate the response to the case of constant concentration at the inlet.

- The modified time domain random walk approach can be coupled with the F_r–κ relationship and the multigene genetic programming-based model to simulate colloid behavior in single fractures and fracture networks under different physical and chemical conditions, which is essential for incorporating the effects of the groundwater-colloid-fracture system's physical and chemical properties. Therefore, the reliability of colloid transport modelling in fractures can be enhanced.
- The modified time domain random walk approach provides a prediction tool for colloid behavior in fractured systems under different physical and chemical conditions, which is essential for the design of effective water quality management and remediation strategies in these systems.

6.3. RECOMMENDATIONS FOR FUTURE RESEARCH

The research presented in this dissertation contributes to the current practise of modelling colloid behavior in fractured aquifers through providing mathematical, analytical, and numerical tools that can efficiently predict colloid behavior under different physical and chemical conditions. Furthermore, the reliability of stochastically generated fracture networks, typically employed for flow and transport simulations in fractured systems, can be enhanced through using the SES-based framework also developed in the present study. In light findings

presented in this dissertation, possible extensions can be carried out to expand the practise of modelling colloid behavior in fractured aquifers.

- The efficacy of the SES-based framework was confirmed both for single fractures with different matrix configurations under different injection scenarios, and for a simple impermeable fracture network. However, the applicability of the framework in more complex systems, where multiple fractures and multiple connections exist, is also crucial.
- The multigene genetic programming-based model was developed using a relatively small dataset. More laboratory experiments under a wider range of physical and chemical conditions are therefore needed to increase the model's accuracy and extend its applicability. This model replicated the observations from laboratory-scale experiments, and verifying its applicability at the field scale is also important.
- Coupling the multigene genetic programming-based model and the F_r–κ relationship can be carried out and applied to laboratory-scale colloid tracer experiments for verification.
- The modified time domain random walk approach, the multigene genetic programming-based model, and the F_r–κ relationship can be coupled and applied at the fracture-network scale to enable the prediction of colloid behavior under multiple physical and chemical conditions.

6.4. NOTATIONS

F_r: Fraction of colloids retained along a fracture

Greek Letters:

κ: Deposition coefficient

6.5. ACRONYMS

SES: Stochastic event synchrony

Appendix - A: Derivation of Equation (4-8)

$F_r(L,t)$ represents the fraction of colloids retained along the full length of a fracture with an impermeable matrix up to time *t*, and under an instantaneous injection at the inlet boundary. At $t = \infty$, the total fraction of colloid retained F_r is evaluated as:

$$F_r = \frac{M_o - M'}{M_o} \qquad (A-1)$$

where *M'* is estimated using Equation (4-6) with $C(L,t)$ defined by Equation (4-5). Instead of using Equation (4-5) to express $C(L,t)$, the transformation introduced by Danckwerts (1953) is applied to the analytical solution developed by Abdel-Salam and Chrysikopoulos (1994) for the case of a constant concentration at the inlet boundary. Therefore, Equation (4-6) is equavilent to:

$$M' = \int_0^\infty Q \times \frac{M_o}{C_o Q} \frac{\partial C'(L,t)}{\partial t}\, dt \qquad (A-2)$$

$$M' = \frac{M_o}{C_o} C'(L,t) + \text{constant} \qquad (A-3)$$

where $C'(L,t)$ is the analytical solution of Equation (4-1) under a constant concentration at the inlet boundary, and is written as (Abdel-Salam and Chrysikopoulos 1994) (with $\zeta = \sqrt{1+KI}$):

$$C'(L,t) = \frac{C_o}{2}\left\{exp\left[\frac{UL}{2D}(1-\zeta)\right] erfc\left[\frac{L-Ut\zeta}{\sqrt{4Dt}}\right] + exp\left[\frac{UL}{2D}(1+\zeta)\right] erfc\left[\frac{L+Ut\zeta}{\sqrt{4Dt}}\right]\right\} \qquad (A-4)$$

Equation (4-8) can then be developed by combining Equations (A – 3) and (A – 4) and applying the following conditions:

$$C'(L,0) = 0 \qquad (A-5)$$

$$\lim_{t\to\infty} erfc\left(\frac{L-Ut\zeta}{\sqrt{4Dt}}\right) = 2 \qquad for\ x>0, U>0, and\ D>0 \qquad (A-6)$$

$$\lim_{t\to\infty} erfc\left(\frac{L+Ut\zeta}{\sqrt{4Dt}}\right) = 0 \qquad for\ x>0, U>0, and\ D>0 \qquad (A-7)$$

REFERENCES

Abdel-salam, Assem, and Constantinos V Chrysikopoulos. 1994. "Analytical Solutions for One-Dimensional Colloid Transport in Saturated Fractures." *Advances in Water Resources* 17(5): 283–96.

Danckwerts, P.V. 1953. "Continuous Flow Systems Distribution of Residence Times." *Chemical Engineering Science* 2(1): 1–13.

Appendix - B: Travel time CDF for colloids in single fractures when longitudinal dispersion is neglected

When longitudinal dispersion is neglected, Equation (5-1) reduces to:

$$\frac{\partial C_{cd}}{\partial t} = -u\frac{\partial C_{cd}}{\partial x} - \frac{2\kappa u}{b^2}C_{cd} + \frac{2\theta D_e}{b}\frac{\partial C_m}{\partial z} \qquad (B-1)$$

where C_{cd} is the colloid concentration in the fracture under a constant concentration at the inlet, when longitudinal dispersion is neglected. As obtaining the travel time is of interest, a constant concentration is assumed at the fracture inlet; and therefore, the following boundary conditions are adopted:

$$C_{cd}(0, x) = 0 \qquad (B-2)$$

$$C_{cd}(t, 0) = C_o \qquad (B-3)$$

$$\left.\frac{\partial C_{ad}}{\partial x}\right|_{x=\infty} = 0 \qquad (B-4)$$

$$C_m(t = 0, x, z) = 0 \qquad (B-5)$$

$$C_m(t, x, z = b/2) = C_{cd}(t, x) \qquad (B-6)$$

$$\left.\frac{\partial C_m}{\partial z}\right|_{z=\infty} = 0 \qquad (B-7)$$

By solving the system of Equations (B-1) and (5-2) under the boundary conditions defined by Equations (B-2) through (B-7), following the same procedures employed by (Tang et al. 1981) to develop an analytical solution for

solute transport in a fracture-matrix system when longitudinal dispersion is neglected:

$$\frac{C_{cd}(x,t)}{C_o} = \exp\left(-\frac{2\kappa x}{b^2}\right) erfc\left(\frac{\theta\sqrt{D_e}x}{ub\sqrt{t - {}^{x}/_{u}}}\right) \qquad (B-8)$$

The ratio C_{ad}/C_o in is equivalent to the ratio between the colloid mass travelling a distance x up to time t and the total colloid mass travelling the same distance up to infinite time. Therefore, it can be used to represent the particle travel time CDF under the condition that $C_{ad}(x, \infty) = C_o$. Although this condition will not be satisfied for Equation (B-8) unless colloid deposition is neglected (i.e., $\kappa = 0$), the CDF of particle travel time can be derived as:

$$F_t(x,t) = \int_0^t QC_i(x,t)dt \Big/ \int_0^\infty QC_i(x,t)dt \qquad (B-9)$$

where the numerator in Equation (B-9) represents the colloid mass travelling a distance x up to the time t, the denominator indicates the total mass travelled the same distance up to infinite time, and C_i is the colloid concentration in the fracture under an instantaneous injection at the inlet. The relationship between C_i and C_{cd} was developed by Danckwerts (1953):

$$C_i(x,t) = \frac{M_o}{QC_o}\frac{\partial C_{cd}}{\partial t} \qquad (B-10)$$

Coupling Equations (B-8), (B-9), and (B-10) results in an analytical description for F_t, that can be written as:

$$F_t(x,t) = erfc\left(\frac{\theta\sqrt{D_e}x}{ub\sqrt{t - {x}/{u}}}\right) \qquad (B-11)$$

Equation (B-11) is equivalent to the CDF of solute travel time reported by Bodin et al. (2007) when Ω is calculated as ${\theta\sqrt{D_e}}/{b}$ instead of ${\sqrt{\theta D_e}}/{b}$.

REFERENCES

Bodin, Jacques, Gilles Porel, Fred Delay, Fabrice Ubertosi, Stéphane Bernard, and Jean Raynald de Dreuzy. 2007. "Simulation and Analysis of Solute Transport in 2D Fracture/Pipe Networks: The SOLFRAC Program." *Journal of Contaminant Hydrology* 89(1–2): 1–28.

Danckwerts, P.V. 1953. "Continuous Flow Systems Distribution of Residence Times." *Chemical Engineering Science* 2(1): 1–13.

Tang, D. H., E. O. Frind, and E. A. Sudicky. 1981. "Contaminant Transport in Fractured Porous Media: Analytical Solution for a Single Fracture." *Water Resources Research* 17(3): 555–64.